SILURIAN-DEVONIAN MICROFOSSILS AT BAN THUNG SAMED SECTION, LA-NGU DISTRICT, SATUN PROVINCE FOR PALEOENVIRONMENTAL INTERPRETATION

ANUCHA PROMDUANG

A Thesis Submitted in Partial Fulfillment of the Requirements for
the Degree of Master of Engineering in Civil, Transportation
and Geo-resources Engineering
Suranaree University of Technology
Academic Year 2024

ซากดึกดำบรรพ์จุลภาคยุคไซลูเรียน-ดีโวเนียน บริเวณหน้าตัดบ้านทุ่งเสม็ด อำเภอละงู จังหวัดสตูล เพื่อการแปลความหมายสภาพแวดล้อมบรรพกาล

นายอนุชา พรมด้วง

วิทยานิพนธ์นี้เป็นส่วนหนึ่งของการศึกษาตามหลักสูตรปริญญาวิศวกรรมศาสตรมหาบัณฑิต
สาขาวิชาวิศวกรรมโยธา ขนส่ง และทรัพยากรธรณี
มหาวิทยาลัยเทคโนโลยีสุรนารี
ปีการศึกษา 2567

SILURIAN-DEVONIAN MICROFOSSILS AT BAN THUNG SAMED SECTION, LA-NGU DISTRICT, SATUN PROVINCE FOR PALEOENVIRONMENTAL INTERPRETATION

Suranaree University of Technology has approved this thesis submitted in partial fulfillment of the requirements for a Master's Degree.

Thesis Examining Committee

.....

(Asst. Prof. Dr. Chatchalerm Ketwetsuriya)
Chairperson

.....

(Assoc. Prof. Dr. Anisong Chitnarin)
Member (Thesis Advisor)

.....

(Asst. Prof. Dr. Prachya Tepnarong)
Member

.....

(Assoc. Prof. Dr. Yupaporn Ruksakulpiwat)
Vice Rector for Academic Affairs and
Quality Assurance

.....

(Assoc. Prof. Dr. Pornsiri Jongkol)
Dean of Institute of Engineering

อนุชา พรมด้วง: ซากดึกดำบรรพ์จุลภาคยุค ไซลูเรียน-ดีโวเนียน บริเวณหน้าตัดบ้านทุ่งเสม็ด อำเภอละงู จังหวัดสตูล เพื่อการแปลความหมายสภาพแวดล้อมบรรพกาล (SILURIAN-DEVONIAN MICROFOSSILS AT BAN THUNG SAMED SECTION, LA-NGU DISTRICT, SATUN PROVINCE FOR PALEOENVIRONMENTAL INTERPRETATION) อาจารย์ที่ปรึกษา: รองศาสตราจารย์ ดร.อานิสงส์ จิตนารินทร์, 121 หน้า.

คำสำคัญ: ออสตราคอด/ โคโนดอน/ เทนทาคูลิทอย/ การวิเคราะห์แผ่นหินบาง/ การลำดับชั้นหินตามลักษณะหิน

วิทยานิพนธ์ฉบับนี้ศึกษาซากดึกดำบรรพ์ขนาดจุลภาค ประกอบไปด้วย ออสตราคอด โคโนดอนและเทนทาคูลิทอย พร้อมทั้งการลำดับชั้นหินจากหน้าตัดบ้านทุ่งเสม็ดในหมวดหินควนทัง จังหวัดสตูล ประเทศไทย ซึ่งมีอายุอยู่ในช่วงไซลูเรียน-ดีโวเนียน หน้าตัดที่ศึกษามีความหนารวมประมาณ 50 เมตร ถูกแบ่งออกเป็น 3 หน่วยหินย่อย โดยส่วนล่างประกอบไปด้วยหินปูนสีเทาแดงที่มีความหนาปานกลางถึงหนาและชั้นดินแทรก จากนั้นเปลี่ยนเป็นหินปูนสีเทาเข้มสลับกับหินดินดานสีดำ โดยที่อัตราส่วนหินดินดานสีดำนั้นเพิ่มขึ้นทางด้านบน หินปูนในหน่วยหินย่อยชั้นล่าง กลาง และส่วนล่างของหน่วยหินย่อยชั้นบน ถูกจำแนกเป็น fine-grained bioclastic sparse wackestone และ bioclastic packed wackestone สำหรับหินปูนของหน่วยหินย่อยชั้นบนที่เหลือ สะท้อนถึงสภาพแวดล้อมทางทะเลที่ลึกขึ้นตามลำดับ

การวิเคราะห์ซากดึกดำบรรพ์ขนาดจุลภาคพบ ออสตราคอด จำนวน 586 ตัวอย่าง ซึ่งจำแนกได้ 34 สปีชีส์ จาก 17 สกุล และ โคโนดอน จำนวน 103 ตัวอย่างจำแนกได้ 7 สปีชีส์ จาก 5 สกุล รวมถึงเทนทาคูลิทอยที่จำแนกได้ 3 สกุล การบ่งชี้อายุของพื้นที่ศึกษา ได้อาศัยกลุ่มซากดึกดำบรรพ์โคโนดอนที่มี *Ozarkodina crispa* (Walliser, 1964) ซึ่งยืนยันอายุสมัยลัดโลวตอนปลาย (Late Ludlow) สำหรับหน่วยหินชั้นล่าง และชั้นหินดินดานที่มี เทนทาคูลิทอย-แกรปโตไลต์ ในหน่วยหินชั้นบนบ่งชี้อายุช่วงยุคดีโวเนียนตอนต้นประมาณสมัยแพรเจี้ยนตอนปลายหรือสมัยเอ็มเซี่ยนตอนต้นสุด (late Pragian or earliest Emsian) ดังนั้น หน้าตัดในงานศึกษานี้ มีอายุในช่วงยุคไซลูเรียนตอนปลายประมาณสมัยลัดโลวถึงยุคดีโวเนียนตอนต้น สมัยแพรเจี้ยนตอนปลายหรือสมัยเอ็มเซี่ยนตอนต้นสุด

การแปลความหมายสภาพแวดล้อมบรรพกาลจากการศึกษากลุ่มสิ่งมีชีวิตของออสตราคอดและการวิเคราะห์ศิลาวรรณาด้วยการศึกษาแผ่นหินบาง บ่งชี้ให้เห็นว่าบริเวณพื้นที่ศึกษานี้สะสมตัวใน

ทะเลน้ำตื้นที่ต่ำกว่าฐานคลื่นในสภาพอากาศปกติ (fair-weather wave base) ที่มีปริมาณออกซิเจนเพียงพอสำหรับสิ่งมีชีวิตที่อาศัยอยู่หน้าดิน (Benthic fauna) ในหน่วยหินย่อยชั้นล่างและกลาง และได้เปลี่ยนแปลงไปสู่สภาพแวดล้อมที่ลึกขึ้น ที่มีออกซิเจนน้อย โดยมีสิ่งมีชีวิตส่วนใหญ่เป็นพวกที่อาศัยอยู่ในมวลน้ำ (Pelagic organisms) ในหน่วยหินย่อยชั้นบน

สาขาวิชาเทคโนโลยีธรณี ลายมือชื่อนักศึกษา .....

ปีการศึกษา 2567 ลายมือชื่ออาจารย์ที่ปรึกษา .....

ANUCHA PROMDUANG: SILURIAN-DEVONIAN MICROFOSSILS AT BAN THUNG SAMED SECTION, LA-NGU DISTRICT, SATUN PROVINCE FOR PALEOENVIRONMENTAL INTERPRETATION
THESIS ADVISOR: ASSOC. PROF. ANISONG CHITNARIN, Ph.D., 121 PP.

Keyword: Ostracod/ Conodont/ Tentaculitoids/ Thin section analysis/ Lithostratigraphy

This thesis examines microfossils (ostracods, conodonts, tentaculitoids) and lithostratigraphy from the Silurian-Devonian Ban Thung Samed section of the Kuan Tung Formation in Satun Province, Thailand. The 50-meter stratigraphic section subdivided into 3 subunits, transitions from thick-bedded reddish-grey limestone with argillaceous layers at the base to interbedded medium-bedded dark grey limestone and black shale toward the top, with an increasing proportion of shale relative to limestone. The lower and middle subunits, including the lower part of the upper subunit, consist of fine-grained bioclastic sparse wackestone, which transitions to bioclastic packed wackestone in the middle and upper portions of the upper subunit, reflecting a deepening marine environment dominated by dacryoconarid pelagic deposits.

Microfossil analysis identified 586 ostracod specimens representing 34 species belonging to 17 genera, 103 conodont specimens representing 7 species, 5 genera and 3 genera from tentaculitoids. The conodont *Ozarkodina crispa* (Walliser, 1964) confirming a Late Ludlow age for the lower subunit and tentaculitoid-graptolites bearing black shale indicate an Early Devonian (late Pragian or earliest Emsian) for the uppermost part of the section. Therefore, the study section ranges from Late Silurian (late Ludlow) to Early Devonian (late Pragian or earliest Emsian). The paleoenvironmental interpretation, based on ostracod assemblages and petrographic analysis conducted on thin sections, suggests subtidal deposition below the fair-weather wave base, well-oxygenated conditions with diverse benthic fauna in the

lower and middle subunits. This progresses to deeper, low-oxygen environments dominated by pelagic organisms in the upper subunit.

School of Geotechnology

Academic Year 2024

Student's Signature .....

Advisor's Signature .....

ACKNOWLEDGEMENT

I am grateful to Suranaree University of Technology (SUT) for the financial support that made this research possible.

I would like to express my deepest gratitude to Assoc. Prof. Dr. Anisong Chitnarin for her invaluable guidance, steadfast support, and encouragement throughout my academic journey. Her mentorship has been a cornerstone of my growth, helping me overcome challenges in both my coursework and research.

I sincerely thank Mr. Jirasak Charoenmit, Mr. Weerachai Paengkaew, and Mr. Sataphon Mitmark from the Department of Mineral Resources for their support during fieldwork and insightful discussions on Paleozoic paleontology in Thailand.

Special thanks to Professor Dr. Sachiko Agematsu-Watanabe from University of Tsukuba, Japan, Professor Dr. Clive Burrett from Maha Sarakham University, Thailand, and Dr. Shuji Niko from Hiroshima University, Japan for their expert guidance and contributions to the study of conodont and tentaculitid specimens.

I also appreciate the constructive feedback from my thesis committee and the unwavering support of my family, whose encouragement has been my greatest source of strength.

Anucha Promduang

TABLE OF CONTENTS

Page

TABLE OF CONTENTS (Continued)

Page

TABLE OF CONTENTS (Continued)

Page

TABLE OF CONTENTS (Continued)

Page

LIST OF FIGURES

Figure **Page**

LIST OF FIGURES (Continued)

Figure **Page**

LIST OF FIGURES (Continued)

Figure **Page**

LIST OF FIGURES (Continued)

Figure **Page**

LIST OF FIGURES (Continued)

Figure **Page**

LIST OF FIGURES (Continued)

Figure **Page**

LIST OF FIGURES (Continued)

Figure **Page**

CHAPTER I

INTRODUCTION

The study of microfossils in Thailand has remained limited, largely due to the scarcity of local specialists. However, the exposed Silurian–Devonian outcrops at Ban Thung Samed in Satun Province presents a valuable opportunity for advancing microfossil research and paleoenvironmental interpretation. This thesis seeks to bridge this gap by investigating microfossils assemblages from the Silurian-Devonian Ban Thung Samed section in Satun Province, Thailand. Through detailed ostracod assemblage analysis and petrographic examination, this research aims to deepen our understanding of the paleoenvironment of the region. The age of the section will be established using conodonts and tentaculitoids, allowing for more precise paleoenvironmental interpretations.

1.1 Background and Rationale

Thailand primarily consists of four geological provinces, as illustrated in Figure 1.1: the west and south of Thailand are comprised of Sibumasu Terrane, the Inthanon zone in the northwest, the Sukhothai Terrane in the center, and the Indochina Terrane in the east (Thassanapak et al., 2019). According to Metcalfe (2017), Sibumasu Terrane was considered to be situated closely to northwest of Australian in Gondwana Supercontinent and then separated in Early Permian. Inthanon Zone was derived from Gondwana (see more discussion in Udchachon et al., 2022). Sukhothai Terrane or Sukhothai arc formed on the margin of the South China-Indochina Superterrane that was subducted by Palaeo-Tethys in Early Carboniferous–Early Permian. Indochina Terrane is a composite terrane that formed by miniterrane derived from peri-Gondwana in Late Silurian to Carboniferous (See Burrett et al., 2021). These terranes (Sibumasu, Inthanon, Indochina) were collided and formed Thailand in Middle to Late

Triassic. This study focuses on Silurian-Devonian section exposed at an abandoned quarry in Ban Thung Samed, La-Ngu District, Satun Province, Thailand.

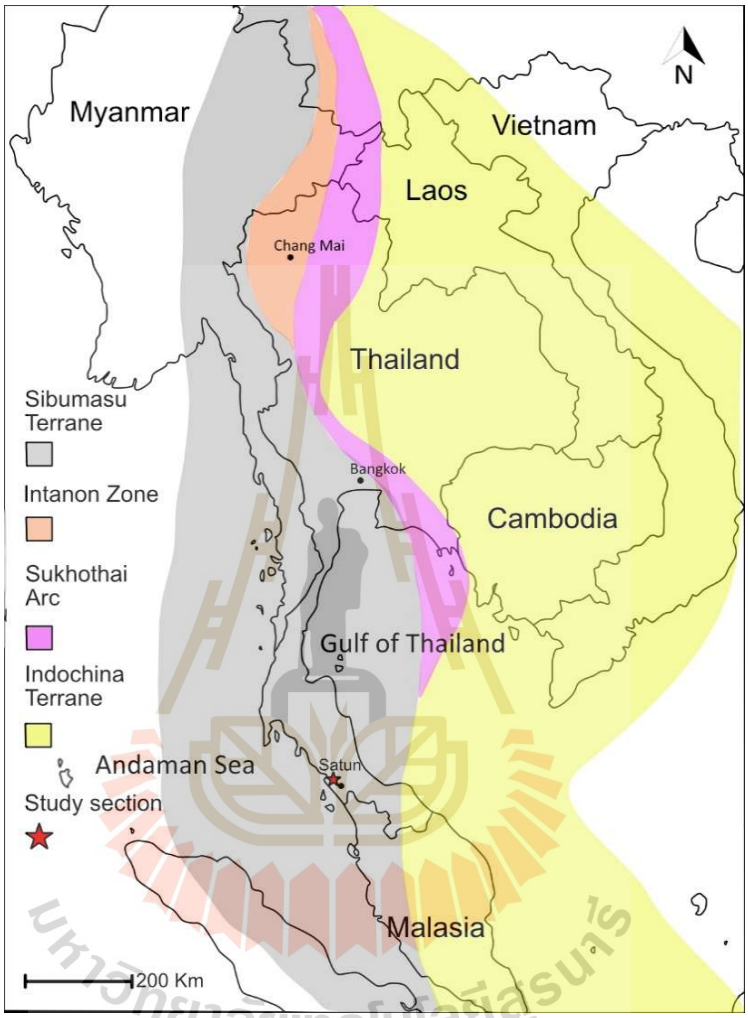

Figure 1.1 Geological Provinces of Thailand (modified after Thassanapak et al., 2019).

On mainland Satun, continuous rock sequences ranging from Upper Ordovician to probably Lower Carboniferous are exposed between Km 9 and Km 11 of the 416 roads from La-Ngu to Thung Wa Districts (Wongwanich et al., 1990). Wongwanich et al. (1990) described five geological units based on lithostratigraphy: the Pa Kae Formation (Ordovician), Wang Tong Formation (Ordovician-Late Silurian), Kuan Tung Formation (Late Silurian-Early Devonian), Pa Samed Formation (Devonian), and Khao Chu Nong Formation (Carboniferous). Later Khao Chu Nong Formation was revised and excluded

(Wongwanich and Boucot, 2011). For a long time, these continuous sequences have been the prime area for Paleozoic rock and fauna research (e.g., Agematsu et al., 2006a, 2007; Boucot et al., 1999; Crônier and Fortey, 2006; Kershaw et al., 2019; Long and Burrett, 1989; Wongwanich et al., 1990).

The Ban Thung Samed abandoned quarry in Satun Province provides well-preserved exposures of Silurian to Devonian strata. Although Itsarapong et al. (2023) conducted detailed lithostratigraphic and geochemical analyses that led to a revised interpretation of the Kuan Tung Formation, studies on microfossils, particularly Paleozoic ostracods, as well as the paleoenvironmental context of this section remain limited. Most Paleozoic ostracod studies in Thailand have focused on the Upper Paleozoic, particularly in central regions (Chitnarin and Ketwetsuriya, 2021; Chitnarin et al., 2008, 2012, 2017). Additionally, Dill et al. (2004) reported Late Paleozoic ostracods from Surat Thani Province in southern Thailand. Despite these contributions, ostracods from the Silurian-Devonian interval remain unexplored. In addition to ostracods, conodonts and tentaculitoids are widely recognized for their biostratigraphic value and have been used globally for age determination. Their integration enhances the potential for a more comprehensive, fossil-based interpretation. This thesis seeks to address these gaps by investigating Silurian-Devonian ostracods from the Ban Thung Samed section in Satun Province. By analyzing ostracod assemblages and thin sections alongside conodonts and tentaculitoids, this study aims to refine age estimates and deepen understanding of the paleoenvironmental conditions preserved in the succession.

1.2 Research objectives

1) To classify and establish a taxonomic record of ostracods, conodonts, and tentaculitoids from the Ban Thung Samed section in Ban Thung Samed, Kamphaeng Sub-district, La-Ngu District, Satun Province.

2) To analyze the depositional environment of the study section using ostracod assemblages with lithology data from thin section analysis.

3) To determine the age of Ban Thung Samed section.

1.3 Scope and limitations

1) The study focuses on rock samples collected from a quarry at Ban Thung Samed, Kamphaeng Sub-district, La-Ngu District, Satun Province.

2) Ostracod preparation follows the methodology of Crasquin-Soleau et al. (2005).

3) The lithology of the study section is analyzed through thin section analysis.

4) Conodonts and tentaculitoids are utilized to determine the age of the study section.

5) Conodont preparation follows Green (2001), with slight modifications.

6) The paleoenvironment is interpreted based on ostracod assemblages and rock lithology.

1.4 Contents of the thesis

This thesis is organized into seven chapters. Chapter I introduces the study, providing an overview of its objectives and scope. Chapter II presents the literature review, covering the geology of Satun Province and foundational knowledge of ostracods, conodonts, and tentaculitoids from the Silurian-Devonian period. Chapter III outlines the methodology, detailing field investigations, sample collection, laboratory processes for ostracods, conodonts, tentaculitoids, and thin section analysis, as well as data interpretation. Chapter IV provides the geology and stratigraphy of the Ban Thung Samed section, including its age determination. Chapter V focuses on the taxonomy of ostracods, conodonts, and tentaculitoids identified in the study section. Chapter VI provides an analysis of the lithology of the study section based on thin sections. Finally, Chapter VII concludes with a discussion of the paleoenvironmental interpretations of the study section and offers recommendations for further research.

CHAPTER II

LITERATURE REVIEW

This chapter covers the fundamentals of ostracods, conodonts, tentaculitoids including their morphology and ecology, and offers a comprehensive overview of the Paleozoic geology in Satun Province, emphasizing the Silurian-Devonian rock formations. This information provides an essential foundation for understanding the geological context in the subsequent parts of the thesis.

2.1 Geology of Satun Province, Southern Thailand

Exposed rocks in Satun Province (Figure 2.1) according to geological map from Department of Mineral Resources (2013) range from Cambrian to Carboniferous-Permian and covered by Quaternary sediments with some Triassic granite intrusions. Most of the Cambrian rocks are exposed on Tarutao Island (Ko Tarutao), covering more than half of the area. Ordovician rocks are exposed in the northeast of Tarutao Island and in the north and east of mainland Satun. Silurian and Devonian rocks are difficult to distinguish precisely, so they are often grouped together as Silurian-Devonian rocks and are mostly exposed on the mainland of Satun. Carboniferous-Permian rocks are also grouped together and exposed in the lower to middle parts of mainland Satun. Quaternary sediments cover the middle and western parts of the mainland. Triassic granite is exposed on Ra Wi Island, Adang Island, and the eastern part of mainland Satun.

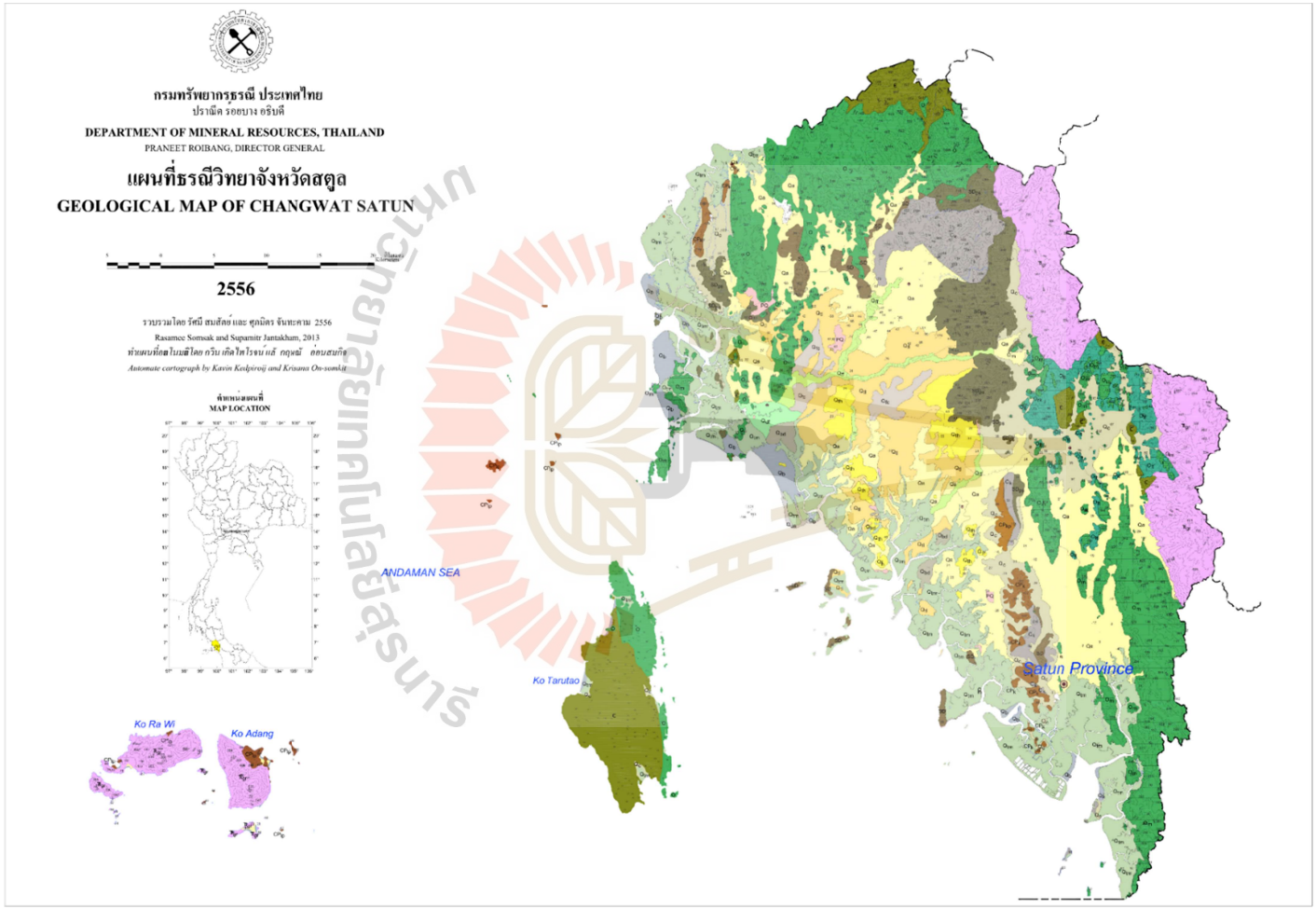

Figure 2.1 Geological map of Satun Province from Department of Mineral Resources (2013).

EXPLANATION

SEDIMENT, SEDIMENTARY AND METAMORPHIC ROCKS	FORMATION/GROUP	PERIOD	AGE (my.)
Qa Alluvial deposits : gravel, sand, silt and clay.			
Qb Beach sand formation : sand, fine to coarse, well sorted, subrounded, light brown or light grey, quartz, loose.			
Qbd Former beach ridges and dunes. (above high water spring tide) : Sand, fine-medium grained, well sorted.			
Qdf Deltaic-flood plain : Fine sand stratied with clay and gravels.			
Qfc Abandoned channels : Fine sand, silt and clay overlies stiff mottle clay.			
Qff Flood plain : Fine grained sand and silt overlies the gravels.			
Qtm Tidal flat vegetated with mangrove (In between high-low water spring tide) : peat, platy clay, fine sand, silty clay and sandy clay of intertidal flat.			
Qua Accretionary plain, tidal delta and bar deposits. (Below-high water spring tide.) : Sand, silty sand, fine-medium grain, with well developed bedforms.		QUATERNARY	0.01-1.6
Ql Lower terraces and undulating upland : elevation from 10-20 meters in the mainland, and 1-5 meters above mean sea levels in the islands : clayey sand, mottle clay, laterite and gravels overlain the weathered surface of bed rock.			
Qth Higher terrace : well dissected surface with elevation from 20-50 maters above sea level. Laterite, gravels and rock fragments, thickness depends on the weathered surface of bed rock.			
Qc Colluvial deposits : fine sand and clay, red, yellow, light brown and light gray, abundant mottled, loose, with some rock fragments and relic structure, partly laterie or laterittic layer.			
PQ Erosion surface of bed rocks : weathered bed rock in situ or bed rock with Quaternary sediment overlains less than 20 meters.			
P Limestone : light gray, massive, fossils of brachiopods, corals and crinoids.	Ratburi Gp.	PERMIAN	245-286
CPkp Mudstone : dark gray, thin bedded to massive, with silt lamination, weathering to reddish brown, interbedded with siltstone; lithic sandstone and pebbly mudstone; sandstone, fine-to medium-grained, thick bedded, moderately sorted, subrounded, pebbles composed of quartz, sandstone, chert and granite.	KHAO PHRA Fm., KAENG KRACHAN Gp.		
CPlp Mudstone : dense, black, thin bedded, well bedded, with silt lamination, intercalated with lithic sandstone; quartzitic sandstone and pebbly mudstone, black, reddish brown and gray, thin bedded to massive.	LAEM MAI PHAI Fm., KAENG KRACHAN Gp.	PERMIAN to CARBONIFEROUS	245-360
CPk Mudstone, shale, siltstone, pebbly greywacke and pebbly mudstone : dark gray, thick-bedded with lamination and lens of sillstone, fine-to coarse- grained, poorly sorted, moderaily rounded.	KAENG KRACHAN Gp.		
Ck Mudstone, shale, sandstone and pebbly mudstone : white, light gray, dark gray, brown, reddish brown, yellowish brown, thin to thick-bedded, fine-to coarse-grained, poorly sorted, moderaily rounded, well cementation, with abundant bivalves, trilobites, cephalopods, brachiopods, crinoids and gastropods.	KUAN KLANG Fm.	CARBONIFEROUS	286-360
SDps Siliceous mudstone : dark gray, greenish gray, thin to medium bedded, well bedded, interbedded with lithic sandstone, siltstone and chert, dark gray, grayish brown and reddish brown.	PA SAMED Fm.	DEVONIAN to SILURIAN	360-445
SD Siliceous mudstone, chert, shale, sandstone and pebbly mudstone : gray, light brown, dark gray, brown, reddish purple and greenish gray, thin-to medium-bedded; very coarse-grained sandstone, poorly sorted, moderatly rounded, well cementation, pebbles consist of sandstone and quartzite with abundant tentaculites, graptolites, trilobites, brachiopods, crinoids and cephalopods			
Orn Limestone, argillaceous limestone : gray to dark gray, thick bedded to massive, with argillaceous laminations and fossil of nautiloid.	RUNG NOK Fm., THUNG SONG Gp.		
Ols Shale, calcareous shale : reddish brown, brown and yellowish brown, thin bedded, interbedded with siltstone, lithic sandstone, fine-grained, well sorted, with limestone lenses at top.	LAE TONG Fm., THUNG SONG Gp.	ORDOVICIAN	445-490
O Argillaceous limestone, limestone : grey and dark grey, and dolomitic limestone with abundant fossils.	THUNG SONG Gp.		
ЄC Sandstone, siltstone, shale and local quartzite : light brown, light gray, reddish brown yellow, thin-to thick-bed; sandstone showing cross-bedding, ripple cross-bedding, lamination and slump structure, with trilobite.	TARUTAO Gp.	CAMBRAIN	490-540
IGNEOUS ROCKS	**PERIOD**		
T_{gr} Granite : biotite-muscovite granite, aplite and pegmatite, fine to coarse crystal, porphyritic texture, with feldspar phenocryst, euhedral crystal.	TRIASSIC		210-245

Figure 2.2 Explanation of rock units in Satun Province from Department of Mineral Resources (2013).

The lithology of rocks in Satun Province, as studied here, is based on the works of Suphakdee (2017), who summarized the lithology and fauna assemblage of the Pa Samet area (Ban Thung Samed). This includes the works of Bunopas (1981) for the Tarutao Group (Cambrian-Ordovician), Wongwanich (1990) and Wongwanich et al. (1990) for establishing the Thung Song Group (Ordovician) and Thong Pha Phum Group (Ordovician-Carboniferous) respectively, and Chaodumrong et al. (2004, 2007) for the Kaeng Krachan Group. The information of Quaternary sediments is adopted from Department of Mineral Resources (2013).

2.1.1 Tarutao Group

This group's type section, situated on Tarutao Island composed of the sequences of siliciclastic rocks including fine-grained sandstone, siltstone, shale, minor limestone, conglomerate, and minor volcaniclastics (Department of Mineral Resources, 2018). Notably, this group contains fossils of brachiopod, conodont and trilobites such as *Pagodiathaiensis*, "*Eosaukia*" *buravasi* (Kobayashi, 1957), and *Coreanocephalus phanulatus* (Kobayashi, 1957) which are typically late Cambrian species.

2.1.2 Thung Song Group

Thung Song Group which overlies Tarutao Group is predominant by limestone with some siliciclastic which includes bedded limestone, nodular limestone, cross-bedded limestone, calcisiltite, calcarenite, graptolitic shale but most distinguish of this group is red stromatolitic limestone which is the topmost of the sequence. The fauna in this group is typically carbonate-platform fauna such as gastropods, brachiopods, bivalves, sponges, trilobites, conodonts, nautiloids, graptolites and stromatolites. Thung Song Group is mostly Ordovician (Wongwanich, 1990; 2001).

2.1.3 Thong Pha Phum Group

The Thong Pha Phum Group was renamed by Bunopas (1981) from the Tanaosi Group of Javanaphet (1969). The type section of this group is exposed along the banks of Huai Thong Pha Phum in Amphoe Thong Pha Phum, Kanchanaburi Province (Bunopas, 1981). In the Satun area, this group was found and redefined by

Wongwanich et al. (1990) in the area between kilometers 9-11 on the side of La-Ngu to Thung Wa Road, known as Ban Pa Samed and Ban Pa Kae. This area (km 9–11) has been named Ban Pa Samed by later researchers, is in fact located at Ban Thung Samed village. Ban Pa Samed village also exists but is located further south of Wongwanich et al, (1990) studied area. The Thong Pha Phum Group consists of three formations: Wang Tong Formation, Kuan Tung Formation, and Pa Samed Formation (Wongwanich 2001; Wongwanich et al., 2002; Wongwanich and Boucot, 2011).

2.1.3.1 Wang Tong Formation

Wang Tong Formation has 50-110 meters thick and can be recognized by graptolitic black shale to dark grey siltstone in the lowermost part and changes into well bedded dark grey-brownish-grey muddy siltstone and very fine grained feldspathic sandstone with a lenticular layer of black graptolite-rich shale in the middle part of formation and the top is consists of thick sequence of grey, well bedded chert with black shale. The fauna of this formation consists of brachiopods and trilobites in the middle part and very abundant graptolites in the top of the Formation (Wongwanich et al., 1990). In sandstone beds of the middle parts contains Hirnantian (Latest Ordovician) brachiopod-trilobite fauna consisting of *Hirnantia sagittifera* (McCoy, 1851), *Onnia*? *Yichangensis* Zeng in Wang 1983, *Aegiromena planissima* (Reed, 1915), *Mirorthis mira* Zeng in Wang 1983, *Cliftonia* sp., *Paramalomena* sp., *Eospirigerina* sp., and *Mucronaspis mucronata* Brongniart (Cocks and Fortey, 1997). Beneath the sandstone beds found trilobites, *Mucranaspis* sp. and *Normalograptus medius*, *N. normalis*, *N. modestus* and *Pseudoclimacograptus* sp., *Parakidinograptus acuminatus*. The graptolite in the top of the Formation are identified as *Normalograptus persculptus* (Wongwanich et al., 1990) and *N. pseudovenustus pseudovenustus* Legrand, 1986 which represents the Uppermost Ordovician (Agematsu et al., 2006b). Therefore, Wang Tong Formation ranges from Late Ordovician to Early Silurian.

2.1.3.2 Kuan Tung Formation

Kuan Tung Formation is approximately 105 meters thick and predominant by limestone. The lower member of this unit is massively bedded, grey calcisiltites with thin argillaceous layers. The middle member consists of calcisiltites that range in color from pink to red and grey with fossils and minor calcarenite with some chert nodule. The upper unit is red, well-bedded micrite, interbedded with thin reddish brown argillaceous layers and small algal polygons of stromatolite (Wongwanich et al., 1990). Based on Emsian trilobites in the lower part, *Reedops megaphacos, R. seleniomma, Decoroproetus* sp., *Cornuproetus (Sculptoproetus) sculptus* and *Platyscutellum* sp. (Fortey, 1989) and Early Devonian conodonts in the upper part, *Pandorinella steinhornensis steinhornensis* Ziegler, 1956, *Polygnathus labiosus mawsonae* Long and Burrett, 1989 and *Pseudooneotodus kuangtungensis* Long and Burrett, 1989 and the formation conformably overlies Upper Silurian Wang Tong Formation (Wongwanich et al., 1990), the age of Kuan Tung Formation is probably Late Silurian to Early Devonian (Wongwanich and Boucot, 2011).

Agematsu et al. (2017) redefined the rock units in this group due to numerous unclear boundaries and discontinuities. The redefined Kuan Tung Formation comprises lower, middle, and upper members. Where the lower member is the whole original Kuan Tung Formation of Wongwanich et al. (1990). The middle member is black tentaculitic shale which is the old member 1 of Pa Samed Formation of Wongwanich et al. (1990). The upper member is nodular limestone overlies unconformably middle member with fault contact. Agematsu et al. (2017) suggested that the Kuan Tung Formation ranges from the Latest Silurian to the Middle Devonian, based on the presence of Late Silurian to earliest Devonian conodonts in the lower member and Givetian conodonts in the upper member.

In a recent study, Itsarapong et al. (2023) conducted a detailed investigation at the study section of this thesis and revised the Kuan Tung Formation (Figure 2.3). The formation is divided into three members. The lower member consists

of medium to thick-bedded grey limestone, overlain by thin to medium-bedded limestone interbedded with black shale. The middle member is composed of thick-bedded black shale and siltstone interbedded with medium-bedded limestone, with pyrite found in the limestone. This member is unconformably overlain by black shale containing abundant fossils. The upper member consists of grey to pink, thin to thick-bedded limestone with observed laminations and argillaceous bands. According to Itsarapong et al. (2023), the upper member is overlain by red sandstone, which could potentially belong to either the Kuan Klang Formation (Suphakdee, 2017) or the Pa Samed Formation (Wongwanich et al., 1990).

2.1.3.3 Pa Samed Formation

Tansuwan et al. (1979) named the discovered black tentaculitic shale in Satun Province as the Pa Samed Formation, which dates from the Silurian to Devonian periods. Wongwanich et al. (1990) redefined Pa Samed Formation as mostly siliciclastic with some grey argillaceous limestone and black carbonaceous shales. The Formation consists of 6 members (Wongwanich et al., 1990) but later has been simplified into 3 units (Department of Mineral Resources, 2018). The lower part (member 1 of Wongwanich et al., 1990) consists of black tentaculitic shale containing abundant dacryoconarids, *Nowakia* (*Turkestanella*) *acuaria acuaria* (Richter), *Striatostyliolina* sp. and *Viriatellina* sp. and suggested a Late Pragian to possibly earliest Emsian age (Boucot et al., 1999). Agematsu et al. (2006a) only recognized *Nowakia acuaria* and interpreted as Emsian. The middle part (members 2–4 of Wongwanich et al., 1990) comprises sandstone interbedded with shale exhibiting Bouma sequences. Its age is interpreted as Carboniferous, based on brachiopods and goniatites reported by Wongwanich et al. (2004), including *Aseptella satunensis* Brunton, *Tornquistia orthogona* Racheboeuf, *Colodium satuni* Boucot and Brunton, *Girtyella* sp., *Crurithyris* sp., *Reticularia* sp., *Plicambocoelia tansathieni* Boucot and Brunton, *Eileenella elegans* Racheboeuf, and goniatites such as *Stenopronorites* cf. *uralensis* (Karpinsky) and

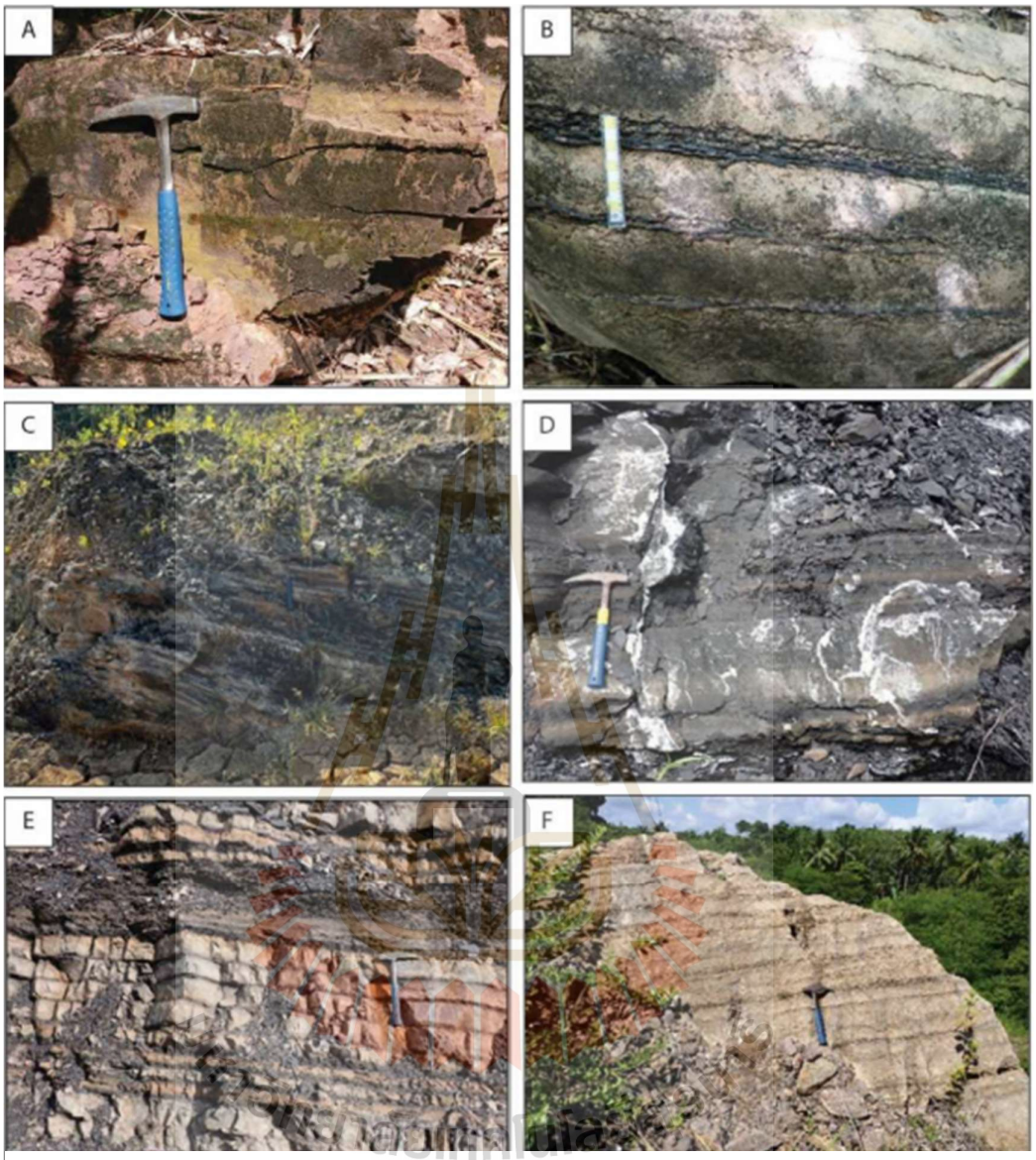

Figure 2.3 Kuan Tung Formation, A. Contact between Upper member and sandstone. B. Upper member. C. Middle member upper part. D. Middle member lower part. E. Lower member upper part. F. Lower member lower part. (Itsarapong et al., 2023).

Syngastrioceras sp. The upper part of the formation (member 5-6 of Wongwanich et al., 1990) consists of grey fine-grained sandstone intercalated by thinly laminated black shales. Therefore, Pa Samad Formation ranges from Early Devonian to Carboniferous.

There is disconformity between the Member 1 (Early Devonian) and Member 2 (Carboniferous), or this could represent a concealed fault (Wongwanich et al., 2004).

2.1.4 Kuan Klang Formation

Kuan Klang Formation is approximately 210 m thick scattered in Satun, characterized by grey, reddish brown to red mudstones and cross bedded sandstones and a 15 m thick dark grey chert at bottom part with cross cutting quartz veins, grey and reddish-brown shale with bivalve (*Posidonomya* sp.), brachiopods and fragments of trilobites. It is interbedded with sandstone, siltstone and chert beds. The ammonoids *Agathiceras* sp. and *Pronorites* sp., which concurrence with *Posidonomya* sp. in upper part suggests Pennsylvanian age with the founding of Tournaisian radiolarian fauna in 2.5 m thick chert located 65 m above its base (Saesaengseerung and Saiid, 2016) which similar to Kubang Pasu Formation of Malaysia suggests Mississippian age (Jasin, 2015). Therefore, this formation possibly ranges from Mississippian to Pennsylvanian (Carboniferous).

2.1.5 Kaeng Krachan Group

Kaeng Krachan Group has been defined by Chaodumrong et al. (2004, 2007) and established 5 formations. In Satun province, this Group exposed inconsistency around the islands and only 3 out of 5 were identified, Laem Mai Phai Formation, Khao Phra Formation, and Khao Chao Formation (Department of Mineral Resources, 2018). Laem Mai Phai Formation is exposed at Ko Bu Lon and its vicinity consists of thin bedded, black mudstone and laminated siltstone with some intercalated sandstone (Tiyapairat, 2004). Khao Phra Formation is characterized by interbedded shales and grey sandstones, well exposed in Adang-Rawi Islands. On mainland Satun, this formation exposed at Khuan Pho, near Satun City contains *Spinomartinia* sp. suggests Sakmarian age (Meesook, 2014). Lastly, Khao Chao Formation is mainly grey to light brown sandstone with some shales exposed on Ko Bitsi, Ko Ta Mui, Ko Lan Ja and north of Ko Adang. The age of this group is probably Early Permian.

2.1.6 Ratburi Group

Ratburi Group lies conformably on the Kaeng Krachan Group and is primarily composed of fossiliferous limestone, predominantly found in western Thailand. In Satun Province, it occurs in Khao Thanan, Ko Taban, and Ko Lidi, where Middle to Late Permian fusulinids have been identified.

2.1.7 Quaternary Sediments

Quaternary sediments cover all undulating terrains in Satun Province. This sequence consists of loose sediments, including clay, silt, sand, and gravel. These sediments can be divided into 11 main units: colluvial, alluvial, mangrove and beach deposits, former beach ridges and dunes, deltaic flood plain, abandoned channels, flood plain, high terrace, low terrace, accretionary plain, and tidal delta and bar deposits (Department of Mineral Resources, 2013).

2.1.8 Igneous Rock

Igneous rocks in Satun Province are predominantly granite, which intruded into Paleozoic rock sequences in Triassic. The granites are exposed in the northern and eastern parts of Khuan Kalong District, extending to the east of Khuan Don District. On the islands, granites are visible at Ko Adang, Ko Lipe, and others. These granites commonly consist of biotite granite, biotite-muscovite granite, aplite, and pegmatite, with fine- to coarse-grained porphyritic textures and feldspar phenocrysts (Department of Mineral Resources, 2013).

2.2 Paleoenvironment of Satun Province

Satun Province offers a detailed record of Paleozoic environmental changes, spanning from Late Cambrian to Permian, based on extensive research. The Department of Mineral Resources (2018) summarized these findings from the accumulated works of many researchers. The deposition of the Tarutao Group during the Upper Cambrian to Lower Tremadoc shows a sandy, barrier-beach complex in shallow tropical seas. During the Lower Ordovician of the Thung Song Group, sedimentation occurred on a homoclinal ramp in predominantly very shallow tropical

sea, characterized by tidal flats, which transitioned to slightly deeper subtidal environments in the Middle Ordovician. By the Late Ordovician of the Thung Song Group, sedimentation took place in deep (approximately 200 meters) and cool (around 15°C) tropical sea, indicated by the presence of large-eyed trilobites, cool-water conodonts, and specific isotopic signatures. These deep-water or deep subtidal conditions persisted through much of the Silurian and Devonian of the Thong Pha Phum Group and likely extended into the Carboniferous. This inference is supported by the brachiopod communities, trilobites with reduced eyes (such as *Plagiolaria* sp.), and the pelagic faunas of graptolites, ammonoids, and radiolarians. The Late Carboniferous to Permian of Satun is correlated to the sediments of Phuket, Krabi, and Langkawi, where there is abundant evidence of deposition near or under glaciers.

2.3 Ostracod

2.3.1 Overview

Ostracods are small, bivalve crustaceans, typically microscopic in size. Most adult ostracods range from 0.5 to 2 mm in length, though certain freshwater species can grow as large as 8 mm. The pelagic marine species *Gigantocypris*, a member of the Myodocopida order, can reach an impressive 32 mm in size (Horne, 2005). Ostracods can be documented as far back as the Early Ordovician (Siveter, 2008; Williams et al., 2008). Renowned for their adaptability, survival, demonstrate vulnerability to environmental factors such as temperature, salinity, substrate, hydrodynamics, and oxygen levels (Jones, 2010; Maillet et al., 2013; Racheboeuf et al., 2012; Song et al., 2019). Despite these sensitivities, ostracods have displayed an impressive capacity for adaptation, facilitating their widespread distribution across ecosystems worldwide. Therefore, the more discoveries of fossil ostracods, the more applications on paleoenvironmental interpretation and paleogeographic reconstructions can be carried out (e.g., Maillet et al., 2016; Meidla et al., 2013; Olempska et al., 2015; Perrier and Siveter, 2013; Schallreuter et al., 1996; Song et al., 2022).

2.3.2 Morphology of ostracod

The ostracod carapace (Figure 2.4) is made up of two valves that encase its body and limbs. It consists of two layers: a rigid outer calcified layer and a soft epidermis layer. During their lifetime, the ostracod's hard layer is covered with a chitinous layer, while the epidermis is enclosed in chitin. The hard layer consists of an inner lamella and an outer lamella. The outer surface of the carapace is mostly made up of the outer lamella, which is calcified and usually remains as a fossil.

The outer lamella covers the carapace's surface and curves inward at the ventral margin to form the inner lamella, which is only the calcified part in that area. The dorsal side is where the two sides of the outer lamella join (interlock) to form a hinge, welded by a thin strip of soft tissue called the ligament. The right and left valves are usually difference in size and have an overlap but in some groups like Myodocopid the valves usually have the same size or very similar in size. The hinges are composed

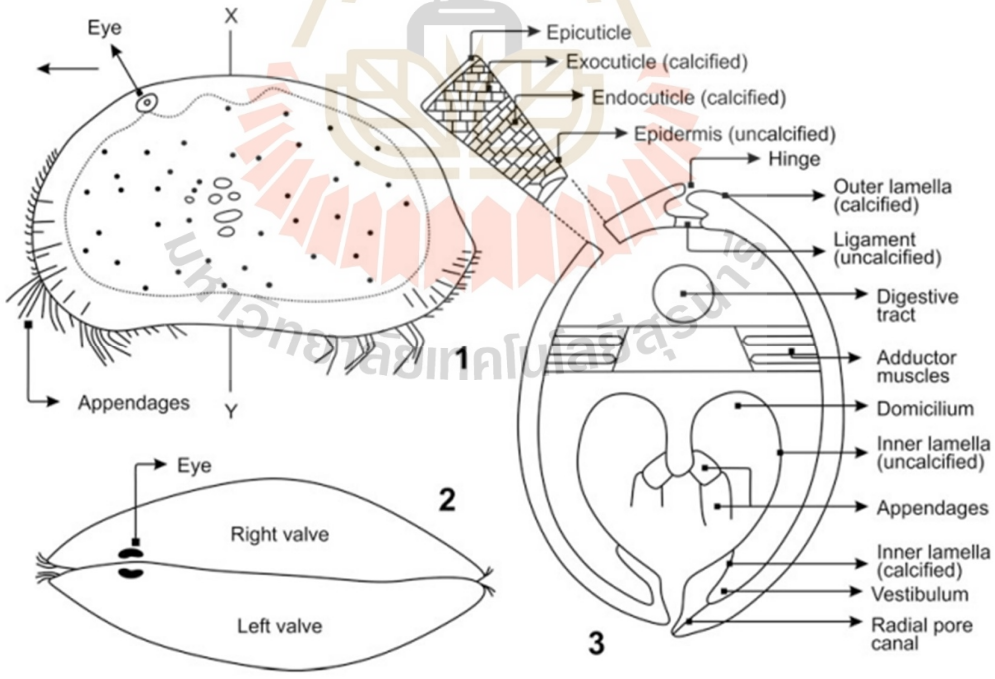

Figure 2.4 Morphology of ostracod carapace (Jain, 2020).

of sockets, bars, grooves, and teeth, whose shapes (Figure 2.5) and arrangements vary and serve as useful tools for identifying ostracods.

The ostracod body is short and laterally compressed, showing no trace of segmentation, with only a slight constriction to distinguish the boundary between the head and thorax. Ostracods have four pairs of appendages: antennae, mandibles, and maxillae, along with one to three pairs of thorax legs and a furca (Figure 2.5).

Antennules function as a locomotor organ (swimming, digging, climbing) or sensory organ or balancing organs.

Antennae also serve as a locomotor organ.

Mandibles function as a tool for feeding (digging, holding, cutting).

Maxillae functions as a support organ for the mandibles to move food into their mouths.

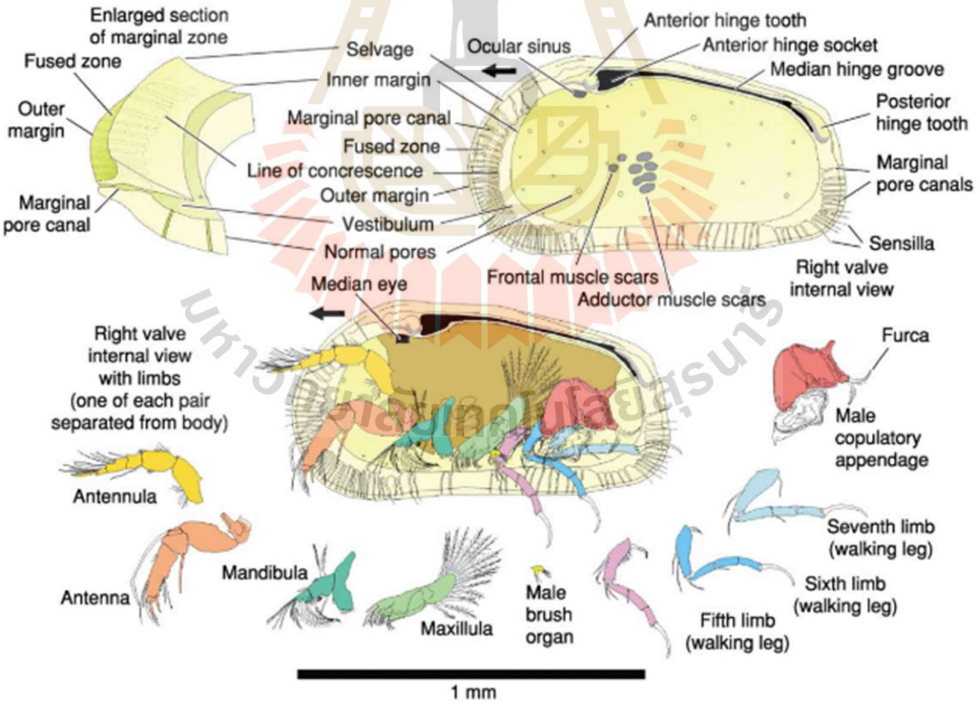

Figure 2.5 Internal valve morphology and limps of a cytheroidean podocopids (Horne, 2005).

Thorax legs develop differently in each group, some groups have developed the legs to function as additional maxillae or to aid the respiration and some groups can develop multiple pairs of thorax legs.

Furcae is probably used as locomotor organs.

Other than internal organs like the heart, digestive organs or genital organs, ostracods have adductor muscles attached to both valves functions to close or open the carapace which leave a scar at both valves (Figure 2.5) that are preserved in a fossil.

2.3.3 Classification criteria of ostracod fossil

The classification of living ostracods is based on carapace morphology, soft part morphology, and DNA analyses. However, since fossilized ostracods rarely preserve soft tissues, their identification relies solely on carapace morphology. Key diagnostic features include carapace shape (e.g., ovate, elongate, spherical, rectangular), valve symmetry, and hinge characteristics, which help distinguish major ostracod groups. Surface ornamentation, such as smooth, pitted, ridged, or spined textures (Figure 2.6), can further refine identification down to the genus or species level.

Dimorphism is common in ostracods, with differences in size, shape, and sculpture observed between males and females or juveniles and adults of the same species. Sexual dimorphism is often linked to reproductive adaptations, where females may have a swollen posterior region to accommodate eggs or a brood pouch, while males are typically smaller. Ontogenetic differences (juvenile vs. adult) are generally limited to size in smooth-shelled species, but many groups exhibit distinct changes in sculpture due to incomplete development in juvenile stages compared to adults.

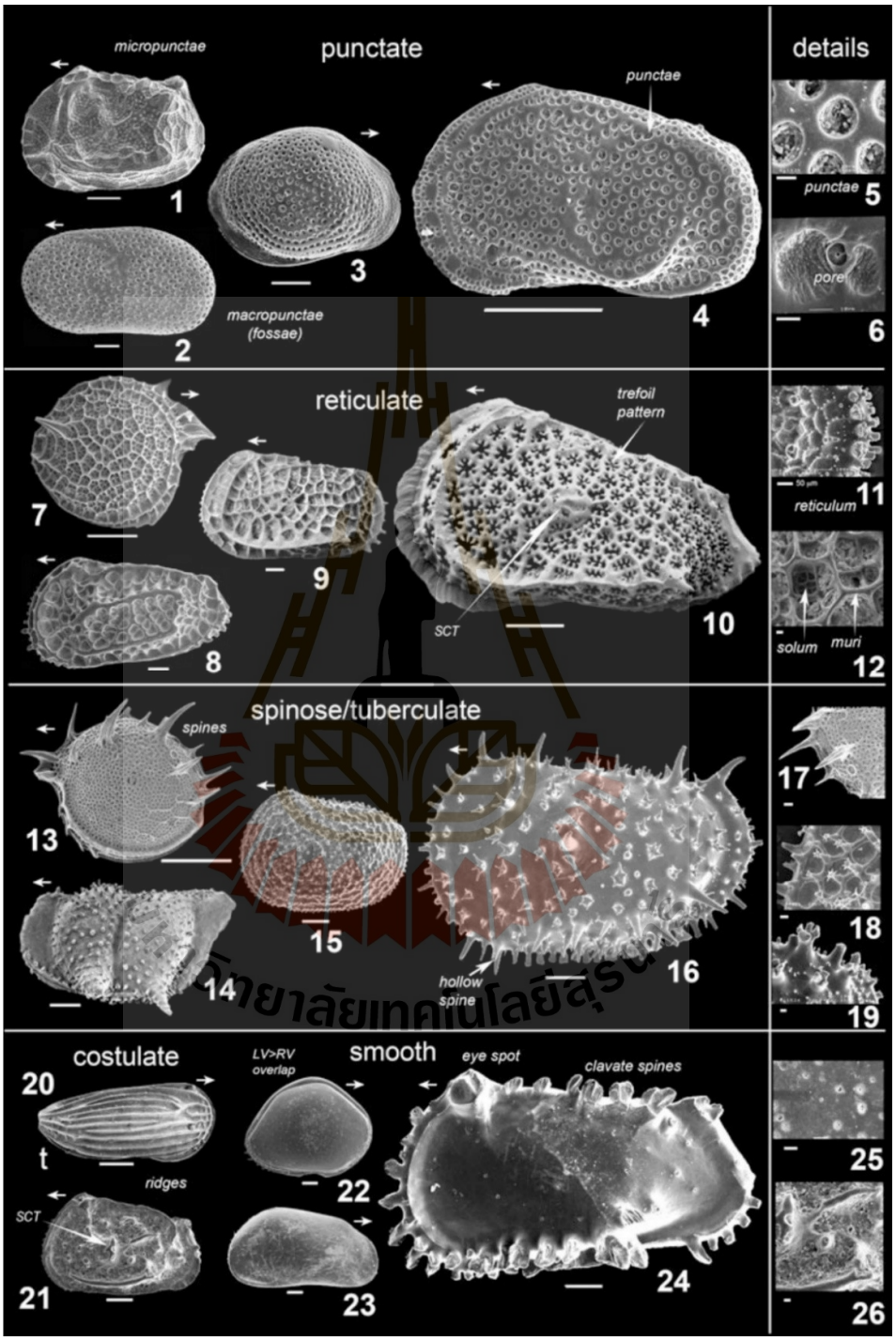

Figure 2.6 Example of ostracod sculptures (Rodriguez-Lazaro and Ruiz-Munoz, 2012).

2.3.4 Study of Silurian-Devonian ostracod in Thailand

Studies on Silurian–Devonian ostracods in Thailand are limited, with only the recent work on the Kuan Tung Formation providing new data (Promduang and Chitnarin, 2025). Most previous research has focused on Upper Paleozoic ostracods, particularly in central Thailand (e.g., Chitnarin and Ketwetsuriya, 2021; Chitnarin et al., 2008, 2017), while Dill et al. (2004) reported late Paleozoic ostracods from Surat Thani Province.

In Southeast Asia, Silurian–Devonian ostracod study is similarly scarce, with notable studies from Vietnam documenting Late Silurian ostracods from the estuarine deposits of the Si Ka Formation, suggesting early estuarine colonization by ostracods (McGairy et al., 2021; Williams et al., 2023).

2.4 Ecology of Silurian-Devonian marine ostracod

2.4.1 Overview of ostracod ecology

Ostracods are predominantly having benthic mode of life with only known pelagic ostracods belonging to Myodocopida (Horne, 2005). The earliest known ostracod dates back to the Early Ordovician period (e.g., Salas et al., 2007; William et al., 2008), probably have benthic lifestyle, dominated by Palaeocopida which included some Podocopida, Platycopida and Leperditicopida having restricted to shelf area and show sign of the assemblage that related to depth (Horne, 2003), also Leperditicopida and leperditelloidean palaeocopids dominated marginal marine tidal flat environment in Ordovician (Williams and Siveter, 1996). In Silurian, most ostracods have benthic lifestyle living mostly on relatively shallow shelves and shelf slopes as a crawler, swimmer or burrower (Perrier and Siveter, 2013). But in Middle Silurian, Myodocopida which may originated in Late Ordovician and been benthic at that time ventured into pelagic niche (Siveter et al., 1991), and by the Late Silurian, ostracods (Palaeocopida and Leperditicopida) began colonizing brackish waters (Horne, 2003; McGairy et al., 2021). During the Carboniferous period, otracods extended their range to include terrestrial aquatic systems (Bennett et al., 2012; Iglikowska, 2014). Today, ostracods are

a highly diverse group, occupying a wide variety of aquatic habitats, from deep-sea bathyal-abyssal regions (Yasuhara et al., 2008; Brandão et al., 2019) to temporary ponds (Ottonello and Romano, 2011).

2.4.2 Ecology of Devonian ostracod

In the Devonian period, three ecotypes of marine ostracods were recognized (Bandel and Becker, 1975). The ecotypes were later revised and reclassified under the term "Mega-Assemblages" (Casier et al., 1995; Casier, 2004, 2017). The Three Mega-Assemblages include Eifelian, Thuringian, and Myodocopid Mega-Assemblages (Figure 2.7).

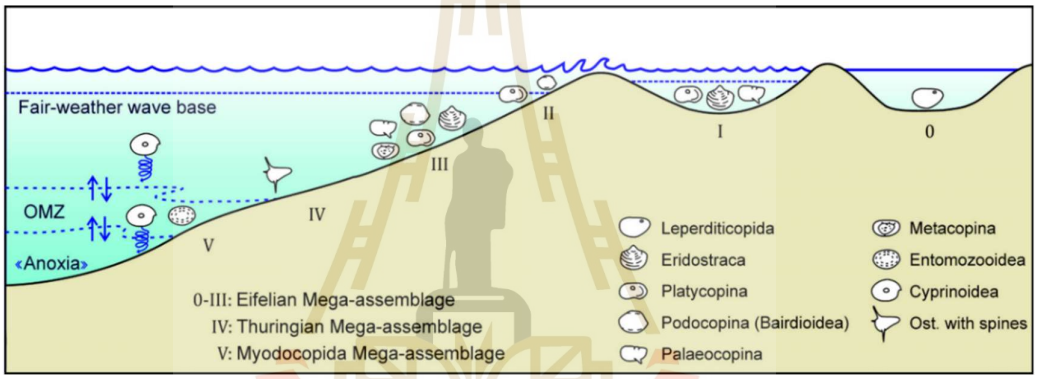

Figure 2.7 Three ostracod mega-assemblages (Crasquin and Horne, 2018).

2.4.2.1 The Eifelian Mega-Assemblages

Comprised 4 assemblages 0-IV

The Assemblage 0: This assemblage, composed solely of large Leperditicopida ostracods, is an indicator of lagoonal environments.

The Assemblage I: This assemblage is characterized by low species diversity, often with a high abundance of specimens, and interprets as a semi-restricted water environment. The species within this assemblage primarily include euryhaline Platycopida, along with Metacopida, Palaeocopida, and Eridostracina. In conditions where salinity nears normal marine levels, some Podocopida may also be present. Additionally, this assemblage may display stacked ostracod valves or a cup-in-cup

structure (Figure 2.8), formed by wavelet induced processes, a phenomenon typically occurs in very shallow, but continuously agitated waters (Boomer et al., 2001).

Figure 2.8 Stacked valves or cup in cup structure of ostracods (Casier, 2007).

The Assemblage II: This assemblage is characterized by a moderately diverse ostracod, predominantly consisting of large, thick-shelled Podocopida and Platycopida. Notably, juvenile ostracods are usually absent, and carapaces are often found fragmented. Assemblage II indicates a very shallow, open-marine environment with constant agitation, situated above the fair-weather wave base. Occasionally, oolites are found accreting around ostracods.

The Assemblage III: This assemblage is characterized by a diverse range of ostracods, including most orders such as Podocopida, Metacopida, Palaeocopida, Platycopida, and Eridostracina. It typically represents environments found below the fair-weather wave base, and sometimes even below the storm-wave base. In Assemblage III, the ratio between Metacopida and Podocopida shifts with increasing water depth: Podocopida shows a decline in both diversity and abundance, while Metacopida become more dominant. As a result, the ratio of Metacopida to Podocopida may be used as an indicator of water depth.

2.4.2.2 The Thuringian Mega-Assemblage

The Assemblage IV: This assemblage consists mainly of thin-shelled, spiny ostracods, mostly from the Podocopid group, with some representation from Metacopids and Palaeocopids. These ostracods are typically found in very calm, possibly colder marine settings, below the storm-wave base. Their fragile shells likely

evolved as an adaptation to such stable conditions. Notably, these ostracods are cosmopolitan and, unlike those in other groups, appear to have experienced slower evolutionary changes during the Palaeozoic. In particularly deep, tranquil waters, some Metacopida species also develop spines on their carapaces.

2.4.2.3 The Myodocopid Mega-Assemblage

The Assemblage V: This assemblage is defined by the presence of Entomozoidea or Cyprinoidea of Myodocopida, which represents the low-oxygen marine environments. Cypridinids were active swimmers, as shown by their large anterior rostrum that allowed swimming limbs to extend. They are typically preserved in oxygen-poor settings, often found with their valves separated but still close together, resembling a butterfly shape (Figure 2.9). Entomozoidea, known for their fingerprint-like shell patterns, hold significant biostratigraphic importance, though their exact lifestyle remains uncertain and debated.

Figure 2.9 Butterfly position of *Palaeophilomedes neuvillensis* Casier, 1988 in Casier (2017).

2.5 Conodont

2.5.1 Overview

Conodonts were jawless, eel-like marine vertebrates (Briggs, 1992; Sansom et al., 1992; Donoghue et al., 2000; Rasmussen and Stouge, 2018). Based on the presence of a tail fin and well-developed eyes, conodonts are thought to have had a pelagic or nektobenthic lifestyle, likely residing in the photic zone (Sweet, 1988; Rigo and Joachimski, 2010; Rasmussen and Stouge, 2018). The fossil record dates back to the Cambrian period, with extinction occurring in the Late Triassic.

Conodonts are commonly discovered as mineralized, tooth-like elements that function as a feeding apparatus within the oral cavity. These conodont elements are composed of phosphatic bioapatite, a material highly resistant to diagenesis, preserving chemical signatures that reflect their original biological composition. Consequently, chemical analyses of these elements provide valuable insights into ocean geodynamics and past climates.

Conodonts have been extensively used in the biostratigraphy of Paleozoic marine carbonates and have played a vital role in paleoecological and biogeographical studies (Sweet and Donoghue, 2001). Despite uncertainties about their ecology and feeding habits, conodont elements are invaluable for biostratigraphy, as their first appearance datum (FAD) and last appearance datum (LAD) help define specific chronological ranges. Their broad geographic distribution, rapid evolutionary changes, and morphological diversity make them essential tools for precisely correlating rock layers across different regions.

2.5.2 Conodont element morphology

Conodont elements are primarily categorized based on their shapes and presumed functions within the conodont feeding apparatus. The main morphological types include:

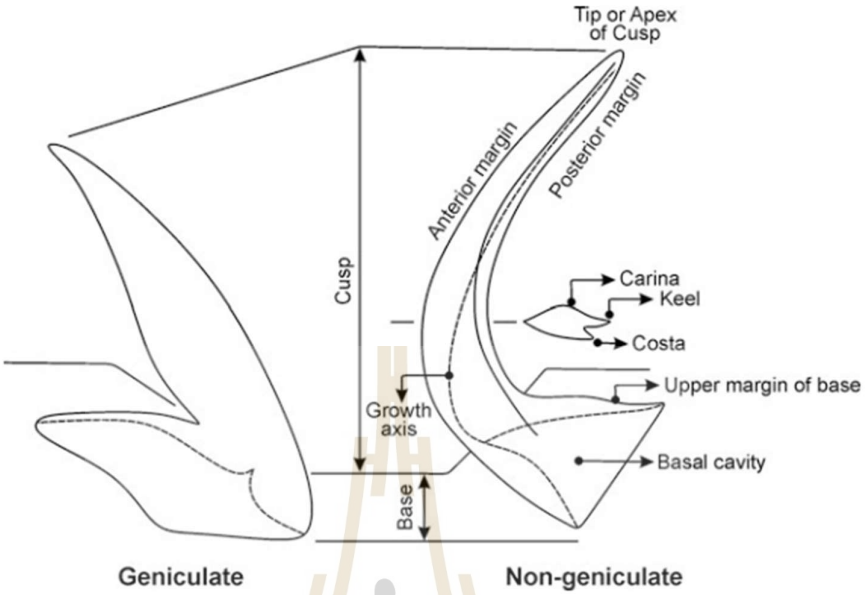

Figure 2.10 Coniform element terminology (Jain, 2020).

Coniform (Cone-shaped): Simple, conical elements resembling single teeth, which can be subdivide into Geniculate and Non-geniculate (Figure 2.10).

Ramiform (Bar-shaped): Elongate, sometimes branched structures that may have multiple cusps or denticles, subdivided into Alate, Digyrate, Quadriramate, Dolabrate, Bipennate Tertiopedate (Figure 2.11).

Pectiniform (Blade, Platform-shaped): Flattened, plate-like elements often bear a series of denticles along one edge, subdivided into Stellate, Pastinate, Angulate, Segminate, Carminate (Figure 2.12).

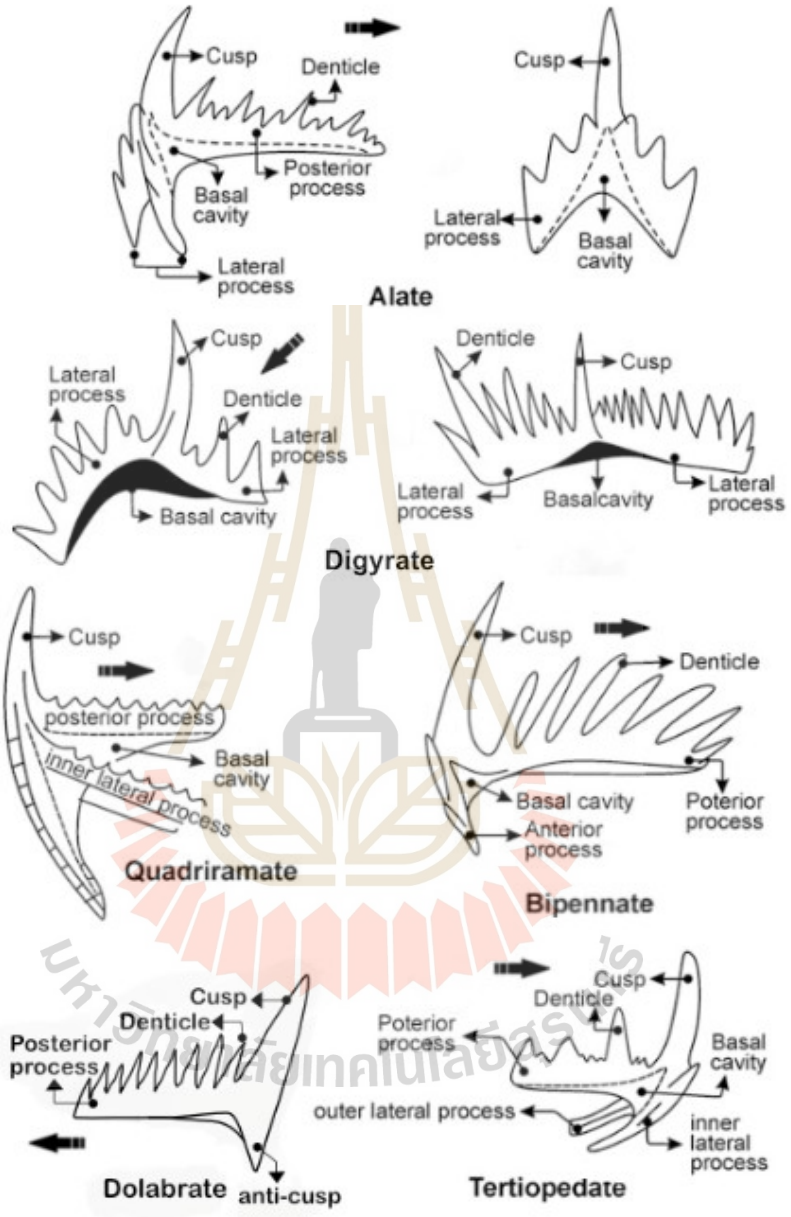

Figure 2.11 Ramiform element: Alate, Digyrate, Quadriramate, Dolabrate, Bipennate, Tertiopedate (Jain, 2020).

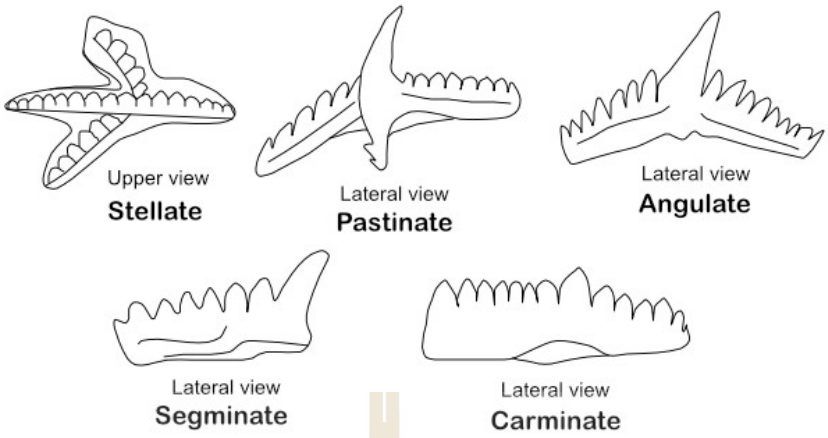

Figure 2.12 Pectiniform element: Stellate, Pastinate, Angulate, Segminate, Carminate (Jain, 2020).

The conodont feeding apparatus is bilaterally symmetrical and consists of distinct elements arranged in the head region. Each species possessed a specific set of elements, divided into an anterior region with M and S elements (Sa, Sb, Sc, and Sd) and a posterior region with P elements (Pa and Pb) (Sweet, 1988; Purnell et al., 2000). Purnell et al. (2000) later refined the classification system, defining element positions based on spatial relationships and body axes, as observed in bedding plane assemblages (Figure 2.13). This led to a standardized nomenclature where elements are labeled with letters and numeric (e.g., P1, P2, S0–S4, M), with S elements numbered outward from S0.

2.5.3 Silurian-Devonian conodonts in Thailand

The Silurian-Devonian boundary has long been a subject of detailed stratigraphic investigation, with conodonts playing a crucial role in refining biozonation schemes (Hušková and Slavík, 2020). The FAD of *Caudicriodus hesperius* serves as a key marker for the base of the Devonian, while taxa such as *Ozarkodina confluens* (Branson and Mehl, 1933), *Zieglerodina remscheidensis* (Ziegler, 1960), and *Caudicriodus woschmidti* (Ziegler, 1960) help further constrain the boundary. Recent taxonomic revisions have shown that many late Silurian–Early Devonian conodont genera, previously classified in broad “waste-basket” categories (such as Genus *Ozarkodina* which has been subdivided into *Ozarkodina*, *Zieglerodina*, and *Wurmiella*),

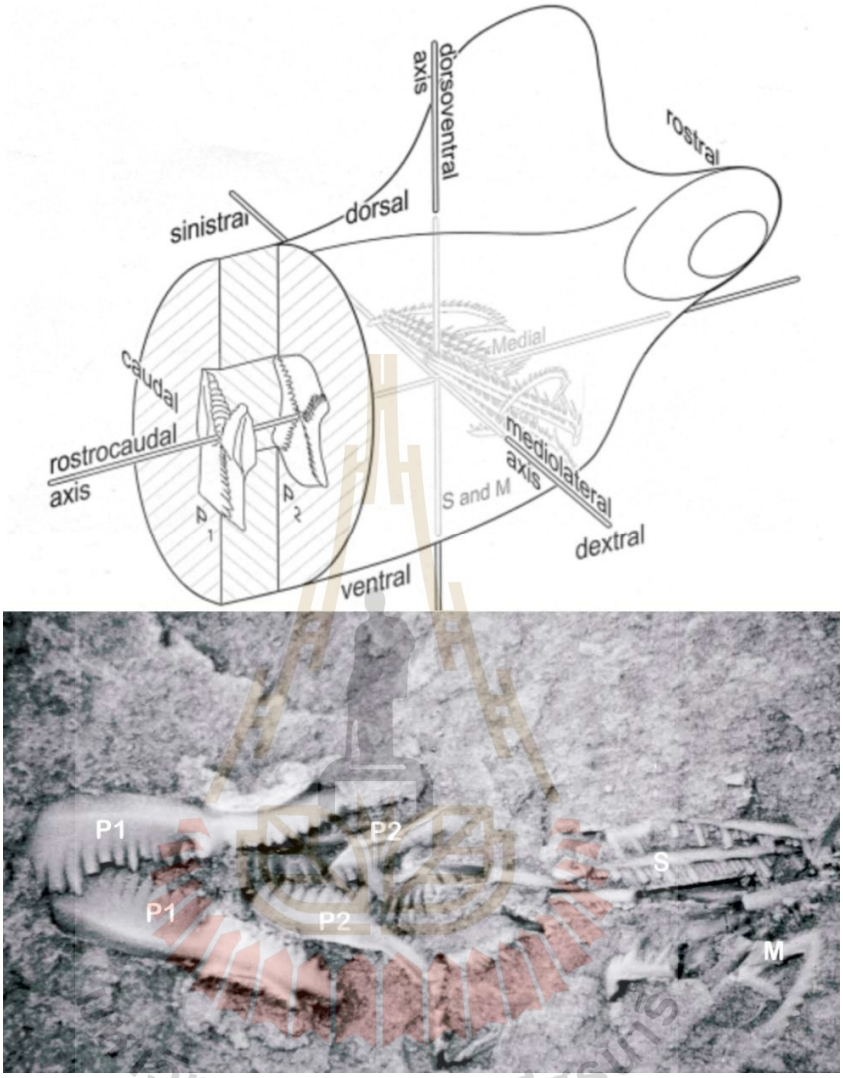

Figure 2.13 The orientation and notation of the Ozarkodinid apparatus drawing (Top) from Purnell et al. (2000) and conodont apparatus in natural assemblage (Bottom) *Idiognathodus* from Sweet and Donoghue (2001).

require re-evaluation to resolve species-level identifications (Ferretti et al., 2022). This refinement is essential for improving the accuracy of conodont-based correlations and biozonation.

In Thailand, studies on the Silurian-Devonian boundary remain limited, partly due to the scarcity of well-preserved boundary strata. Hagen and Kemper (1976)

reported Late Silurian conodonts from the Thong Pha Phum area, Kanchanaburi Province, western Thailand, but did not specify the taxa. A study of specimens from a limestone unit by Long and Burrett (1989) marking the boundary between the middle and upper sections of the Kuan Tung Formation of Wongwanich et al. (1990), identified *Pandorinellina steinhornensis steinhornensis*, *Polygnathus lahiosus mawsonae* Long and Burrett, 1989 (later considered synonymous with *Polygnathus bultyncki* Weddige, 1977 by Klapper and Vodrážková, 2013), and *Pseudooneotodus kuangtungensis* Long and Burrett, 1989, indicating an Emsian age. More recently, a conodont assemblage including *Zieglerodina remscheidensis* s.l., *Belodella resima* (Philip, 1965), and *Decoriconus fragilis* (Branson and Mehl, 1933), co-occurring with plate loboliths of scyphocrinitid crinoids, was documented from the Ban Tha Kradan area, Kanchanaburi. This assemblage suggests an age ranging from the late Ludlow (Silurian) to early Lochkovian (Devonian) (Burrett et al., 2024).

2.6 Tentaculitoid

2.6.1 Overview

These organisms (Figure 2.14) often referred to by many researchers as Tentaculites (which can lead to confusion with the genus *Tentaculites*), are enigmatic

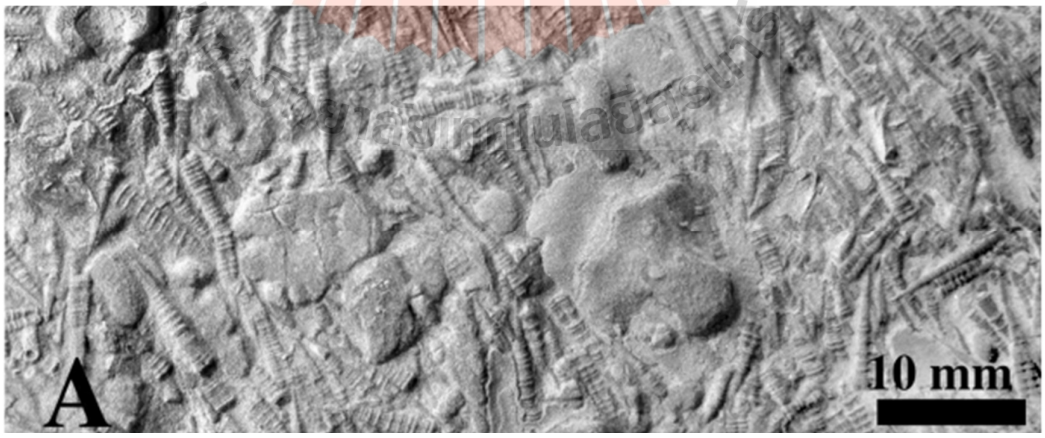

Figure 2.14 *Tentaculites gyracanthus* of Lower Devonian, Manlius Formation, New York State, USA (Cornell et al., 2003).

marine invertebrates with an unresolved taxonomic position. These organisms first appeared in the fossil record during the Ordovician period, underwent significant diversification in the Silurian, and became extinct by the Late Devonian. Despite their widespread fossil records, their biological affinities remain uncertain, and their classification continues to be debated among paleontologists.

Two main theories exist regarding their classification (Wei et al., 2012). The first suggests that tentaculitoids, due to their similarities in shell morphology such as wall structure, septal neck, and siphuncular cord belong to an independent class within Mollusca (e.g., Bouček, 1964; Farsan, 1994). The second theory suggests a closer relationship between tentaculitoids and microconchids, based on shared characteristics like wall microstructure, including microlamellar layers, cross-bladed fabric, and pseudopuncta (Vinn et al., 2008; Vinn, 2010), or an affinity with lophophorates (Larsson, 1979).

The fossil remains of tentaculitoids are small, ringed, conical-shaped shells found in various marine deposits. Their distribution across the seafloor provides valuable insights into paleocurrents (Hladil et al., 1991, 2014; Gügel et al., 2017). Although the origin and affinity of tentaculitoids remain uncertain, their ecological roles are still debated. Overall, thick-walled tentaculitoids are widely thought to have had a benthic lifestyle in shallower waters and are commonly associated with siliciclastic rocks. In contrast, small and thin-walled tentaculitoids were likely planktonic or nektoplanktonic and are more frequently found in deeper sedimentary deposits (Schindler, 2012). Additionally, their broad distribution, short stratigraphic range, and rapid evolutionary rate make tentaculitoids valuable tools in global biostratigraphy (for a comprehensive overview, see Becker et al., 2020).

2.6.2 Classification criteria of Tentaculitoid shell

Tentaculitoids are predominantly discovered as shells embedded in rock, making shell morphology the primary criterion for classification. While some researchers have reported organic remains of Tentaculitoids through palynological studies (e.g., Wood et al., 2004; Jarzynka and Filipiak, 2009; Marshall and Telnova,

2012), these specimens are often extracted in a folded or distorted state, making it difficult to accurately discern shell morphology. Consequently, the characteristics of a solid-calcareous shell continue to provide a more reliable basis for classification.

The shell, or conch, of Tentaculitoids is generally straight, ringed, and conical in shape, with an initial chamber that is often used to determine their order. The overall shell shape (e.g. length, width, growth angle), along with the pattern and shape of transverse rings and/or longitudinal ribs (e.g. number of rings, interspace between rings), serves as key features for identifying specimens at the genus and species levels (Figure 2.15). Order Tentaculitida generally has large, thick-walled, ringed, layered shell with narrow apex and mostly represent by genus *Tentaculites.* Order Dacryoconarida has a small, ringed or without ringed, thin shell, bulbous or tear-shaped initial chamber have commonly known group Nowakiidae. Order Homoctenida has

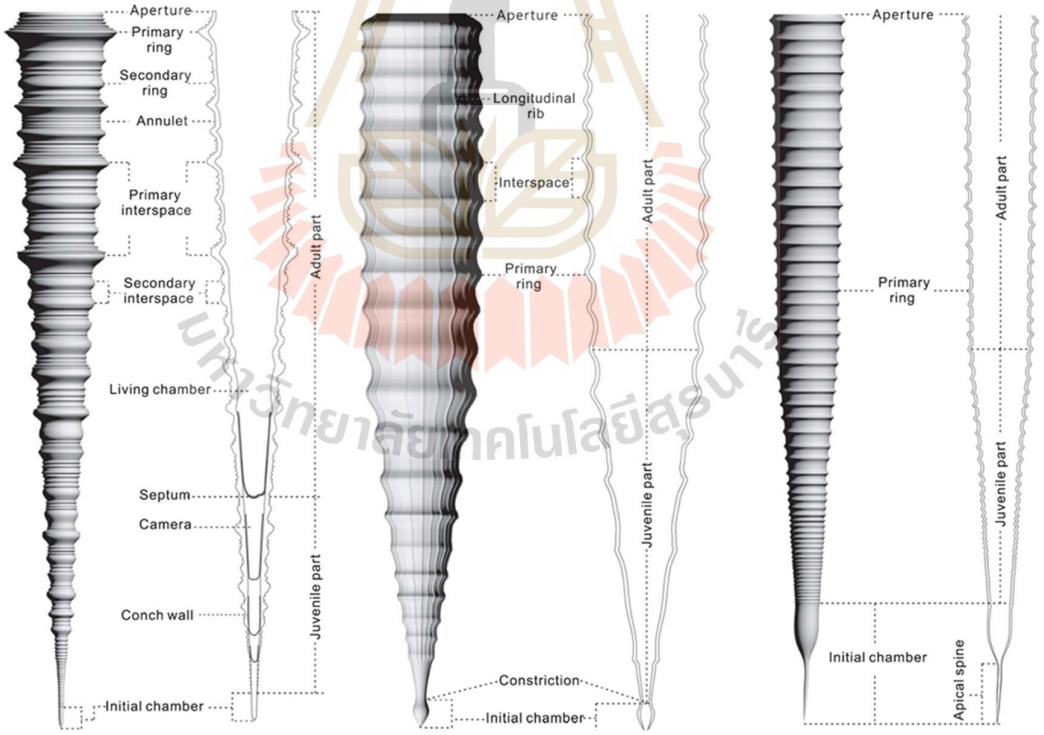

Figure 2.15 Morphology of Tentaculitoids shell, represents left: Tentaculitida (*Tentaculites*); middle: Dacryoconarida (*Nowakia*); right: Homoctenida (*Homoctenus*) from Wei (2019).

small, ringed, thin-shelled, and apical spine in initial chamber and represent by genus *Homoctenus*.

2.6.3 Tentaculitoids in Thailand

One of the earliest reports on tentaculitoids in Thailand was by Pitakpaivan et al. (1969), who identified *Tentaculites elegans* (Barrande, 1852) and *Styliolina clavula* in Silurian sandy shale underlying Permian limestone in Si Sawat District, Kanchanaburi Province. Later, Hahn and Siebenhüner (1982) documented fossil assemblages included dacryoconarids, *Nowakia holynensis* Bouček, 1964, *N. sulcata* (Roemer, 1843), *Styliolina* sp., and *Homoctenus hanusi* (Bouček, 1964), from Thong Pha Phum area, with an age range extending from the Ordovician to the Carboniferous. In the 1990s, Dr. Ruan Yi-Ping examined dacryoconarid samples from the Pa Samed Formation (Wongwanich et al., 1990), identifying *Nowakia acuaria*, *N.* cf. *matlockiensis* (Chapman, 1904), *N.* cf. *hercyniana* Alberti, *N.* sp. 1, *Styliolina* sp., *Striatostyliolina* sp., and *Viriatellina* sp., dating from the late Pragian to earliest Emsian (Boucot et al., 1999). Agematsu et al. (2006a) also reported *Nowakia acuaria* from the Pa Samed Formation and documented its presence in Lower Devonian (Emsian) black shale in Satun Province. More recently, Maneerat (2021) identified a diverse tentaculitoid assemblage from the Silurian-Devonian sedimentary rocks of the Thong Pha Phum Group in Ban Tha Kradan, Si Sawat District. The recorded species include *Nowakia acuaria*, *N.* (*Cepanowakia*) *pumilio* Alberti, *Styliolina fissurella* (Hall, 1843), *S. clavulus* Fisher, 1962, *S.* sp. A, *Homoctenus tikhyi* Ljashenko, 1959, and *H. arctus* Li, 1995, suggesting Early Devonian to Late Devonian. Additionally, associated graptolites bearing bed (*Monograptus* sp. and *Diplograptus* sp.) suggesting Silurian? to the Early Devonian.

CHAPTER III

RESEARCH METHODOLOGY

This chapter outlines the research methodology, encompassing field investigation and sample collection, laboratory work, data analysis and interpretation, and thesis writing and presentation. Fieldwork and sample collection were conducted at the quarry in Ban Thung Samed, Satun Province. Laboratory work involved the extraction of ostracods and conodonts, the preparation of samples for tentaculitoid identification, and thin section analysis. Data analysis and interpretation are described in Section 3.3, while thesis writing and presentation are covered in Section 3.4.

3.1 Field investigation and sample collection

The study section is referred to as Ban Thung Samed section, is named after Ban Thung Samed village. It is located in an abandoned quarry at coordinates 6°58’05"N, 99°46’04"E, on the western side of Highway No. 416, near the 88-kilometer marker, in Ban Thung Samed village, La-Ngu District, Satun Province. It is located about 4 kilometers northwest of La-Ngu Hospital (Figure 3.1).

In total, 21 rock samples were gathered from the study section (see Figure 3.2 for sampling locations). Among these, 12 samples (designated 19KT01-12) were extracted from limestone layers, each weighing around 500 grams. These samples were treated following the hot-acetolysis method (Crasquin-Soleau et al., 2005) for ostracod analysis. Additionally, 8 rock samples extracted from limestone layers (U1L, U1M, U1U, U2L, U2U, U3L, U3M, and U3U) provided by Mr. Jirasak Charoenmit from the Department of Mineral Resources and each weighing about 3 kg, were treated with 10-15% acetic acid (Green, 2001) to extract conodonts. From these conodont samples,

eight limestone samples (U1L-U3U) were selected for thin section analysis, and one dark calcareous shale sample, located near a tentaculitoid-rich bed (19KT12), was collected for the study of tentaculitoids.

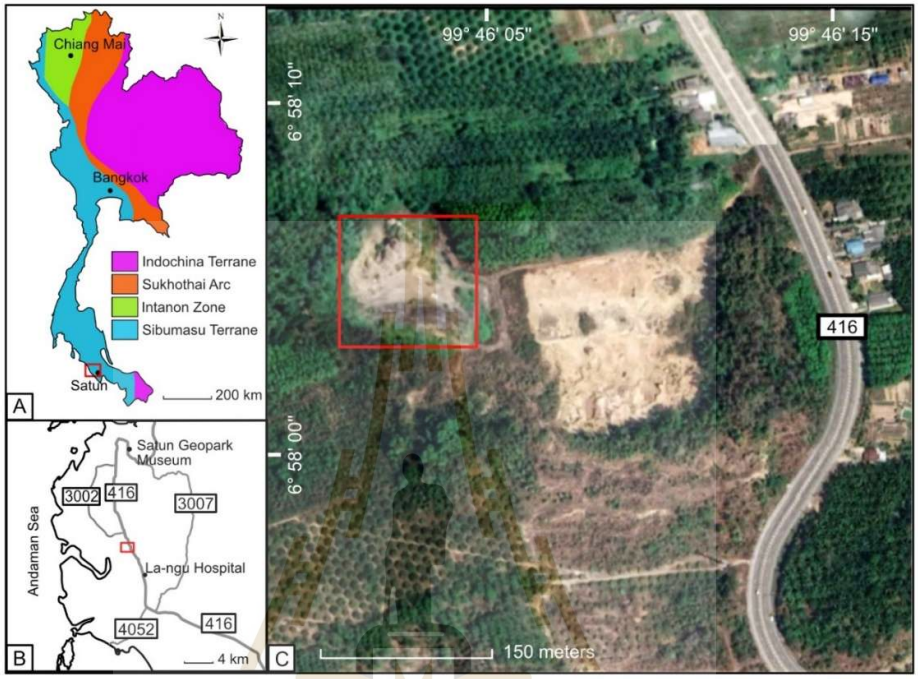

Figure 3.1 Location of the study section.

3.2 Laboratory works

3.2.1 Ostracod preparation

The limestone samples were treated using the hot acetolysis technique, which is suitable for rocks with high carbonate content. Each 500-gram sample was crushed and washed to remove any residue particles. The samples were placed in a glass jar on a hot sand bath at 60-100°C to dehydrate for 48-72 hours, ensuring they were completely dry. Once dried, the samples were covered with 99.99% acetic acid (CH_3COOH) and placed back on the hot sand bath, maintaining a temperature at 60°C. The jar was covered with a lid, leaving a small hole to vent the vaporized acid, and these procedures were performed within an extractor hood. After sufficient residue had formed, typically within 24 hours to several weeks, the residues were sieved using

a series of 0.1, 0.5, and 2.0-mm mesh sieves and then washed, repeated the process to obtain 2 sets of each sample. Once dried, the residue was hand-picked under a stereomicroscope and photographed using a JEOL Neoscope JCM-5000 Scanning Electron Microscope (SEM) housed in Facility Building 10 at Suranaree University of Technology.

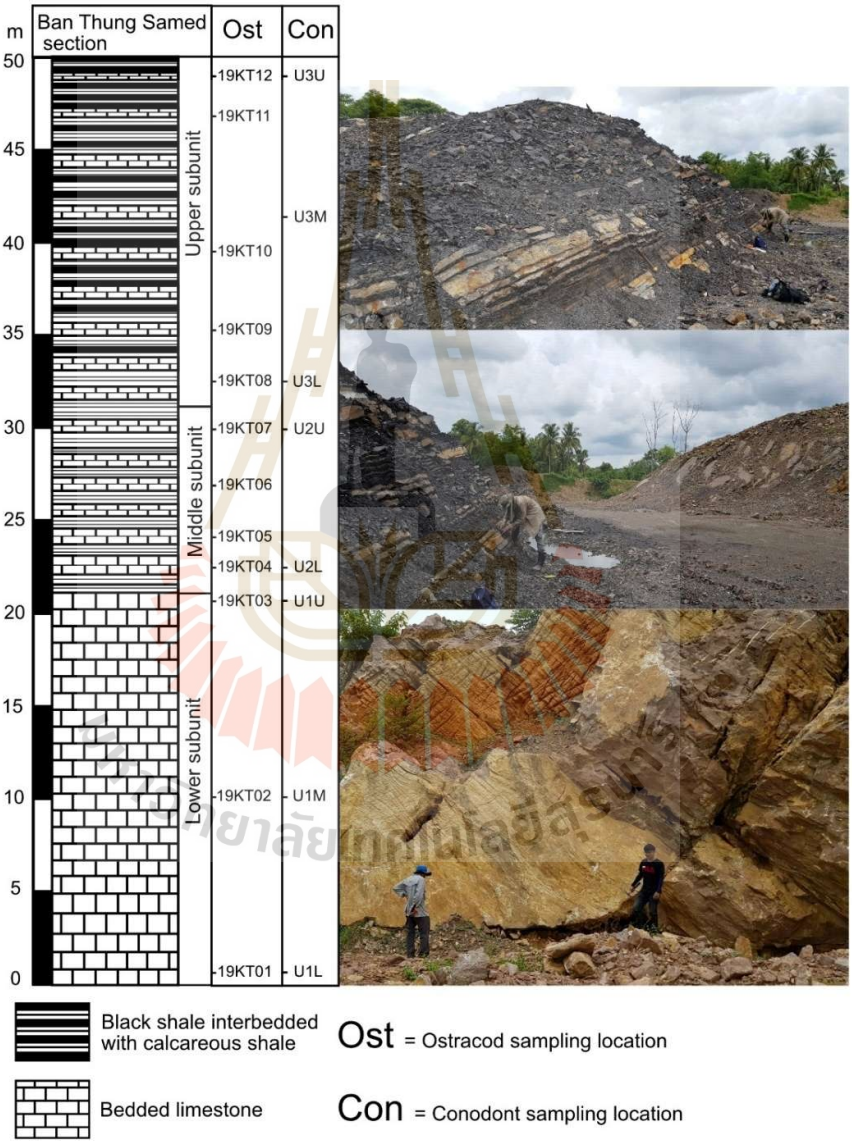

Figure 3.2 Lithostratigraphy of the Ban Thung Samed section, with sampling locations and the outcrop shown on the right.

3.2.2 Conodont preparation

The limestone samples were processed following the method of Green (2001), with modifications. According to Jeppsson et al. (1985), mixing the acid solution with a buffer acid enhances the recovery rate while minimizing sample damage. Green (2001) used a mixture of 10% acetic acid (CH_3COOH) with either sodium acetate (CH_3COONa) or calcium acetate [$(CH_3COO)_2Ca$] in a 100 mL/3–4 mg ratio. The rock samples were submerged in the acid solution, washed, and the residue was collected, with the acid being replaced every eight hours. This process continued for several weeks to obtain a sufficient amount of residue or until the rock samples completely disintegrated.

Due to limitations in equipment, space, and laboratory time, modifications were made to this study. Initially, the limestone samples were broken into 2–3 cm fragments and thoroughly washed to remove any contaminants. They were then placed in a plastic bucket with a lid and dissolved in a 10–15% acetic acid solution (without a buffer solution, as the process was sufficient to yield conodont elements) for seven days. Once the reaction ceased, the residues were wet-sieved using 0.1 mm, 0.5 mm, and 2.0 mm mesh sieves, then rinsed with water to remove any remaining acid (to prevent the recrystallization of calcium acetate on the conodont samples) and dried in hot oven. This process was repeated to obtain two sets from each sample.

Traditionally, the residue material undergoes heavy liquid treatment to separate conodont elements from other debris and concentrate the recovered elements. However, due to the high cost and hazardous nature of heavy liquids, this step was omitted in this study. Instead, the remaining residues were carefully hand-picked under a stereomicroscope. The recovered conodonts were then photographed using a JEOL Neoscope JCM-5000 Scanning Electron Microscope (SEM) housed in Facility Building 10 at Suranaree University of Technology.

3.2.3 Thin section analysis

The rock samples (took some from conodont samples) were prepared for 4 slides of thin sections for each sample from lower subunit (U1L, U1M, U1U from lower, middle, and upper of the subunit respectively); from middle subunit (U2L, U2U from lower and upper of the subunit); and from upper subunit (U3L, U3M, U3U from lower, middle, and upper of the subunit).

The rock sample was first cut into a slab using a diamond saw and then trimmed to the desired size (2×3 cm) for mounting onto a glass slide. The surface of the sample was grinded to achieve smooth and even texture using a grinding machine. To enhance adhesion, the glass slide was pre-treated by polishing with coarse-grained abrasive dust (silicon carbide, SiC) to create a rough surface. The prepared sample was then affixed to the slide using epoxy adhesive. Once the epoxy had fully cured, the mounted sample was processed using a thin sectioning machine to reduce its thickness to approximately 1–2 mm. The section was further polished using fine-grained silicon carbide abrasive dust until the desired final thickness was achieved. The thin sections were studied under polarized-light microscope.

3.2.4 Tentaculitoid preparation

The rock samples were carefully chipped to expose additional tentaculitoid fossils. The surfaces were then cleaned by gently brushing away any dust or debris to ensure clear visibility of the specimens. Once prepared, the samples were securely packed and sent to Dr. Shuji Niko at Hiroshima University, Japan, for identification and photographic documentation.

3.3 Data analysis and interpretation

3.3.1 Ostracod

Ostracods were identified based on their morphology and analyzed to interpret the paleoenvironment of the study section through their assemblages.

3.3.2 Conodont and tentaculitoid

Conodonts and tentaculitoids were identified and analyzed to determine the age of the study section in accordance with global biostratigraphy (Becker et al., 2020).

3.3.3 Thin section analysis

The lithology of the study section was analyzed by the thin section following Dunham's limestone classification (Dunham, 1962) and the depositional environment was interpreted following Flügel (2010).

3.4 Thesis writing and presentation

This dissertation records all research methods and outcomes, with some findings presented at conferences and published in the journal.

CHAPTER IV

STRATIGRAPHY OF BAN THUNG SAMED SECTION

This chapter summarizes the stratigraphy of the Ban Thung Samed section based on primary field investigations, integrated with biostratigraphic data from ostracod, conodont, and tentaculitoid studies. These findings also help establish the age of the section.

4.1 Geology of Ban Thung Samed section

The study area, located near the previous research sites of Wongwanich et al. (1990) and Agematsu et al. (2006a), is part of the Kuan Tung Formation (Wongwanich et al., 1990), originally described as comprising calcisiltite and stromatolitic algal polygons. Following the revision by Itsarapong et al. (2023), the Kuan Tung Formation is now subdivided into three members. The lower member consists of medium to thick-bedded grey limestone, overlain by thin to medium-bedded limestone interbedded with black shale. The middle member comprises thick-bedded black shale and siltstone interbedded with pyrite-bearing limestone and is unconformably overlain by fossil-rich black shale. The upper member consists of grey to pink, thin to thick-bedded limestone with laminations and argillaceous bands. The Ban Thung Samed section includes only the lower and middle members of the revised Kuan Tung Formation. The area is also characterized by the presence of multiple faults (Figure 4.1).

4.2 Stratigraphy of Ban Thung Samed section

The Ban Thung Samed section (Figure 4.2), part of the Kuan Tung Formation and previously studied by Itsarapong et al. (2023), extends approximately 50 meters

and features well-exposed, well-bedded rock layers. On average, the bedding orientation is around 080°/40° (strike/dip). This section is subdivided into lower, middle,

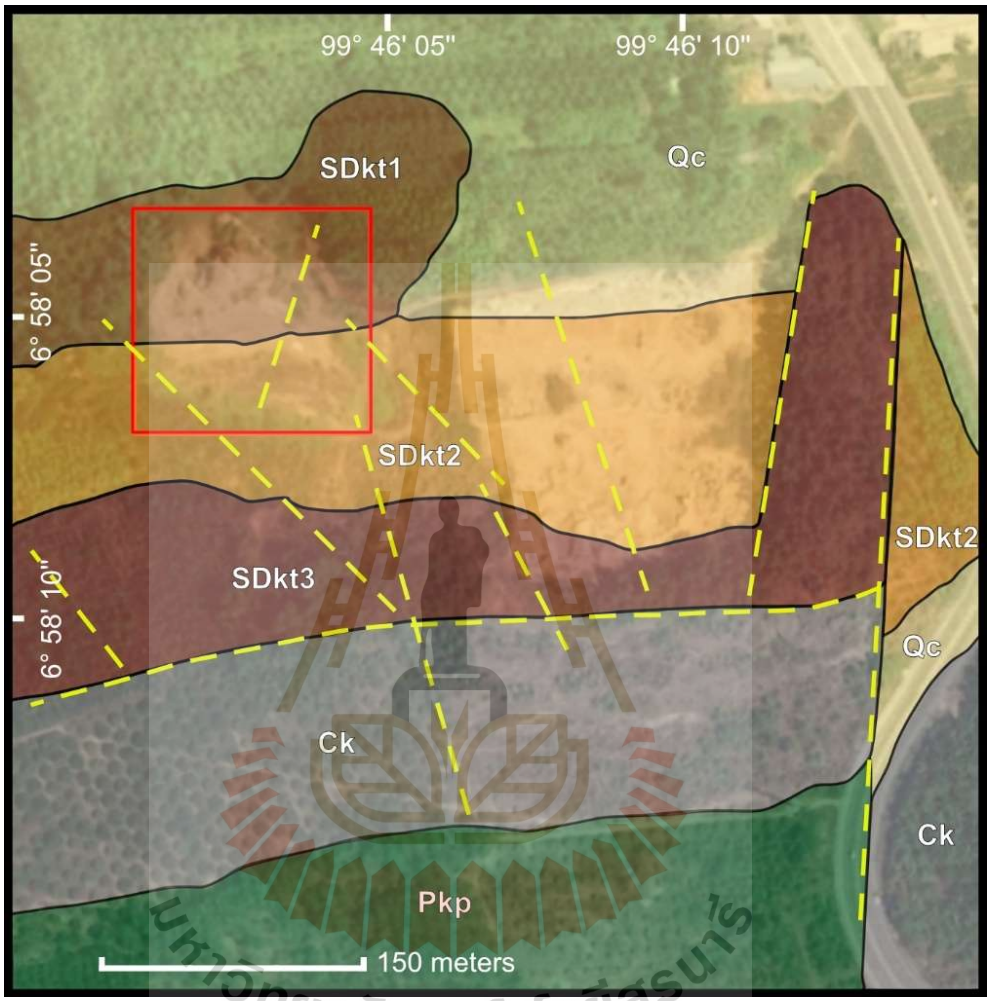

Figure 4.1 Geological map of study area. The geological data is adopted from Itsarapong et al. (2023). Red box = study area, yellow dashed line = fault, SDkt1 = Lower member of revised Kuan Tung Formation, SDkt2 = Middle member of revised Kuan Tung Formation, SDkt3 = Upper member of revised Kuan Tung Formation, Ck = Kuan Klang Formation, Pkp = Kao Phra Formation, Qc = Quaternary sediment.

and upper subunits. The lower subunit, about 22 meters thick, primarily consists of medium to thick-bedded, red-grey limestone associated with thin argillaceous layers. The middle subunit is approximately 8 meters thick, and is mostly covered by soil, composed of medium-bedded red-grey limestone interbedded with black shale. The upper subunit, approximately 20 meters thick, is well exposed and primarily composed of black shale and thin to medium-bedded dark grey limestones, with an increasing concentration of black shales toward the top.

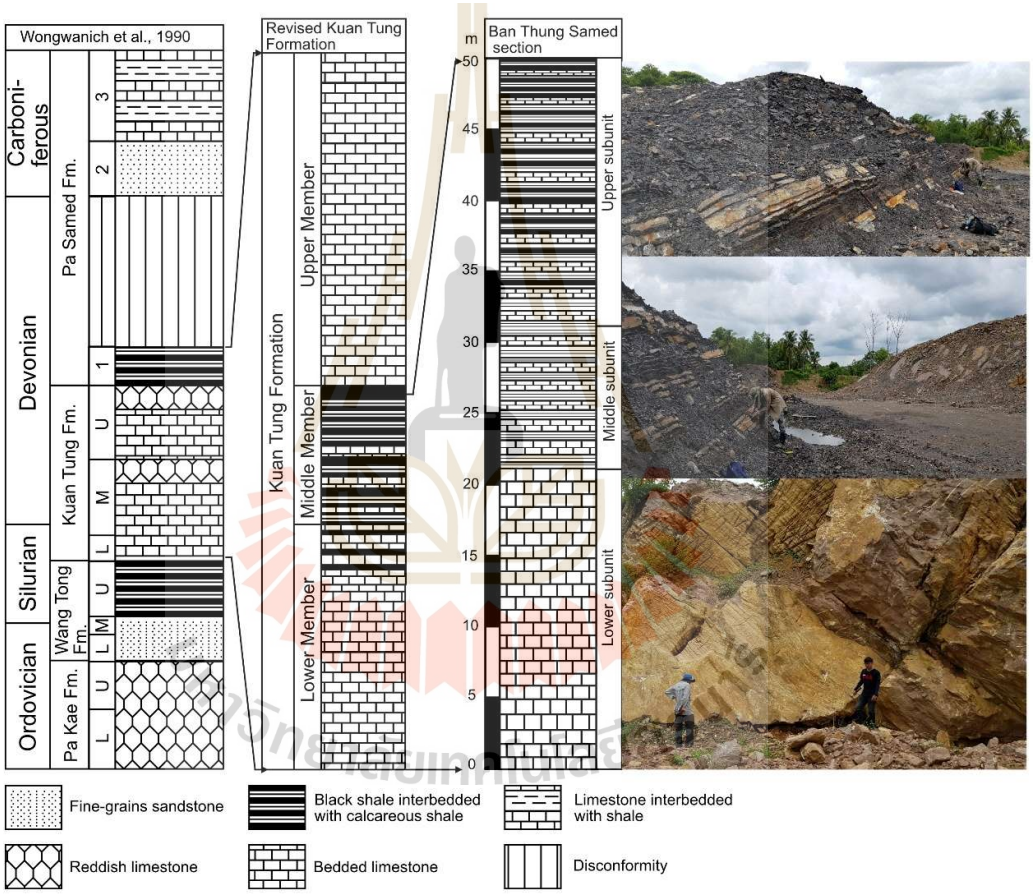

Figure 4.2 The lithostratigraphy of Ban Thung Samed section with previous study. The revised Kuan Thung Formation is after Itsarapong et al. (2023).

4.3 The age of Ban Thung Samed section

The concurrence of conodonts (Figure 4.3) such as *Pseudooneotodus beckmanni* (Bischoff and Sannemann, 1958), *Zieglerodina eladioi* Valenzuela-Ríos, 1994, and *Belodella resima* (Philip, 1965) in the middle and upper subunits suggests a stratigraphic range from the Late Silurian to Early Devonian. These species, particularly *B. resima*, *P. beckmanni*, and *Z. eladioi*, are commonly associated with the Silurian–Devonian boundary (Corradini et al., 2020). In the lower subunit, the presence of *Ozarkodina crispa* (Walliser, 1964) marks the *O. crispa* Biozone (Corradini et al., 2015), which is defined by the First Appearance Datum (FAD) of *O. crispa* in the uppermost Ludlow and continues to its Last Appearance Datum (LAD), marking the Ludlow–Pridoli boundary. Although *O. crispa* may extend slightly beyond this boundary into the lower Pridoli (Bancroft and Cramer, 2020), its stratigraphic range remains confined to the Late Silurian. However, due to the limited sample size and frequency, it remains unclear whether the occurrence of *O. crispa* represents its FAD or LAD. Therefore, the lower subunit can only be broadly assigned to the Upper Silurian, likely the uppermost Ludlow.

Tentaculitoids such as *Nowakia* sp., *Guerichina* sp., and *Striatostyliolina* sp., identified in the upper subunit (Figure 4.3) are typically Devonian in age. Although these identifications are restricted to the genus level, the associated presence of the graptolite genus *Monograptus* (see Itsarapong et al., 2023; Promduang and Chitnarin, 2025) suggests correlation with the dacryoconarid–monograptid bearing shales. These shales have been sparsely documented in Thailand, Malaysia, Myanmar, and Yunnan, and are dated to the Early Devonian (late Pragian or earliest Emsian) (Hassan et al., 2013). Further research is needed to more precisely constrain the age of the upper part of the section.

In conclusion, the Ban Thung Samed section spans from the Late Silurian to the Early Devonian, specifically from the late Ludlow to the late Pragian or earliest Emsian.

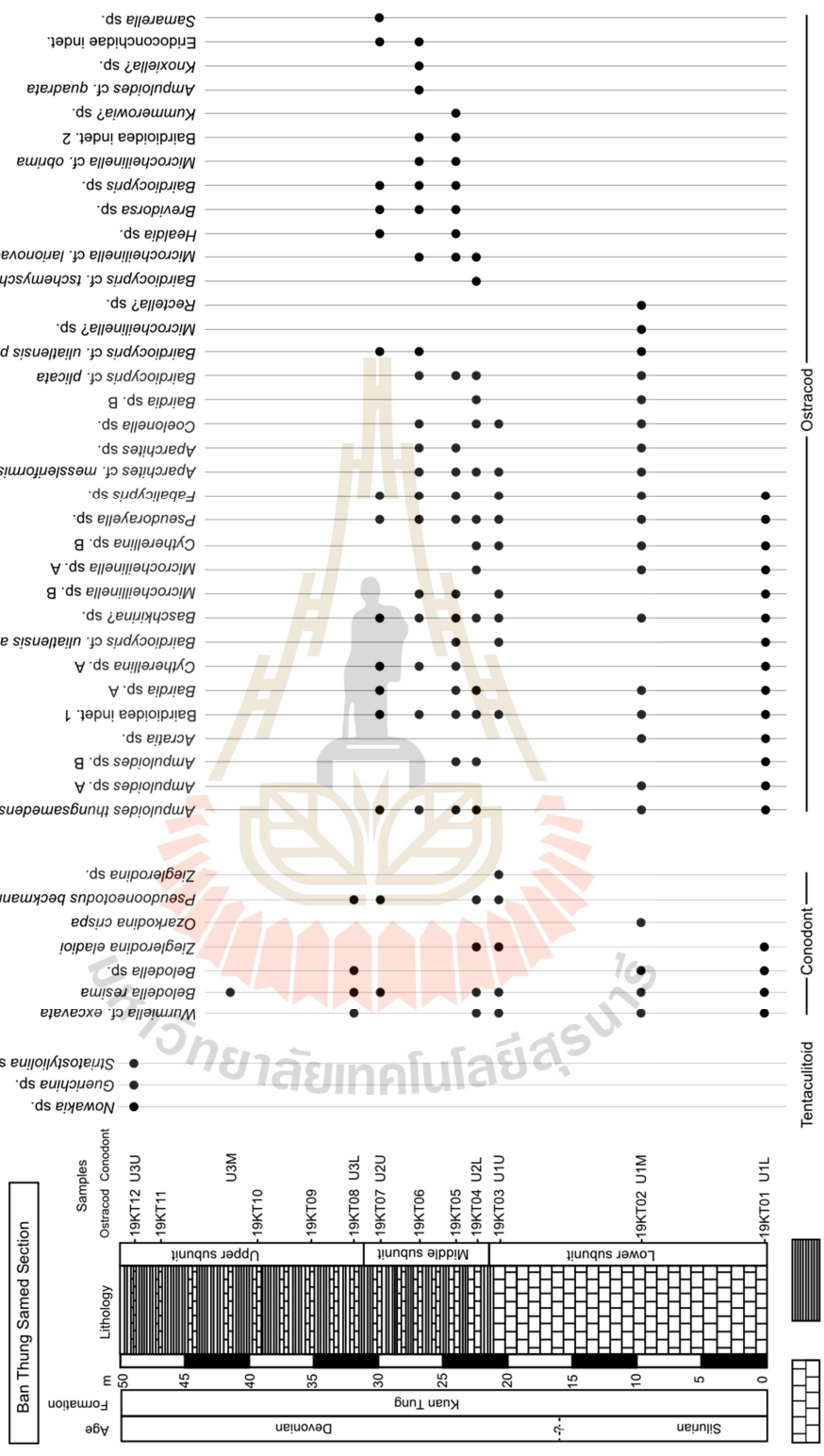

Figure 4.3 Distribution of ostracods, conodonts and tentaculitoids found in this study.

CHAPTER V

SYSTEMATIC PALEONTOLOGY

This chapter presents the findings from microfossils study included ostracods, conodonts and tentaculitoids, emphasizing the taxonomy, classification, and identification. Descriptions of morphological features are provided to aid in the accurate identification of species.

5.1 Ostracod

A total of 586 complete carapaces without disarticulated valves, adults and juvenile mixed assemblage were recovered from 12 limestone samples (19KT01-03 collected from lower unit, 19KT04-08 collected from middle unit, 19KT09-12 collected from upper unit) and deposited at micropaleontological laboratory, Suranaree University of Technology. A total of 34 ostracod species were identified, belonging to 17 genera and 11 families.

The classification in this study follows the framework established by Moore (1961).

Class OSTRACODA Latreille, 1802

Subclass PODOCOPA Müller, 1894

Order PODOCOPIDA Sars, 1866

Suborder PODOCOPINA Sars, 1866

Superfamily BAIRDIOCYPRIDOIDEA Shaver, 1961

Family PACHYDOMELLIDAE Berdan and Sohn, 1961

Genus *Ampuloides* Polenova, 1952

Type species: *Ampuloides verrucosa* Polenova, 1952

Ampuloides* cf. *quadrata Jiang in Wei et al., 1983

(Figure 5.1)

Occurrence: Sample 19KT06**.**

Study material: 2 specimens.

Dimension: Length = 0.58 – 0.60 mm, Height = 0.33 – 0.36 mm

Remarks: The specimen resembles *Ampuloides quadrata* Jiang, 1983, discovered in the Middle Devonian Huaning Formation in Yunnan (Wei et al., 1983). The carapace has a straight ventral border, giving it a sub-rectangular shape in lateral view. However, the posterior border of *A. quadrata* is bigger than the specimens in this study.

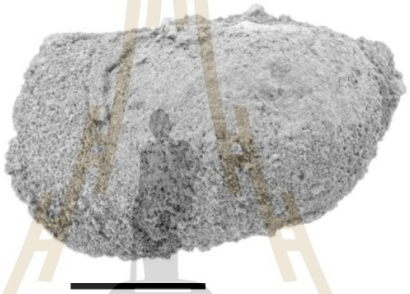

Figure 5.1 *Ampuloides* cf. *quadrata*; left lateral view. Scale bar = 0.2 mm.

Ampuloides thungsamedensis Promduang and Chitnarin, 2025

(Figures. 5.2)

Occurrence: Samples 19KT01, 02, 04, 05, 06, 07.

Study material: 46 specimens.

Dimensions: Length = 0.46-0.62 mm, Height = 0.28-0.35 mm.

Remarks: The new ostracod species *Ampuloides thungsamedensis* is distinguishable from *A. quadrata* from the Middle Devonian of Guizhou (Wei et al., 1983) by the absence of the sub-rectangular carapace in lateral view. Although the overall shape and size of the carapace closely resemble *A. beckeri* Nazik, 2020, from the Late Devonian of Mongolia (Nazik et al., 2020), the cardinal extremities of the left valve in *A. thungsamedensis* are positioned at the dorsal border. This species shares similarities with *A. vissouensis* Casier and Préat, 1996, from the upper Eifelian to lower Givetian in

the Pic de Vissou quarry, Montagne Noire, France (Casier and Préat, 1996) but can be differentiated by its smoothly rounded free margin on the left valve and a small surface protuberance. Juveniles are fusiform when viewed dorsally and ventrally (Figure 5.2F), while adults possess a robust carapace with an inflated posterior section (Figures 5.2D-E).

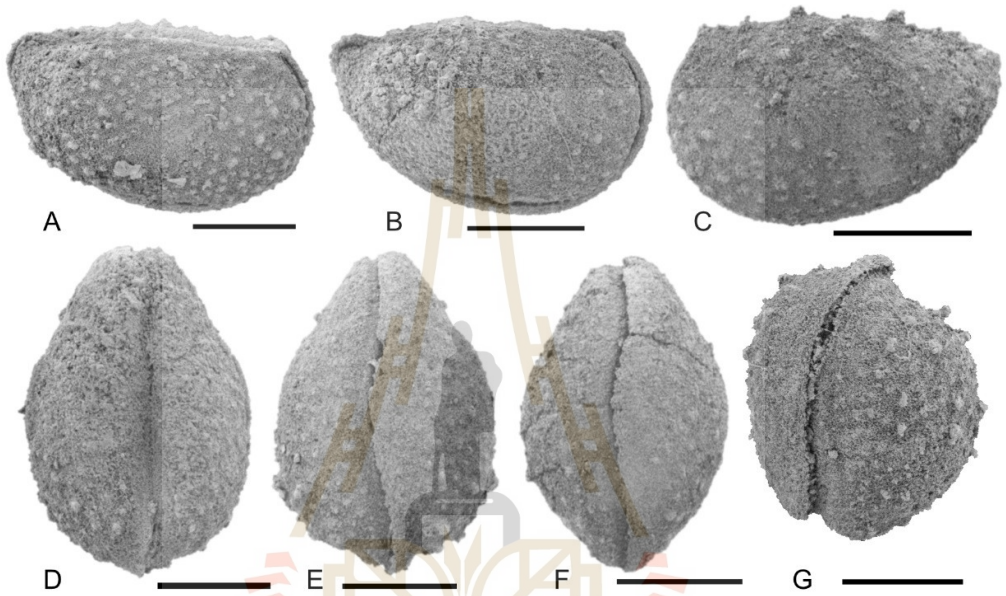

Figure 5.2 *Ampuloides thungsamedensis*, A-B, left lateral view, C. right lateral view. D. dorsal view, E-F, ventral view, G. oblique postero-ventral view showing shallow furrow that run parallel to free margin. Scale bar = 0.2 mm.

***Ampuloides* sp. A**

(Figure 5.3)

Occurrence: Samples 19KT01-02**.**

Study material: 7 specimens.

Dimension: Length = 0.44-0.58 mm, Height = 0.30-0.41 mm.

Remarks: The specimens can be distinguished from *Ampuloides thungsamedensis* by having greater Height/Length ratio, pointed cardinal extremities, and a swollen dorsal border that arches higher than the dorsum.

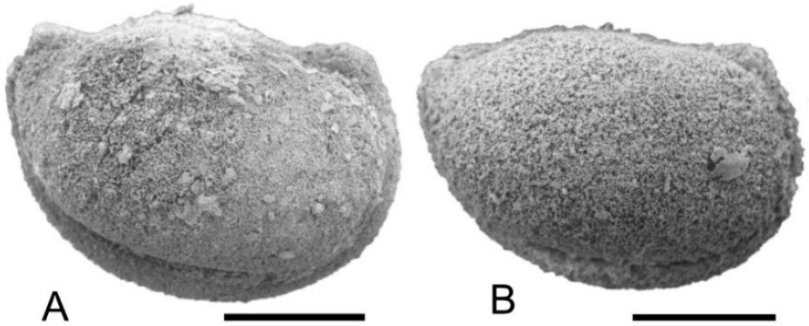

Figure 5.3 *Ampuloides* sp. A; right lateral view. Scale bar = 0.2 mm.

Ampuloides **sp. B**

(Figure 5.4)

Occurrence: Samples 19KT01, 04, 05.

Study material: 9 specimens.

Dimension: Length = 0.58-0.59 mm, Height = 0.41-0.47 mm.

Remarks: The specimen is set apart from *Ampuloides thungsamedensis* by having sub-rectangular shape, straight posteroventral border, rounded yet prominent cardinal extremities that rise higher than the dorsal border, a swollen median area, and a prominent surface protuberance.

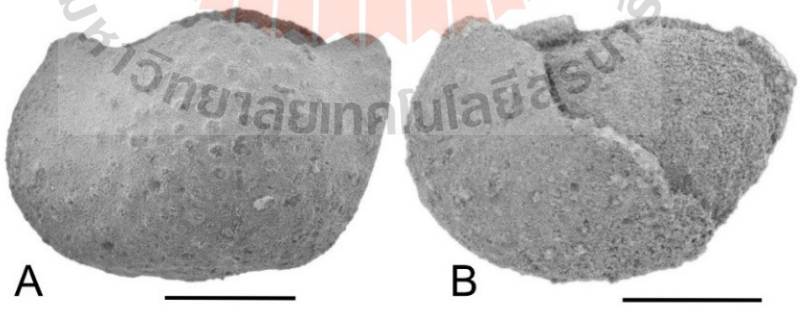

Figure 5.4 *Ampuloides* sp. B; left lateral view. Scale bar = 0.2 mm.

Genus *Microcheilinella* Geis, 1933

Type species: *Microcheilinella distortus* Geis, 1932

Microcheilinella* cf. *larionovae Polenova 1955 in Wei et al., 1983

(Figure 5.5)

Occurrence: samples 19KT04-06.

Study material: 13 specimens.

Dimension: Length = 0.53-0.54 mm, Height = 0.29-0.30 mm.

Remarks: The species closely resemble *Microcheilinella larionovae* Polenova, 1955 in Wei et al. (1983) from the Middle Devonian of Ghuizhu (Wei et al., 1983) due to its ovate-oblong shape in lateral view and a dorsal border that is straight to slightly convex, running parallel to the ventral border.

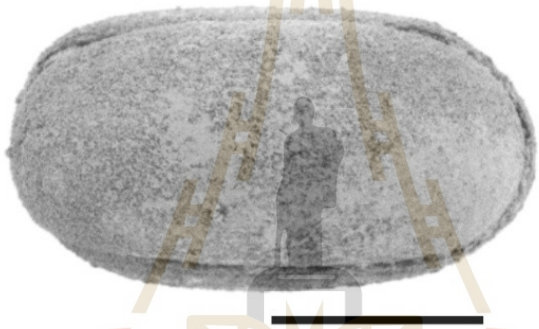

Figure 5.5 *Microcheilinella* cf. *larionovae*; right lateral view. Scale bar = 0.2 mm.

Microcheilinella* cf. *obrima Jiang in Wei et al., 1983

(Figure 5.6)

Occurrence: Samples 19KT05, 06.

Study material: 12 specimens.

Dimension: Length = 0.37-0.65 mm, Height = 0.18-0.36 mm.

Remarks: This species has a similarity with *Microcheilinella obrima* Jiang in Wei et al., 1983, from the Middle Devonian of the Ghuizhu (Wei et al.,1983). However, differences are observed at the anterior border and posterior border, where the maximum convexities are positioned at mid-height in the specimens from this study, but below mid-height in *M. obrima* Jiang in Wei et al. (1983).

Figure 5.6 *Microcheilinella* cf. *obrima*, A. right lateral view, B. dorsal view. Scale bar = 0.2 mm.

***Microcheilinella* sp. A**

(Figure 5.7)

Occurrence: Samples 19KT01, 02, 04**.**

Study material: 12 specimens.

Dimension: Length = 0.47-0.53 mm, Height = 0.30-0.34 mm.

Remarks: The specimen is distinguished from *Microcheilinella* species by having a more swollen carapace. In contrast to *M. xuanheensis* Wang, 2015 in Song et al., 2022 from the Late Silurian of southern Tibet, China, it exhibits a less pronounced swelling and features more rounded AB and PB.

Figure 5.7 *Microcheilinella* sp. A; right lateral view. Scale bar = 0.2 mm.

***Microcheilinella* sp. B**

(Figure 5.8)

Occurrence: Samples 19KT01, 03, 05, 06.

Study material: 26 specimens.

Dimension: Length = 0.44-0.55 mm, Height = 0.28-0.35 mm.

Remarks: This *Microcheilinella* species shows some resemblance to the genus *Newsomites* Morris and Hill, 1952 but lacks the pointed posterior ends. Its overall shape closely matches *Decoranewsomites multicavus* Rozhdestvenskaja, 1972 from Montagne Noire, France (Casier and Lethiers, 1997), though it lacks ornamentation, preventing its classification within *Decoranewsomites* Casier and Lethiers, 1997.

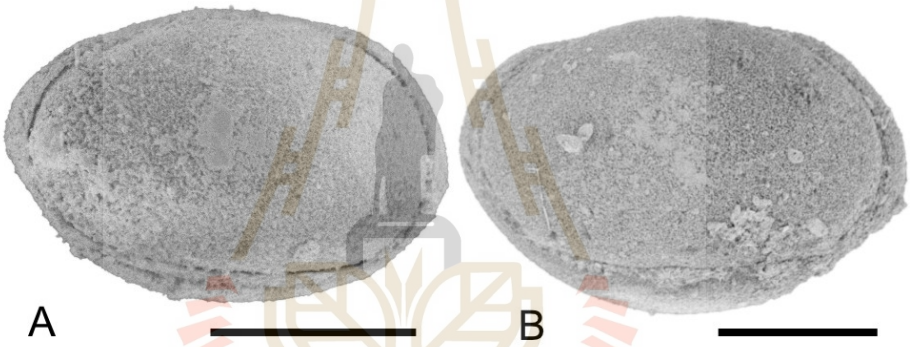

Figure 5.8 *Microcheilinella* sp. B; right lateral view. Scale bar = 0.2 mm.

***Microcheilinella*? sp.**

(Figure 5.9)

Occurrence: Sample 19KT02.

Study material: 2 specimens.

Dimension: Length = 0.46-0.51 mm, Height = 0.26-0.29 mm.

Remarks: This species generally resembles *Microcheilinella* sp. B described in this study, but is distinctly shorter in height, resulting in a more oblong outline. The dorsal margin is nearly straight. Although its overall shape is similar to *Decoranewsomites angelicus* Casier and Lethiers, 1997, the specimen cannot be confidently assigned to *Decoranewsomites* because it is poorly preserved and does not show the surface

ornamentation that typically characterizes the genus. Given these limitations and its closer resemblance to other members of this community, the specimen is provisionally referred to *Microcheilinella.*

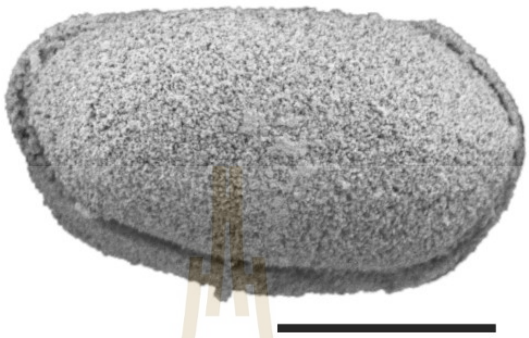

Figure 5.9 *Microcheilinella*? Sp.; right lateral view. Scale bar = 0.2 mm.

Family BAIRDIOCYPRIDIDAE Shaver, 1961

Genus Bairdiocypris Kegel, 1932

Type species: Bairdiocypris gerolsteinensis Kegel, 1932

Bairdiocypris* cf. *uliatlensis prava Wang and Shi in Hou, 1988

(Figure 5.10)

Occurrence: Samples 19KT02, 06, 07.

Study material: 19 specimens.

Dimension: Length = 0.36-0.88 mm, Height = 0.22-0.56 mm.

Remarks: The specimen closely resembles *Bairdiocypris uliatlensis prava* Wang and Shi (in Hou et al., 1988) from the Lower Devonian Yangmaba Formation at the Guixi-Shawozi section.

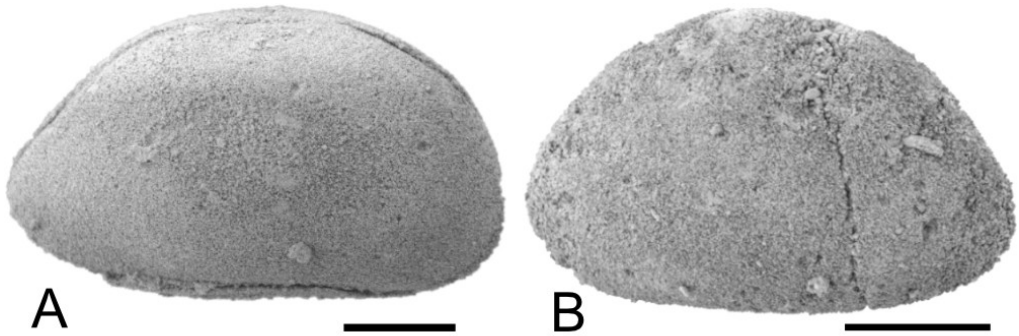

Figure 5.10 *Bairdiocypris* cf. *uliatlensis prava*; A. right lateral view, B. left lateral view. Scale bar = 0.2 mm.

Bairdiocypris* cf. *uliatlensis alta Wei in Hou, 1988

(Figure 5.11)

Occurrence: Samples 19KT01, 03, 05.

Study material: 18 specimens.

Dimension: Length = 0.52 - 0.73 mm, Height = 0.35 – 0.45 mm.

Remarks: In lateral view, the specimen exhibits a subtriangular shape, resembling *Bairdiocypris uliatlensis alta* Wei in Hou, 1988 from the Upper Devonian Tuqiaozi Formation, China. However, it is distinguished by a longer carapace.

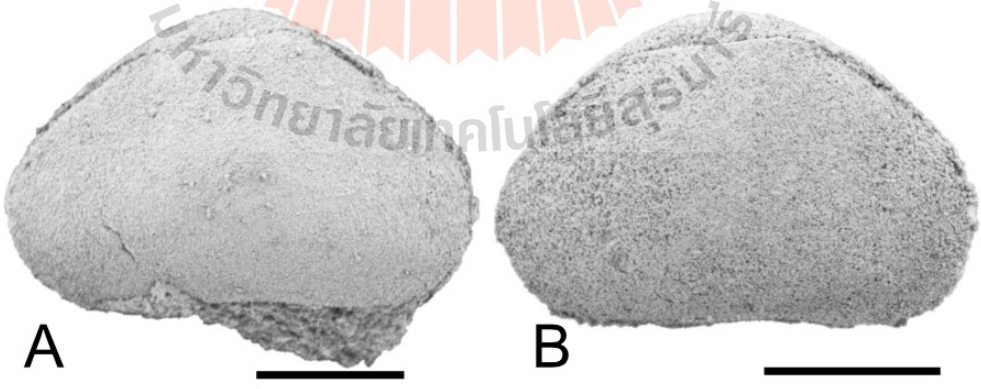

Figure 5.11 *Bairdiocypris* cf. *uliatlensis alta;* right lateral view. Scale bar = 0.2 mm.

Bairdiocypris* cf. *plicata Wang, 1983

(Figure 5.12)

Occurrence: Samples 19KT02, 04, 05, 06.

Study material: 15 specimens.

Dimension: Length = 0.41 - 1.20 mm, Height = 0.29 – 0.77 mm.

Remarks: The specimen having a similarity with *Bairdiocypris plicata* Wang, 1983 of the Middle Devonian Sipai Formation, China (Wang, 1983) but is distinguished by a less inclined posterodorsal border.

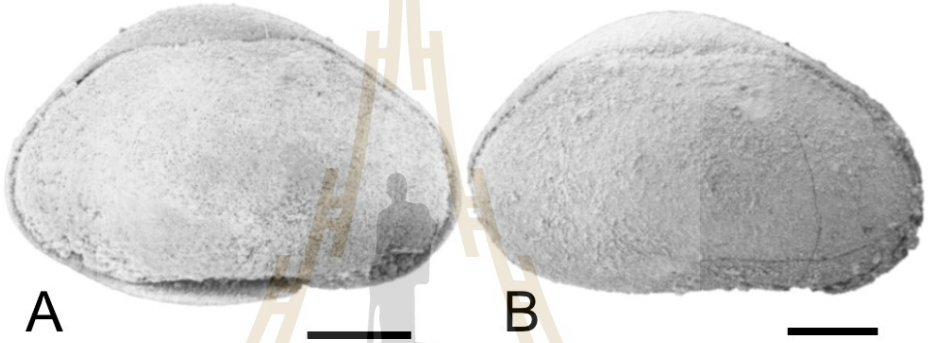

Figure 5.12 *Bairdiocypris* cf. *plicata*; right lateral view. Scale bar = 0.2 mm.

Bairdiocypris* cf. *tschemyschensis (Samoilova et Smirnova) in Hou, 1988

(Figure 5.13)

Occurrence: Sample 19KT04.

Study material: 14 specimens.

Dimension: Length = 0.71 - 1.02 mm, Height = 0.47 - 0.68 mm.

Remarks: The specimen features a small, rounded anterior border and a large, rounded posterior border, with maximum Height at mid-Length, resembling *Bairdiocypris tschemyschensis* (Samoilova and Smirnova) in Hou et al., 1988 from the Upper Devonian Tuqiaozi Formation, China.

Figure 5.13 *Bairdiocypris* cf. *tschemyschensis*; A. right lateral view, B. left lateral view, C. dorsal view. Scale bar = 0.2 mm.

***Bairdiocypris* sp.**

(Figure 5.14)

Occurrence: Samples 19KT05-07.

Study material: 6 specimens.

Dimension: Length = 0.33 - 0.69 mm, Height = 0.22 – 0.46 mm

Remarks: This species has a subtriangular shape in lateral view, but its outline is more round compared to other *Bairdiocypris* species examined in this study. However, due to poor preservation and the limited number of available carapaces, it is not possible to assigned to a species.

Figure 5.14 *Bairdiocypris* sp.; right lateral view. Scale bar = 0.2 mm.

Genus *Baschkirina* Rozhdestvenskaja, 1959

Type species. *Baschkirina memorabilis* Rozhdestvenskaja, 1959

***Baschkirina*? sp.**

(Figure 5.15)

Occurrence: Samples 19KT01-07.

Study material: 15 specimens.

Dimension: Length = 0.45 – 0.51 mm, Height = 0.25 – 0.29 mm.

Remarks: This species shows a subtriangular outline, with a broadly rounded anterior and a narrower, rounded posterior. The dorsal and ventral margins are straight, with the dorsal margin inclined posteriorly. It is uncertainly assigned to *Baschkirina* due to its irregular trapezoidal shape in lateral view and the presence of angular bends along the dorsal margin. However, due to poor preservation and the morphological resemblance to certain *Acratia* forms, a definitive assignment remains problematic.

Figure 5.15 *Baschkirina*? sp.; left lateral view. Scale bar = 0.2 mm.

Family RECTELLIDAE Neckaja, 1966

Genus *Rectella* Neckaja, 1958

Type species: *Mica inaequalis* Neckaja, 1952

***Rectella*? sp.**

(Figure 5.16)

Occurrence: Samples 19KT02.

Study material: 3 specimens.

Dimension: Length = 0.67 mm, Height = 0.31 mm.

Remarks: This species has been assigned to *Rectella* based on its overall shape, characterized by parallel, straight dorsal and ventral margins, and rounded anterior and posterior ends. However, due to poor preservation and the limited number of specimens, a specific identification is difficult, as this form also closely resembles several other genera.

Figure 5.16 *Rectella*? sp.; left lateral view. Scale bar = 0.2 mm.

Family KRAUSELLIDAE Berdan, 1961

Genus *Pseudorayella* Neckaja in Abushik et al.1960

Type species: *Pseudorayella scala* Neckaja in Abushik et al., 1960

***Pseudorayella* sp.**

(Figure 5.17)

Occurrence: Samples 19KT01-07.

Study material: 128 specimens.

Dimension: Length = 0.41 – 0.83 mm, Height = 0.21 – 0.41 mm.

Remarks: The specimen closely resembles *Pseudorayella*? *ellipsis* (Li, 1989) in Wang, 2015 from the Upper Ordovician of Sichuan, China, which is noted for its oblong-elliptical carapace in lateral view, with nearly symmetrical dorsal and ventral convexity, and convex anterior and posterior ends. In dorsal view, it has a biconvex shape, with maximum convexity at the middle. However, the studied specimens show a more pronounced dorsal convexity and are larger than *P*? *ellipsis* (Li, 1989).

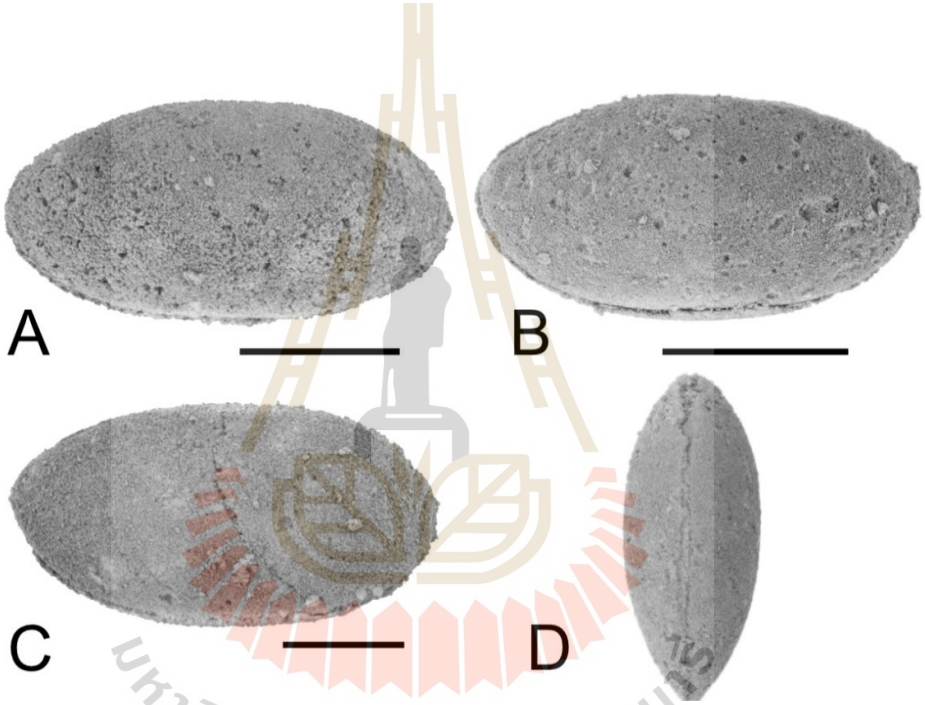

Figure 5.17 *Pseudorayella* sp.; A-C, right lateral view, D. dorsal view Scale bar = 0.2 mm.

Superfamily BAIRDIOIDEA Sars, 1888

Family ACRATIIDAE Gründel, 1962

Genus *Acratia* Delo, 1930

Type species: *Acratia typica* Delo, 1930

***Acratia* sp.**

(Figure 5.18)

Occurrence: Samples 19KT01-02.

Study material: 10 specimens.

Dimension: Length = 0.69 – 0.80 mm, Height = 0.28 – 0.31 mm.

Remarks: This species has been assigned to *Acratia* based on its beaked anterior, which points downward, and its narrow posterior, with convex dorsal and ventral margins. It shares similarities with *Acratia (Cooperuna) tichonovitchi* Egorov, 1953, from the Late Devonian of the Holy Cross Mountains, Poland (plate 21, fig. 6 in Olempska, 1979), particularly the flattened, downward-deflected anterior and the pointed posterior. However, it differs in possessing a concave posteroventral border and a convex ventral margin.

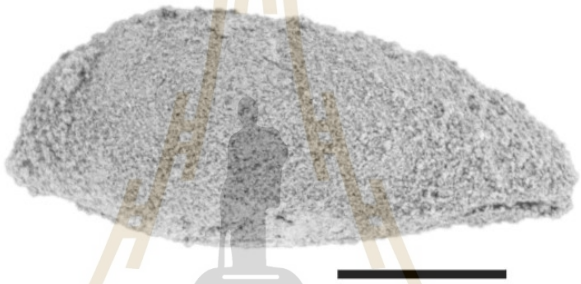

Figure 5.18 *Acratia* sp.; left lateral view. Scale bar = 0.2 mm.

Family BAIRDIIDAE Sars, 1888

Genus *Bairdia* McCoy, 1844

Type species: *Bairdia curtus* McCoy, 1844

***Bairdia* sp. A**

(Figure 5.19)

Occurrence: Samples 19KT01, 02, 04, 05, 07.

Study material: 21 specimens.

Dimension: Length = 0.61 - 0.90 mm, Height = 0.31 – 0.44 mm.

Remarks: The specimens exhibit a typical bairdian shape, characterized by a gently convex dorsal border and a straight hinge line that accounts for approximately one-third of the total length. The left valve is larger than the right and overlaps along the

free margin, although this overlap is less distinct along the ventral border. The ventral margin is straight to slightly concave. Both anterior and posterior ends are pointed but asymmetrical. The overall outline resembles that of *Bairdia (Orthobairdia)* nov. sp. C, aff. *philippovae* Egorov, 1953, from the Late Devonian Schmidt Quarry in Germany (Casier et al., 1999) but differs in exhibiting a biconvex dorsal view. It also closely resembles *Bairdia* sp. A aff. *buschminae* Crasquin, 1985 (plate 4, figs. 4a, b, Casier et al., 2005) but can be distinguished by its more pointed anterior end.

***Bairdia* sp. B**

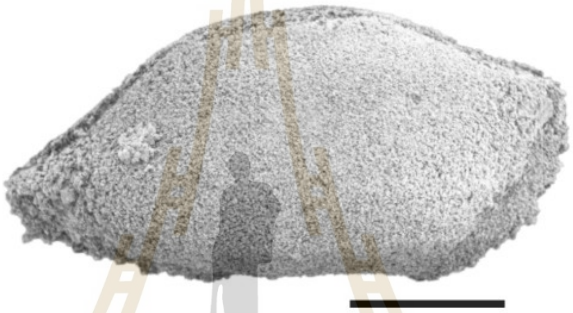

Figure 5.19 *Bairdia* sp. A; right lateral view Scale bar = 0.2 mm.

(Figure 5.20)

Occurrence: Samples 19KT02, 04.

Study material: 2 specimens.

Dimension: Length = 0.58 - 0.73 mm, Height = 0.30 – 0.36 mm.

Remarks: The specimens have a similar outline to *Bairdia* sp. A from this study but differ from having punctate surface. This species also shares a very similar outline with *Bairdia* (*Bairdia*) cf. *finifracta* Blumenstengel, 1970, from the Late Devonian Schmidt quarry in Germany (figs. 4.8a, b Casier et al., 1999) but differs by its punctate surface.

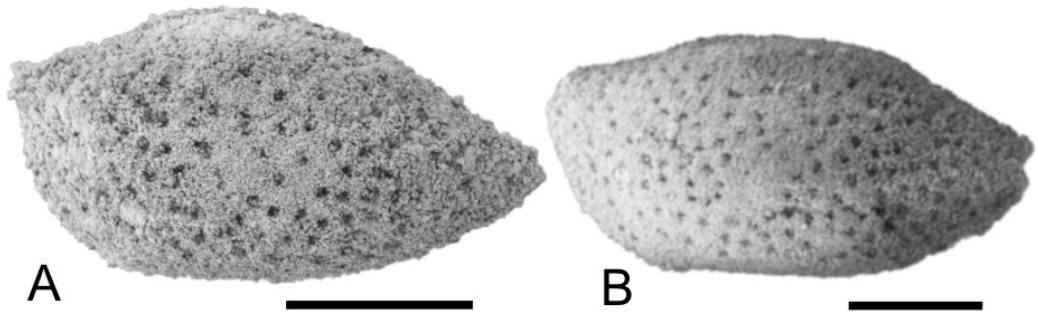

Figure 5.20 *Bairdia* sp. B; left lateral view. Scale bar = 0.2 mm.

Genus *Fabalicypris* Cooper, 1946

Type species: *Fabalicypris wileyensis* Cooper, 1946

***Fabalicypris* sp.**

(Figure 5.21)

Occurrence: Samples 19KT01-03, 05-07.

Study material: 56 specimens.

Dimension: Length = 0.40 - 0.61 mm, Height = 0.18 – 0.31 mm.

Remarks: This species has been assigned to *Fabalicypris* based on its elongate subovate shape in lateral view, with a rounded anterior and a rounded to subtriangular posterior. However, due to its simple morphology and poor preservation, it is difficult to assign it accurately to a specific species.

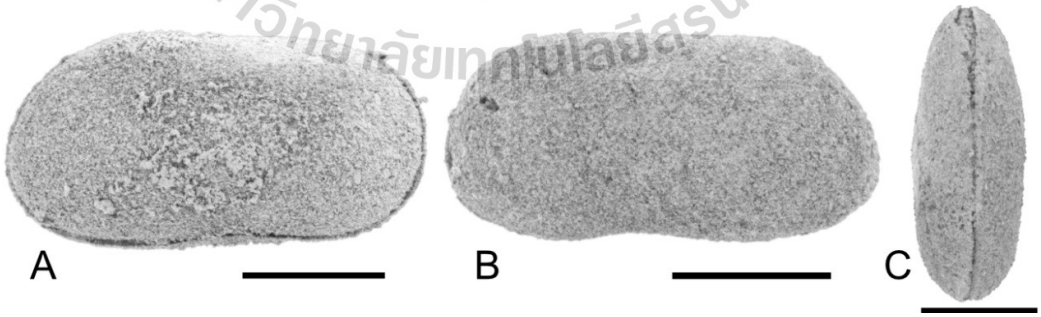

Figure 5.21 *Fabalicypris* sp.; A. right lateral view, B. left lateral view, C. dorsal view. Scale bar = 0.2 mm.

Bairdioidae indet.1

(Figure 5.22)

Occurrence: Samples 19KT01-07.

Study material: 36 specimens.

Dimension: Length = 0.53 - 0.73 mm, Height = 0.29 – 0.36 mm.

Remarks: This species exhibits a straight dorsal margin, a gently convex ventral margin, a broadly rounded anterior, and a posterior that tapers gradually to a small, rounded end. The left valve is larger than the right and overlaps it along the free margin. In dorsal view, the carapace appears biconvex with a smooth surface. Its general morphology resembles several genera, including *Bairdia*, though the anterior is more rounded, and *Fabalicypris*, but the ventral margin lacks the straight or concave. As a result, the species remains undetermined.

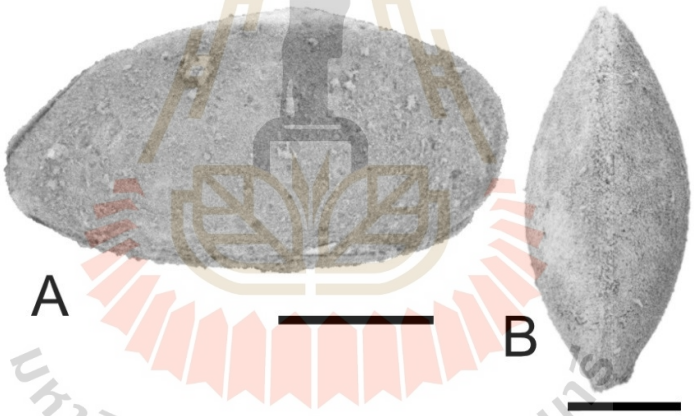

Figure 5.22 Bairdioidae indet.1; A. right lateral view, B. dorsal view. Scale bar = 0.2 mm.

Bairdioidae indet.2

(Figure 5.23)

Occurrence: Samples 19KT05, 06.

Study material: 1 complete and 4 broken carapaces.

Dimension: Length = 0.43 mm, Height = 0.21 mm.

Remarks: The carapace is oblong in lateral view. The dorsal border is straight and slopes posteriorly, while the ventral border is also straight. Both the anterodorsal and posterodorsal borders are convex. The anterior border has an acute point located approximately one-third of the distance from the ventral margin. The posterior border is subangular, with its pointed end positioned lower than that of the anterior border. The right valve is slightly larger than the left and exhibits weak overlap along the free margin. Prominent spines are present at mid-length on the lateral surface of the ventral border of both valves, oriented posteriorly. In dorsal view, the carapace is gently biconvex. Due to poor carapace preservation and the limited number of specimens, determination is challenging, as they do not appear to fit within any known genus of Bairdioidea.

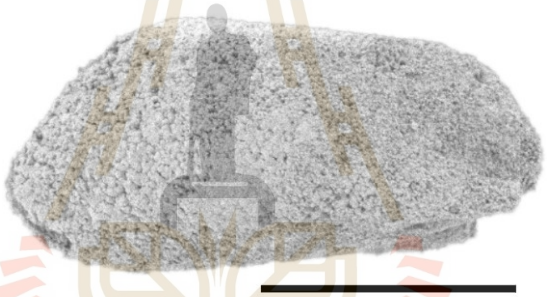

Figure 5.23 Bairdioidae indet. 2; left lateral view. Scale bar = 0.2 mm.

Suborder METACOPINA Sylvester-Bradley, 1961

Superfamily HEALDIOIDEA Harlton, 1933

Family HEALDIIDAE Harlton, 1933

Genus *Cytherellina* Jones and Holl, 1869

Type species: *Beyrichia siliqua* Jones, 1855 subsequently designated by Jones and Holl, 1869

***Cytherellina* sp. A**

(Figure 5.24)

Occurrence: Samples 19KT01, 05, 06, 07.

Study material: 7 specimens.

Dimension: Length = 0.36 - 0.39 mm, Height = 0.18 – 0.20 mm.

Remarks: The specimens have been assigned to *Cytherellina* based on their elongate carapace, with the greatest height situated in the posterior half, rounded anterior and posterior margins, and smooth surface texture. However, due to poor preservation and the limited number of specimens, determination at the species level is not possible.

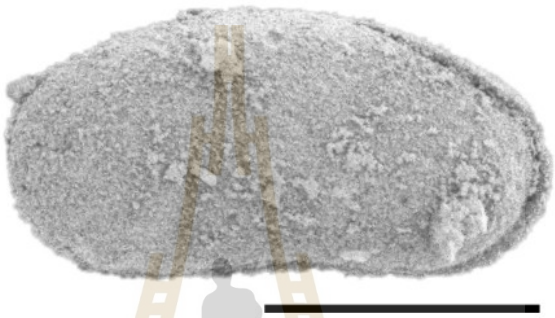

Figure 5.24 *Cytherellina* sp. A; right lateral view. Scale bar = 0.2 mm.

***Cytherellina* sp. B**

(Figure 5.25)

Occurrence: Samples 19KT01-04.

Study material: 18 specimens.

Dimension: Length = 0.54 – 1.27 mm, Height = 0.26 – 0.58 mm.

Remarks: The species has been assigned to *Cytherellina* based on its elongate carapace, with the maximum height located in the posterior half, rounded anterior and posterior margins, and smooth surface. However, the specimens differ from *C.* sp. A by having longer carapaces and a narrower, almost pointed posterior. Due to the poor preservation of the carapaces, specific classification remains difficult.

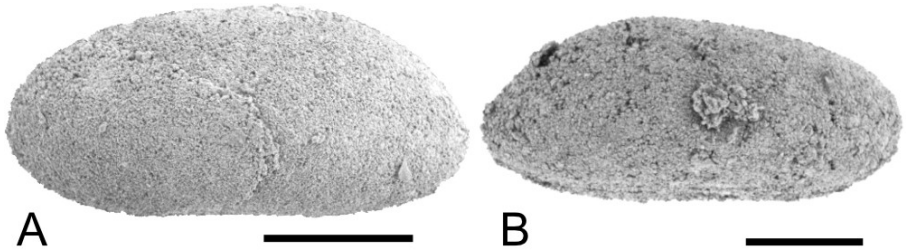

Figure 5.25 *Cytherellina* sp. B; A. left lateral view, B. right lateral view. Scale bar = 0.2 mm.

Genus *Healdia* Roundy, 1926

Type species: *Healdia simplex* Roundy, 1926

***Healdia* sp.**

(Figure 5.26)

Occurrence: Samples 19KT05, 07.

Study material: 3 specimens.

Dimension: Length = 0.58 – 1.05 mm, Height = 0.35 – 0.67 mm.

Remarks: The specimen is assigned to the family Healdiidae due to its short, smooth carapace. It is placed in *Healdia* based on a distinct, sub-vertical posterior ridge on both valves, which differentiates it from *Healdianella* Posner, 1951. Additionally, it is distinguished from *Waylandella* Coryell and Billings, 1932 by its shorter carapace and dorsal angulation. Despite these characteristics, the specimen does not fully correspond to any previously described *Healdia* species.

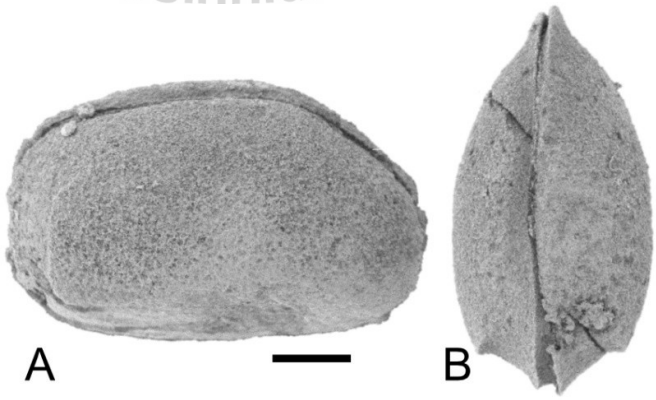

Figure 5.26 *Healdia* sp.; A. right lateral view, B. dorsal view. Scale bar = 0.2 mm.

Genus *Kummerowia* Adamczak, 1976

Type species: *Kummerowia prima* Adamczak, 1976

***Kummerowia*? sp.**

(Figure 5.27)

Occurrence: Sample 19KT05.

Study material: 4 specimens.

Dimension: Length = 0.56 - 0.81 mm, Height = 0.30 – 0.43 mm.

Remarks: The species is classified uncertainty as *Kummerowia*. The carapace shape closely resembles that of *Kummerowia prima*, which has been identified in the Middle Devonian of Poland (Adamczak, 1976) and the Middle Devonian Yangmaba Formation in China (Hou, 1988).

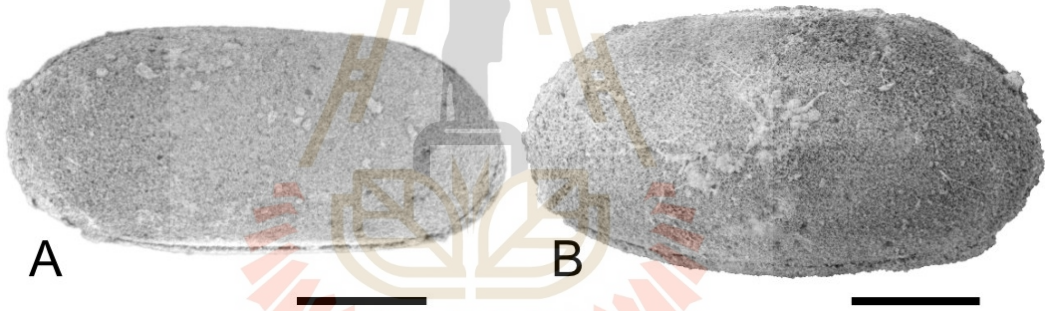

Figure 5.27 *Kummerowia*? Sp.; right lateral view. Scale Bar = 0.2 mm.

Order PALAEOCOPIDA Henningsmoen, 1953

Suborder PALAEOCOPINA Henningsmoen, 1953

Superfamily APARCHITOIDEA Ulrich and Bassler, 1923

Family APARCHITIDAE Ulrich and Bassler, 1923

Genus *Aparchites* Jones, 1889

Type species: *Aparchites whiteavesi* Jones, 1889

Aparchites* cf. *messleriformis Polenova, 1960 in Polenova, 1968

(Figure 5.28)

Occurrence: Sample 19KT02-06.

Study material: 19 specimens.

Dimensions: Length = 0.48 – 0.61 mm, Height = 0.38 – 0.47 mm.

Remarks: The species is classified under the genus *Aparchites* due to their carapace shape. They are similar to *A. messleriformis* Polenova, 1960 in Polenova, 1968, which has been found in the Lower Devonian of Salair, Russia, and in the Middle Devonian Sipai Formation, China (Wang, 1983).

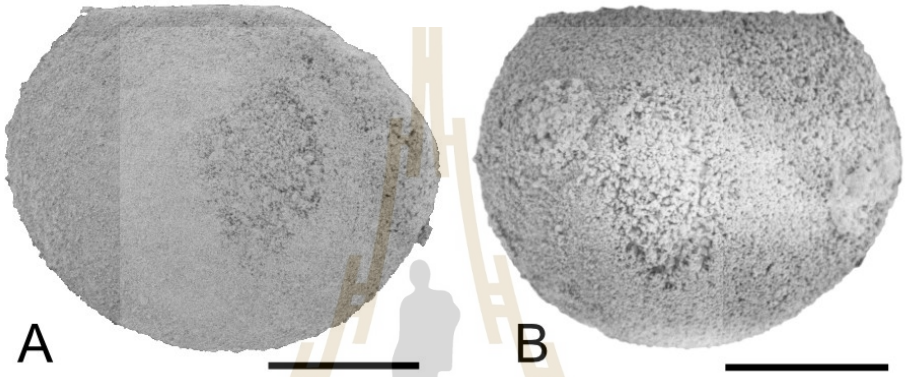

Figure 5.28 *Aparchites* cf. *messleriformis*; left lateral view. Scale bar = 0.2 mm.

***Aparchites* sp.**

(Figure 5.29)

Occurrence: Samples 19KT02, 05, 06.

Study material: 7 specimens.

Dimension: Length = 0.40 – 0.60 mm, Height = 0.31 – 0.44 mm.

Remarks: The species is similar to *Aparchites productus* Polenova, 1960 *sensu* Polenova, 1968), which has been documented in the Lower Devonian rocks of Salair, Russia, and the Lower Devonian Ganxi Formation in China (Hou, 1988). However, more well-preserved material is required for a more detailed assessment of their classification.

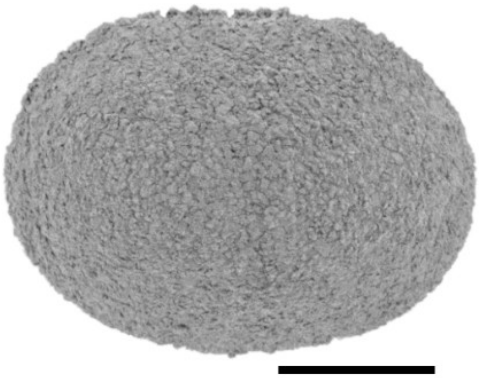

Figure 5.29 *Aparchites* sp. left lateral view. Scale bar = 0.2 mm.

Genus *Brevidorsa* Neckaja, 1973

Type species: *Brevidorsa brevidorsata* Neckaja, 1973

***Brevidorsa* sp.**

(Figure 5.30)

Occurrence: Samples 19KT05-07.

Study material: 12 specimens.

Dimension: Length = 0.49 – 0.95 mm, Height = 0.38 – 0.75 mm.

Remarks: This species has been assigned to *Brevidorsa*, based on right valve overlapping left valve and overreaching right valve in dorsal border with short ridges on free margin of both valves. Compared to *B. sichuanensis* Wang, 2015 from the Silurian Pulu Formation, Nyalam region, southern Tibet, China (fig. 3B, Song et al., 2022), the species has a straighter and longer dorsal border.

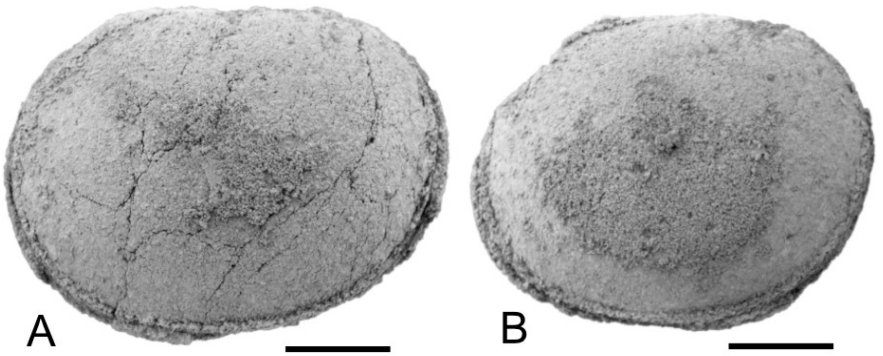

Figure 5.30 *Brevidorsa* sp.; left lateral view. Scale bar = 0.2 mm.

Suborder PARAPARCHITICOPINA Gramm in Gramm and Ivanov (1975)

Superfamily PARAPARCHITOIDEA Scott, 1959

Family PARAPARCHITIDAE Scott, 1959

Genus *Samarella* Polenova, 1952

Type species: *Samarella crassa* Polenova, 1952

***Samarella* sp.**

(Figure 5.31)

Occurrence: Sample 19KT07.

Study material: 1 specimen.

Dimension: Length = 0.38 mm, Height = 0.26 mm.

Remarks: This species has been assigned to *Samarella* by having a convex dorsal border, both rounded ends, and right valve overlapping left valve in ventral border and reverse overreach in dorsal border. The outline in lateral view is very similar to *S.* cf. *laevinodosa* Becker, 1964 from the Givetian of the Fromelennes Formation, Ardennes, France (fig. 8C, Maillet et al., 2013) but differs in having more overlapping in ventral border and less overlapping in anterodorsal. Compared to *S.* cf. *laevinodosa* Becker, 1964 from the Early Givetian, Hanonet Formation, France (plate 1, fig. 14, Casier et al., 2011), the species is very similar in lateral outline, but without a detailed description or a figure of the dorsal view, it could possibly be a different species.

Figure 5.31 *Samarella* sp.; left lateral view. Scale bar = 0.2 mm.

Genus *Coelonella* Stewart, 1936

Type Species: *Isochilinal scapha* Stewart, 1930

***Coelonella* sp.**

(Figure 5.32)

Occurrence: Sample 19KT02-04, 06.

Study material: 31 specimens.

Dimension: Length = 0.35-0.50 mm, Height = 0.47-0.77 mm.

Remarks: This species has been assigned to *Coelonella* based on its subovoid shape. Right valve overlapping left valve along the free margin, extending to the ventral margin. The posterior margin is depressed along the hinge. However, due to poor preservation, assigning it to a specific species is not possible.

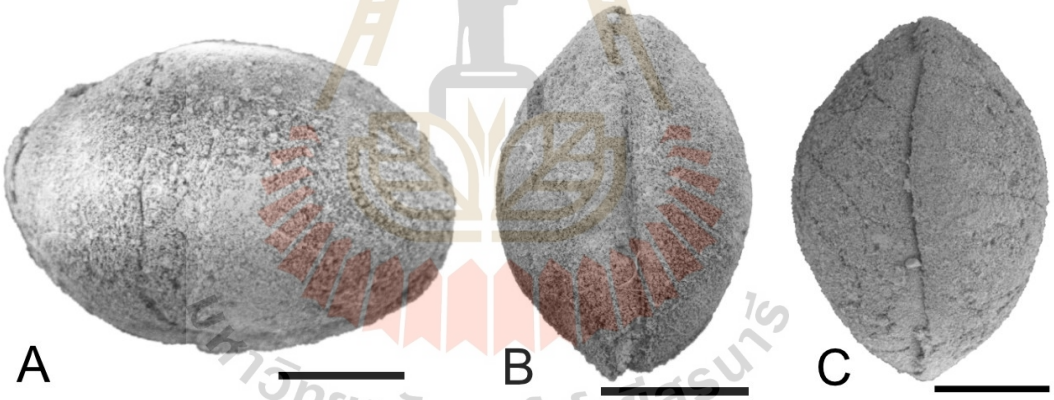

Figure 5.32 *Coelonella* sp.; A. right lateral view, B. dorsal view, C. ventral view. Scale bar = 0.2 mm.

Suborder PLATYCOPINA Sars, 1866

Superfamily KLOEDENELLOIDEA Ulrich and Bassler, 1908

Family KNOXITIDAE Egorov, 1950

Genus *Knoxiella* Egorov, 1950

Type species: *Knoxiella semilukiana* Egorov, 1950

***Knoxiella*? sp.**

(Figure 5.33)

Occurrence: Sample 19KT06.

Study material: 1 specimen.

Dimension: Length = 0.60 mm, Height = 0.36 mm.

Remarks: The specimens show characteristics resembles *Knoxiella cf. tuqiaoensis* Wei, 1988 *sensu* Song et al., 2018 from Yangdi section in Guangxi, South China (Song et al., 2018); however, poor preservation limits further identification. Additionally, they are comparable to *K. complanata* Kummerow, 1939 *sensu* Guillam et al., 2022 from the Blue Snake Section, Guizhou, China (Guillam et al., 2022), but they can be differentiated by the lack of a reticulated surface.

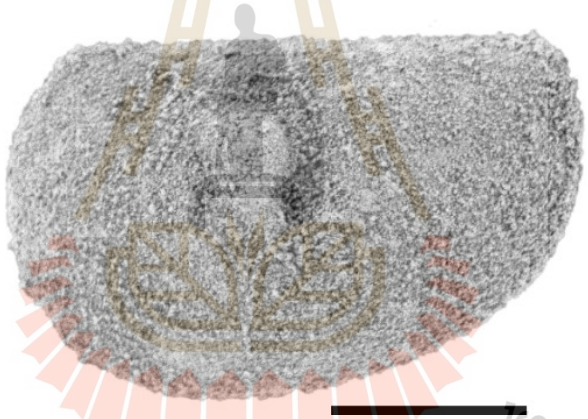

Figure 5.33 *Knoxiella*? sp.; left lateral view. Scale bar = 0.2 mm.

Suborder ERIDOSTRACA Adamczak, 1961

Family ERIDOCONCHIDAE Henningsmoen, 1953

Eridoconchidae indet.

(Figure 5.34)

Occurrence: Samples 19KT06-07.

Study material: 6 specimens.

Dimension: Length = 0.56-0.68 mm, Height = 0.43-0.48 mm.

Remarks: The specimens have concentric ridges which are closely spaced and much thinner than those found in *Eridostracina* species (e.g., Olempska et al., 2015; Song et al., 2016), which may be a result of poor preservation.

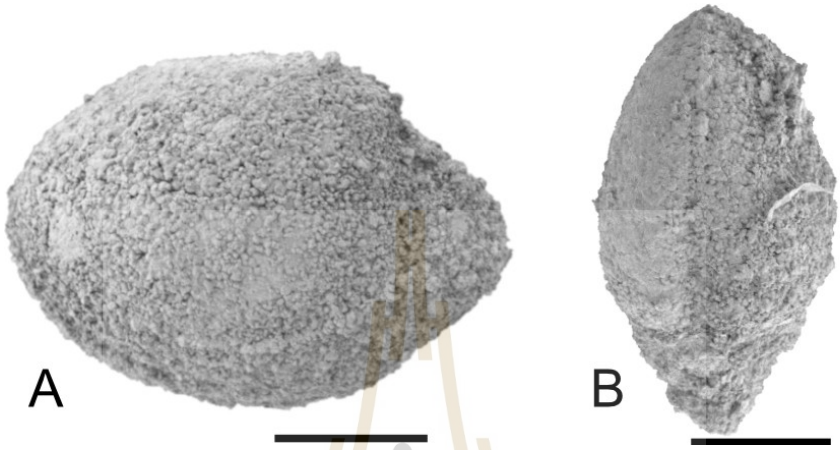

Figure 5.34 Eridoconchidae indet.; A. left lateral view, B. dorsal view. Scale bar = 0.2 mm.

5.2 Conodont

A total of 103 specimens were recovered from 8 limestone samples (U1L, U1M, U1U from the lower unit; U2L, U2U from the middle unit; U3L, U3M, U3U from the upper unit). These specimens, identified as 7 species, 5 genera, and are housed at the micropaleontological laboratory of Suranaree University of Technology

The suprageneric classification is followed Sweet (1988). The synonymy list is shortened and contains only the first or necessary description.

Phylum CHORDATA Bateson, 1886

Class CAVIDONTI Sweet, 1988

Order BELODELLIDA Sweet, 1988

Family BELODELLIDAE Khodalevich and Chernikh, 1973

Genus *Belodella* Ethington, 1959

Type species - *Belodella devonicus* (Stauffer, 1940)

Belodella resima (Philip, 1965)

(Figure 5.35)

1965 *Belodella resimus* Philip, pl. 8, figs. 15–17.

Occurrence: sample U1L, U1M, U1U, U2L, U2U, U3L, U3M.

Study materials: 62 specimens.

Remarks: The specimens have been assigned to *Belodella resima* based on the compressed, symmetrical triangular or subtriangular cross-section of the basal cavity, the presence of small denticles on the posterior, and an anterolateral flange-like costa visible in the inner lateral view (Anderson, 2003). In this study, only S0 and S1 elements were recognized. The S0 element has an untwisted cusp, while the S1 element has a similar shape but with a twisted cusp. The S0 and S1 elements of *B. resima* are very similar in shape to the S3 element of *B. anomalis* Cooper, 1974, differing only in the presence of denticles on the anterior of the element. If these denticles cannot be discerned, the specimen should be assigned to *B. resima* (Farrel, 2004). This may lead to an inflated count of *B. resima* elements. However, since the S0 and S1 elements of *B. anomalis*, which have denticles appearing laterally at the base of the cusp, could not be identified, the specimens should be assigned to *B. resima*.

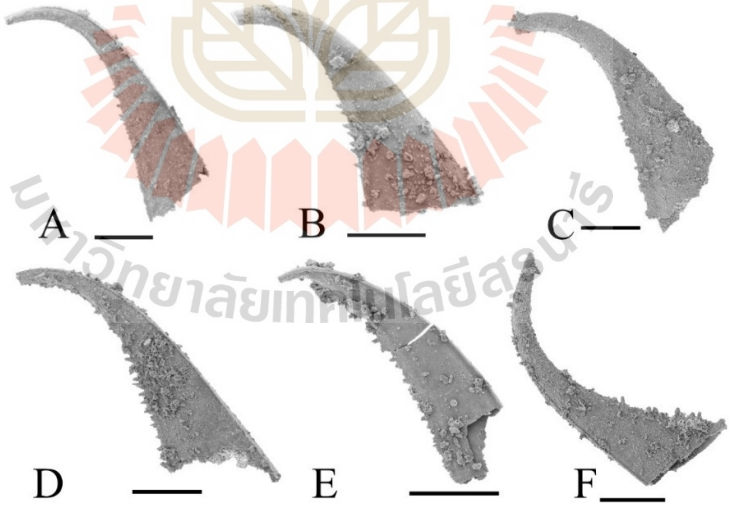

Figure 5.35 *Belodella resima;* A. Inner lateral view of S0 element, B. Outer lateral view of S0 element, C. Outer lateral view of S0 element D. Inner lateral view of S0 element, E. Inner lateral view of S1 element, F. Inner lateral view of S1? element. Scale bar = 0.2 mm.

***Belodella* sp.**

(Figure 5.36)

Occurrence: U1L, U1M, U3L.

Study materials: 10 specimens.

Remarks: the specimen differs from *Belodella resima* from having asymmetrical triangular cross-section of basal cavity (the inner side is shorter than outer side), the shape has less compressed and has longitudinal costae (or ridges) that appear on posterior and anterior.

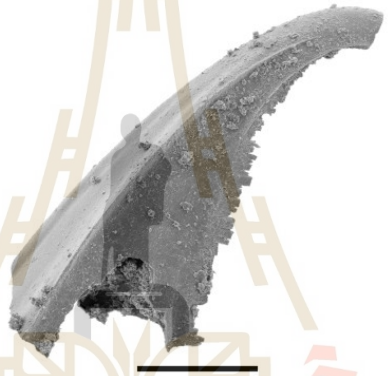

Figure 5.36 *Belodella* sp.; Inner lateral view. Scale bar = 0.2 mm.

Class CONODONTA Pander, 1856

Order OZARKODINIDA Dzik, 1976

Family SPATHOGNATHODONTODAE Hass, 1959

Genus *Ozarkodina* Branson and Mehl, 1933

Type species - *Ozarkodina confluens* Branson and Mehl, 1933

Ozarkodina crispa (Walliser, 1964)

(Figure 5.37)

1964 *Spathognathodus crispus* Walliser, p. 74-75, Pl. 9, fig. 3; Pl. 21, figs. 7-13.

Occurrence: U1M.

Study materials: 2 specimens.

Remarks: The specimens have been assigned to *Ozarkodina crispa* based on the presence of fused denticles above the basal cavity toward the posterior end, an asymmetrical basal cavity, and the termination of the blade at the posterior of the basal cavity. The specimen in this study (Figure 5.37D) exhibits unfused denticles, which align with the description of the alpha$_3$ morph by Viira and Aldridge (1998).

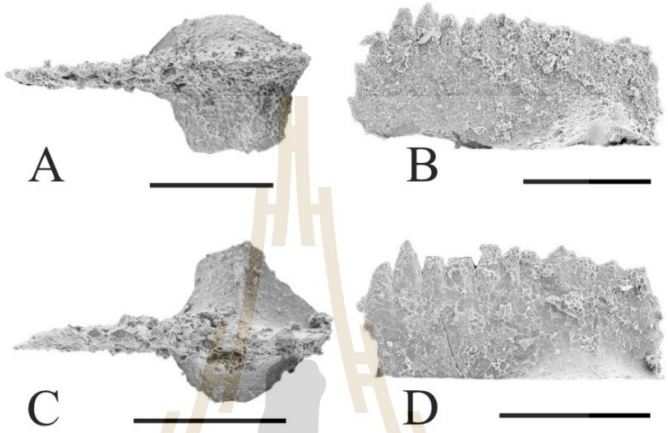

Figure 5.37 *Ozarkodina crispa*; A-B same specimen: A, Top view of P1 element, B. lateral view of P1 element; C-D same specimen: C. Top view of P1 element, D. Lateral view of P1 element. Scale bar = 0.2 mm.

Genus *Wurmiella* Murphy, Valenzuela-Rios and Carls, 2004

Type species - *Ozarkodina excavata tuma* Murphy and Matti, 1983

Wurmiella* cf. *excavata (Branson and Mehl, 1933)

(Figure 5.38)

Occurrence: U1L, U1M, U1U, U2L, U3L.

Study materials: 15 specimens.

Remarks: The genus *Wurmiella* was proposed by Murphy et al. (2004) to include the *excavata* group, which was previously classified under the genus *Ozarkodina*. The specimens examined in this study resemble *W. excavata* based on the presence of uniformly sized denticles, a basal cavity extending along the entire process of the elements, and a straight or slightly curved P1 element. *W. excavata* exhibits a high

degree of variation in P1 elements (e.g., Corradini and Corriga, 2010; Mathieson et al., 2016). In this study, two variants were recognized. Figures 5.38A–E show similarities to those illustrated by Corradini and Corriga (2010) and Corriga et al. (2014), while Figures 5.38F and G resemble those of Takahashi et al. (2017).

Figure 5.38C was previously assigned to *W.* cf. *inclinata* by Promduang and Chitnarin (2025) based on its overall shape. Upon reconsideration, however, the specimen was found to lack the prominent cusp characteristic of *W. inclinata* and instead exhibits greater similarity to *W. excavata*, as illustrated by Corriga et al. (2014) and Corradini and Corriga (2010). Therefore, the specimen has been reassigned to *W.* cf. *excavata*.

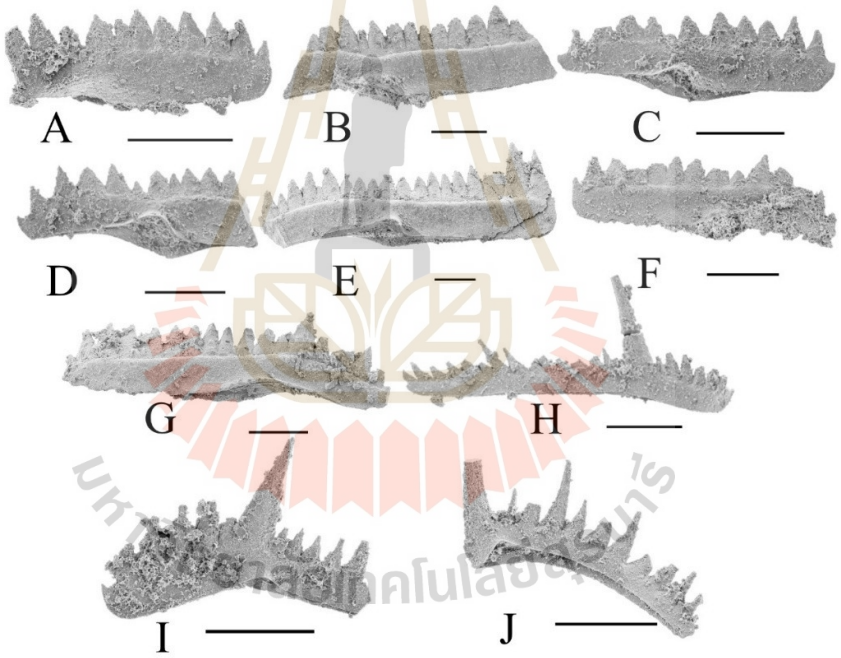

Figure 5.38 *Wurmiella* cf. *excavata*; A. Lateral view of a juvenile P1 element, B. Lateral view of an adult P1 element, C. Lateral view of a juvenile P1 element, D. Lateral view of a juvenile P1 element, E. Lateral view of an adult P1 element, F. Lateral view of a Juvenile P1 element, G. Lateral view of an adult P1 element, H. Lateral view of S2 element, I. Lateral view of P2 element, J. Lateral view of M element. Scale bar = 0.2 mm.

Genus *Zieglerodina* Murphy, Valenzuela-Rios and Carls, 2004

Type species *Spathognathodus remscheidensis* Ziegler, 1960

Zieglerodina eladioi Valenzuela-Ríos, 1994

(Figure 5.39)

1994 *Ozarkodina eladioi* n. sp. Valenzuela-Ríos, p. 59-63, pl. 5, figs 1-35.

2019 *Zieglerodina eladioi* (Valenzuela-Ríos, 1994) Corriga and Corradini, figs 2-3

Occurrence: U1L, U1U, U2L.

Study materials: 8 specimens.

Remarks: *Zieglerodina* was established by Murphy et al. (2004) to include the "remscheidensis Group" of Ozarkodinids. *Z. eladioi* was recently reconstructed with a complete apparatus by Corriga and Corradini (2019), consisting of P1 carminate, P2 angulate, M dolabrate, S0 alate, S1 digyrate, and S2 bipennate elements. In this study, only P2, M, S1, and S2 elements were recognized, characterized by "the alternate denticulation with spike-like denticles" (Corriga and Corradini, 2019).

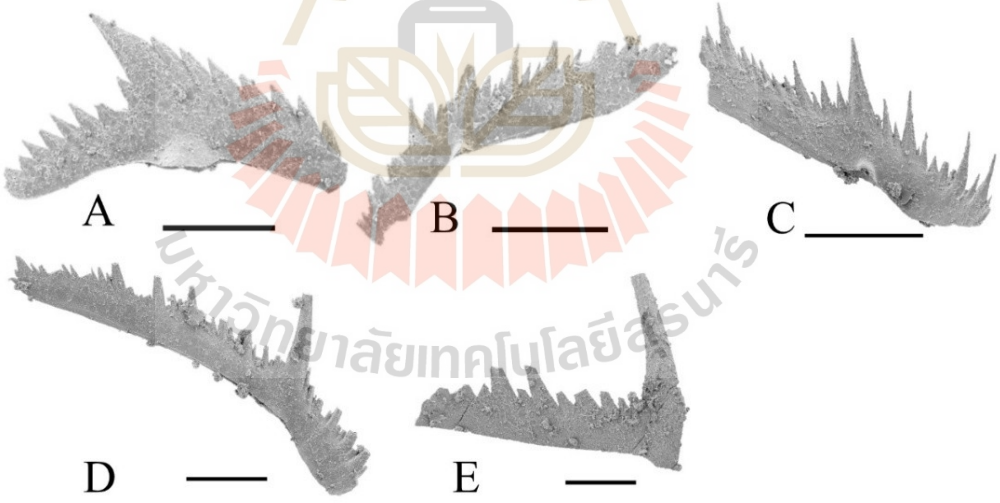

Figure 5.39 *Zieglerodina eladioi*; A. Lateral view of P2 element, B. Lateral view of S2 element, C. Lateral view of S2 element, D. Lateral view of S1 element, E. Lateral view of M element. Scale bar = 0.2 mm.

***Zieglerodina* sp.**

(Figure 5.40)

Occurrence: U1U.

Study materials: 1 specimen.

Remarks: The specimen has a very similar outline to *Zieglerodina remscheidensis* Ziegler, 1960; however, the cusp is broken, preventing accurate identification. The study sample also shares similarities with *Z.* sp. (Figure 6H) illustrated by Hušková and Slavík (2020).

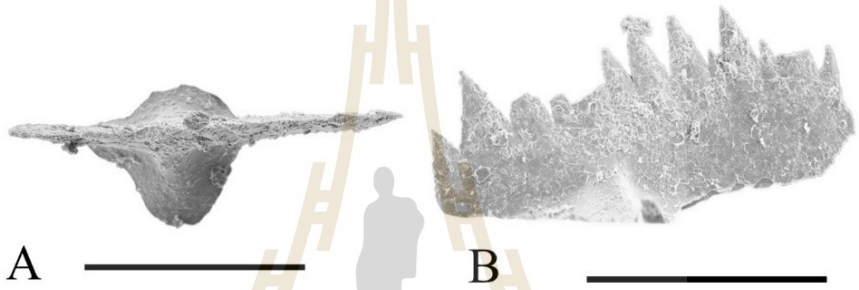

Figure 5.40 *Zieglerodina* sp.; A-B same specimen; A. Top view of P1 element, B. Lateral view of P1 element. Scale bar = 0.2 mm.

Family STRACHANOGNATHIDAE Bergström, 1981

Genus *Pseudooneotodus* Drygant, 1974

Pseudooneotodus beckmanni (Bischoff and Sannemann, 1958)

(Figure 5.41)

1958 *Oneotodus*? *beckmanni* Bischoff and Sannemann, p. 98, pl. 15, figs. 22-25.

Occurrence: U1U, U2L, U2U, U3L.

Study materials: 5 specimens.

Remarks: The specimens have been assigned to *Pseudooneotodus beckmanni* based on their "squat conical element with a single apical denticle and an ovoidal to subtriangular base" (Corradini, 2007).

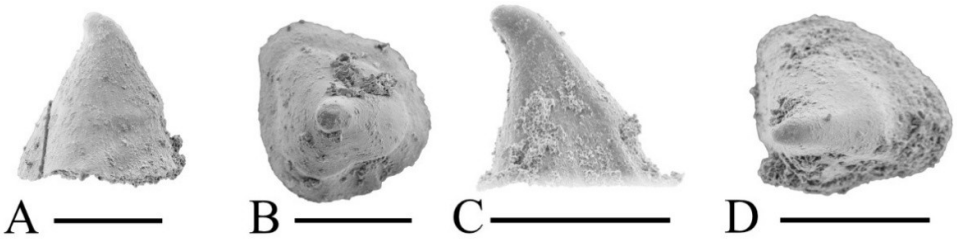

Figure 5.41 *Pseudooneotodus beckmanni*; A-B same specimen, A. Lateral view of the element, B. Top view of the element; C-D same specimen, C. Lateral view of element, D. Top view of element. Scale bar = 0.2 mm.

5.3 Tentaculitoid

The specimens from the rock surface on sample 19KT12 were photographed and identified by Dr. Shuji Nikko from Hiroshima University.

The suprageneric classification of tentaculitoids is still debated mainly difference in how to defined class, subclass or order. In this study the classification were followed Lardeux (1969), Larsson (1979).

Class TENTACULITOIDEA Ljashenko 1957

Order DACRYOCONARIDA Fisher, 1962

Family NOWAKIIDAE Bouček and Prantl, 1960

Genus *Nowakia* (Gürich, 1896)

***Nowakia* sp.**

(Figure 5.42)

Occurrence: 19KT12.

Remarks: The specimens exhibit a straight conch shape with both transverse rings and longitudinal ribs (difficult to discerned). The initial chamber is difficult to observe but is likely bulbous in shape (Figure 5.42A). When compared to the specimens described by Agematsu et al. (2006a), those in this study appear to belong to *Nowakia*. However, due to the low-quality image and poor preservation, a definitive identification is not possible.

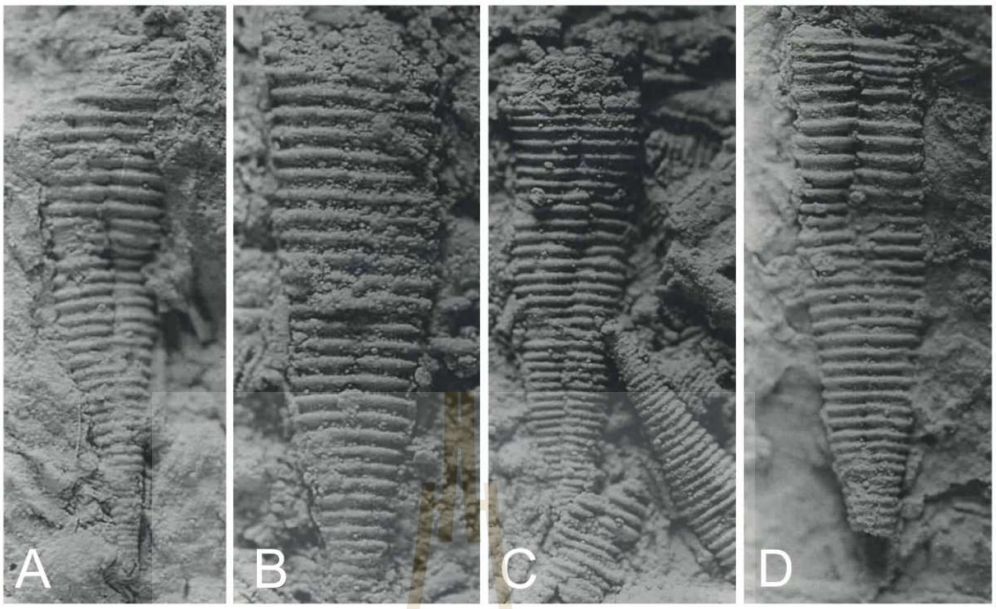

Figure 5.42 A-D *Nowakia* sp. SEM image, 15x magnification.

Family PENEAUIIDAE Lardeux, 1969

Genus *Guerichina* Bouček and Prantl, 1961

***Guerichina* sp.**

(Figure 5.43)

Occurrence: 19KT12

Remarks: The specimens exhibit a straight conch with only transverse rings, while the external wall displays annulations composed of smaller rings (Figure 5.43C). Although the low-quality image and poor preservation prevent accurate determination, the characteristic annulations suggest that the specimens belong to *Guerichina*.

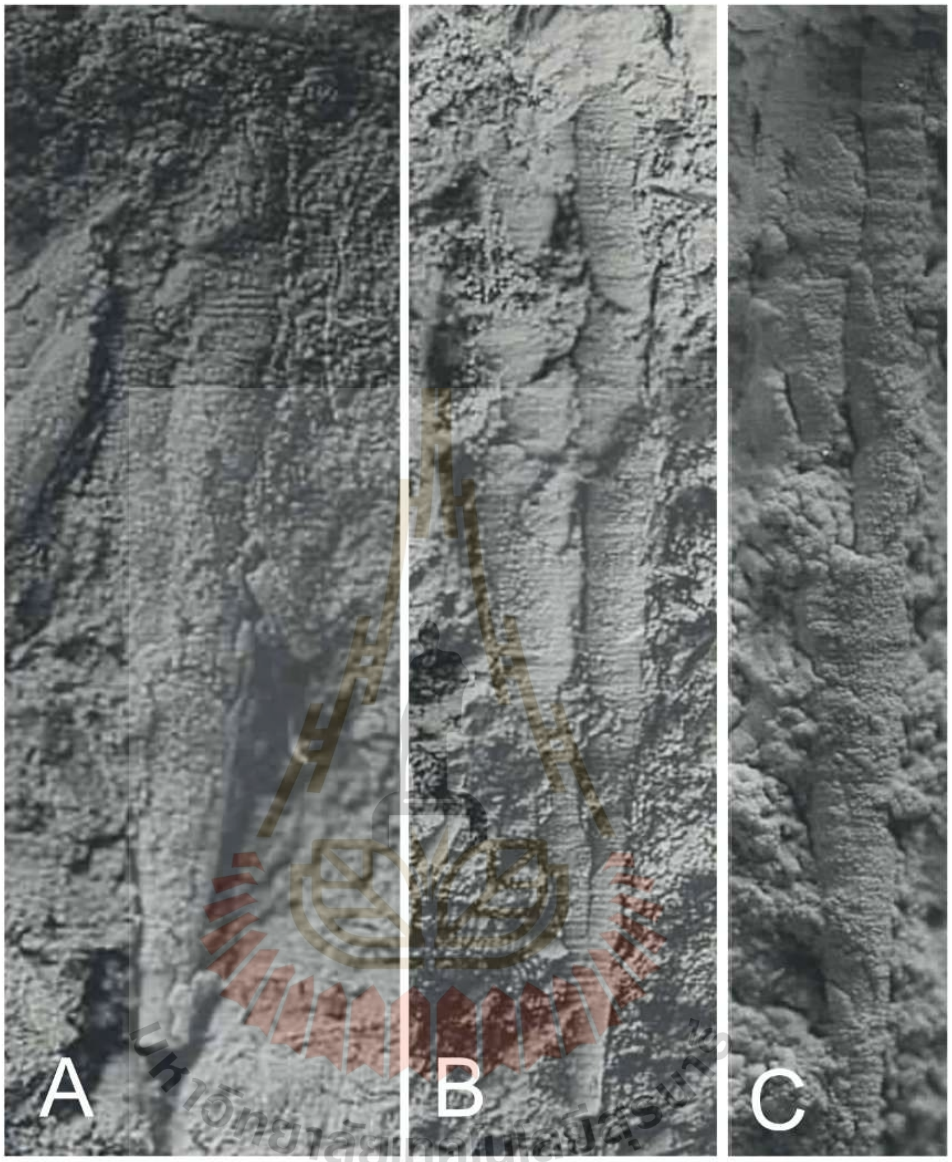

Figure 5.43 A-C *Guerichina* sp. SEM image, 15x magnification.

Family STRIATOSTYLIONIDAE Bouček, 1964

Genus *Striatostyliolina* Bouček and Prantl, 1961

***Striatostyliolina* sp.**

(Figure 5.44)

Occurrence: 19KT12

Remarks: The specimens exhibit a straight conch with a smooth surface and faintly discernible longitudinal ribs, a characteristic feature of *Striatostyliolina*. However, due to the low-quality image and poor preservation, a definitive identification is not possible.

Figure 5.44 *Striatostyliolina* sp. SEM image, 15x magnification.

CHAPTER VI

THIN SECTION ANALYSIS

This chapter presents a detailed analysis of the rock subunits in the Ban Thung Samed section. By utilizing thin section descriptions and interpretations, it offers valuable insights into the environmental conditions that influenced the formation of these rock units.

6.1 Thin section analysis

The rock samples, collected from conodont study, which is limestone, were prepared into 4 thin sections per sample. The samples included U1L, U1M, and U1U from lower, middle and upper of the lower subunit; U2L and U2U from lower and upper of the middle subunit; and U3L, U3M, and U3U from lower, middle and upper of the upper subunit. These thin sections were examined using a polarized-light microscope, following the classification outlined by Dunham (1962) (Figure 6.1).

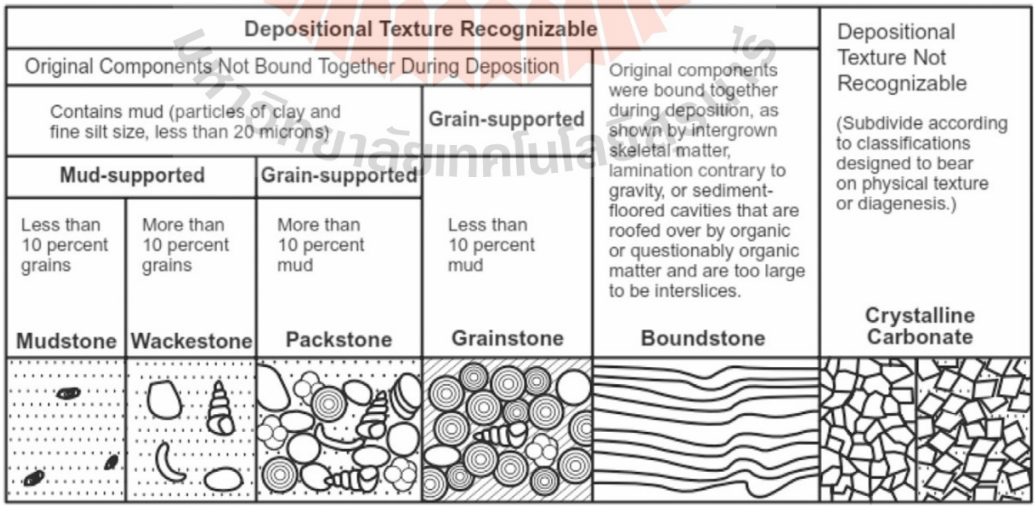

Figure 6.1 Dunham's carbonate rock classification (Al Omari et al., 2016).

Dunham's (1962) classification defines carbonate rocks based on their texture and the ratio of grains (allochems) to matrix (mud/micrite). Mudstone is characterized by less than 10% grains, with the rock being predominantly matrix-supported. Wackestone contains more than 10% grains while remaining matrix-supported; if grain content is below 50%, it is classified as sparse wackestone, whereas grain content above 50% qualifies as packed wackestone.

Packstone is a grain-supported limestone that contains more than 10% matrix, indicating some remaining micrite, while Grainstone is also grain-supported but contains less than 10% matrix, reflecting a well-washed and compact texture.

Boundstone refers to carbonate rocks where grains were bound together during deposition and includes reef-building organisms as well as microbial structures like stromatolites.

Crystalline Carbonate encompasses limestone or dolomite that has undergone diagenetic processes, which obscure the original depositional texture.

6.1.1 The lower subunit

The limestone of lower subunit composed of unsorted, fine-grained bioclasts, most of which are less than 1 mm in size and are embedded in a lime mud matrix. These bioclasts contribute between 10% to 50% of the total volume, with

Figure 6.2 Photomicrographs of sample U1L under ppl, scale bar = 1 mm. A. bioclastic wackestone with argillaceous seams (Arg), tentaculitoid (Ten), and microfilaments. B. bioclastic wackestone with argillaceous seams (Arg) and microfilaments.

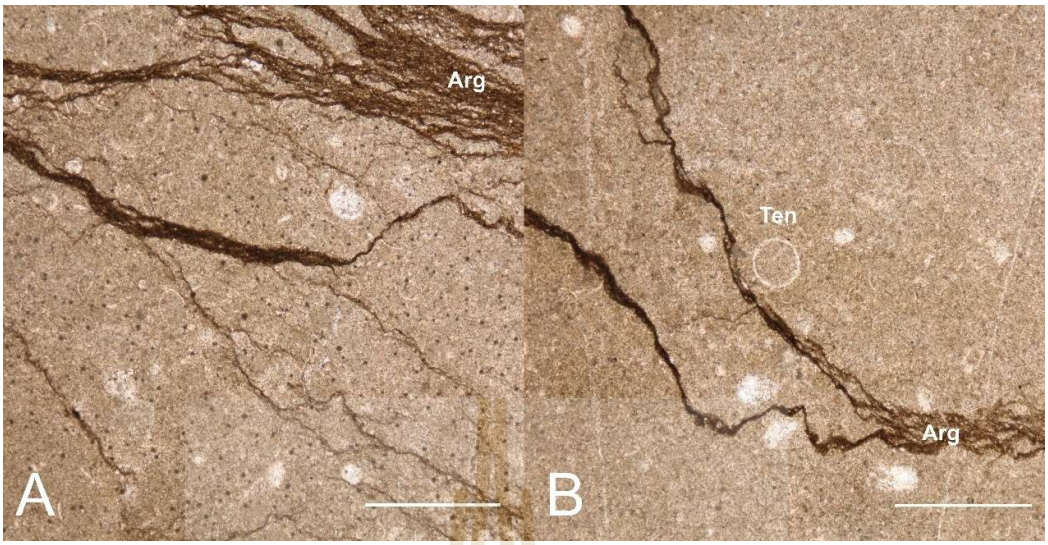

Figure 6.3 Photomicrographs of sample U1M under ppl, scale bar = 1 mm. A. bioclastic wackestone with argillaceous seams (Arg) and microfilaments. B. bioclastic wackestone with argillaceous seams (Arg), transverse cross-sectioned tentaculitoid? (Ten) and microfilaments.

sample U1L ranging from approximately 15-40%; sample U1M from 10-20%; sample U1U from 15-30%. Based on this composition, the subunit is classify as fine-grained bioclastic sparse wackestone. Argillaceous seams are observed in all samples and appear to have formed after lithification, as they frequently crosscut multiple bioclasts. Their development may be attributed to pressure solution processes (Figures 6.2-6.4). The bioclasts includes tentaculitoids (Figures 6.2A, 6.3B, 6.4A), gastropods (Figure 6.4B), trilobite fragments (Figure 6.4B), and microfilaments (Figures 6.2-6.4). The microfilaments are difficult to precisely identify, as they may originate from bivalves, brachiopods, or ostracods (Figures 6.2-6.4).

The fine-grained bioclastic sparse wackestone of lower subunit can be compared to standard microfacies (SMF) 8 of Flügel (2010), characterized by “wackestone with whole fossils and well-preserved infauna and epifauna, burrows are common”. According to Wilson’s facies zone (FZ), SMF 8 can occur in shallow open

shelf lagoon or just below fair-weather wave base (FZ 7), deep open shelf (FZ 2) (Flügel, 2010).

The presence of unsorted, fine-grained bioclasts suggests deposition in a low energy environment, where limited transport prevented significant grain sorting (Flügel, 2010). based on regional stratigraphic studies, carbonate deposition from the Late Ordovician to Silurian in the area occurred in subtidal ramp to deep shelf settings under cool-water tropical conditions, which continued into the Devonian (Department of Mineral Resources, 2018). This broader paleoenvironmental context indirectly supports the interpretation of SMF 8 in this study as representing deposition in subtidal below the fair-weather wave base to deep open shelf environment. A regression to lagoonal conditions is unlikely, particularly given the absence of large skeletal fauna typically associated with shallow, high-energy settings such as inner ramp shoals and lagoons (Flügel, 2010). Although burrows are absent in the lower subunit thin section, the presence of diverse benthic taxa (e.g. gastropods, trilobites, microfilaments), along with bioturbation reported by Itsarapong et al. (2023), suggests normal bottom-water

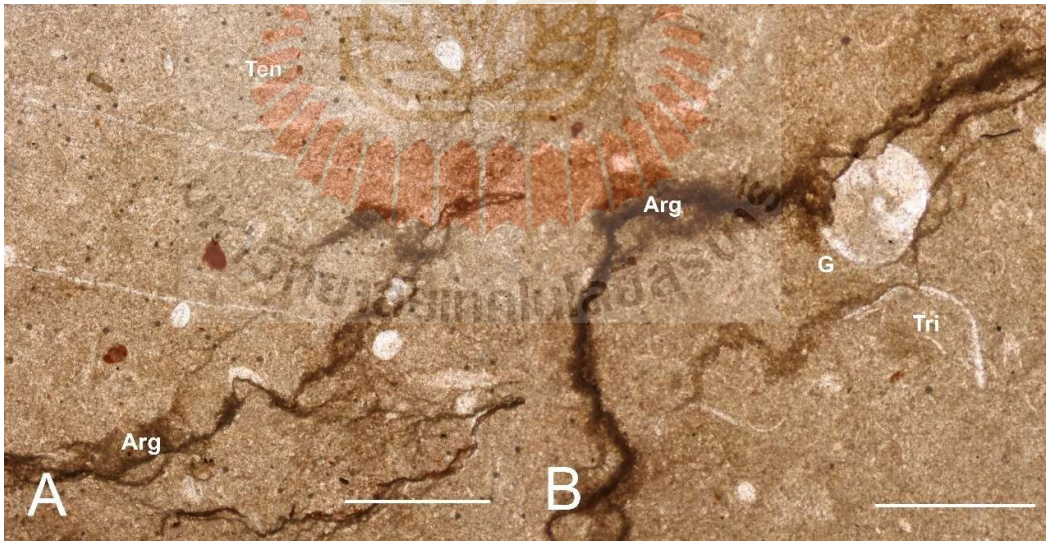

Figure 6.4 Photomicrographs of sample U1U under ppl, scale bar = 1 mm. A. bioclastic wackestone with argillaceous seams (Arg), longitudinal cross-sectioned tentaculitoid (Ten) and microfilaments. B. bioclastic wackestone with argillaceous seams (Arg), gastropod (G), trilobite (Tri) and microfilaments.

oxygenation (Allison et al., 1995). The scarcity of pelagic organisms such as tentaculitoids, coupled with the dominance of benthic fauna, points to a shallower setting than the deep shelf. This supports an interpretation of deposition in subtidal settings below the fair-weather wave base, rather than in deeper waters where pelagic microfossils are typically more abundant (Flügel, 2010).

In conclusion, SMF 8 represents subtidal open marine conditions below the fair-weather wave base. The faunal assemblage suggests a moderately deep, well oxygenated, low energy environment, rather than a deep shelf or restricted lagoonal setting.

6.1.2 The middle subunit

The middle subunit is composed of limestone interbedded with black shale. However, thin section analysis was limited to the limestone, as samples from the black shale beds were not successfully obtained. The limestone comprises unsorted, fine-grained bioclasts, most of which are less than 1 mm in size, with a minority exceeding 1 mm, within a lime mud matrix. These bioclasts make up more

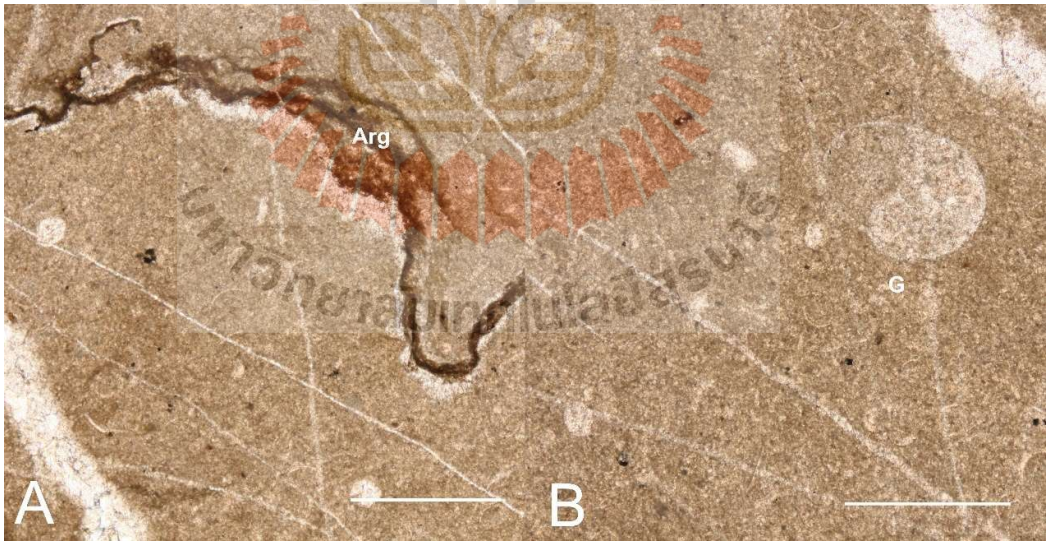

Figure 6.5 Photomicrographs of sample U2L under ppl, scale bar = 1 mm. A. bioclastic wackestone with argillaceous seams (Arg) and microfilaments. B. bioclastic wackestone with gastropod (G) and microfilaments.

than 10% but less than 50% of the total volume, with sample U2L contributing approximately 10-25% and sample U2U contributing 30-40%, classifying the subunit as fine-grained bioclastic sparse wackestone. Argillaceous seams, likely the result of pressure solution processes, are observed in all samples (Figures 6.5A, 6.6A). The bioclast assemblage includes gastropods (Figure 6.5B), tentaculitoids (Figure 6.6), ostracods (Figure 6.6A), echinoderms (Figure 6.6A), and microfilaments (figures 6.5, 6.6).

The fine-grained bioclastic sparse wackestone of the middle subunit can be compared to SMF 8 and likely indicates subtidal open marine conditions below the fair-weather wave base, as the thin section features are consistent with those of the lower subunit. However, this subunit was likely deposited in a slightly deeper setting, as suggested by the lithological shift from bedded limestone to interbedding with black shale.

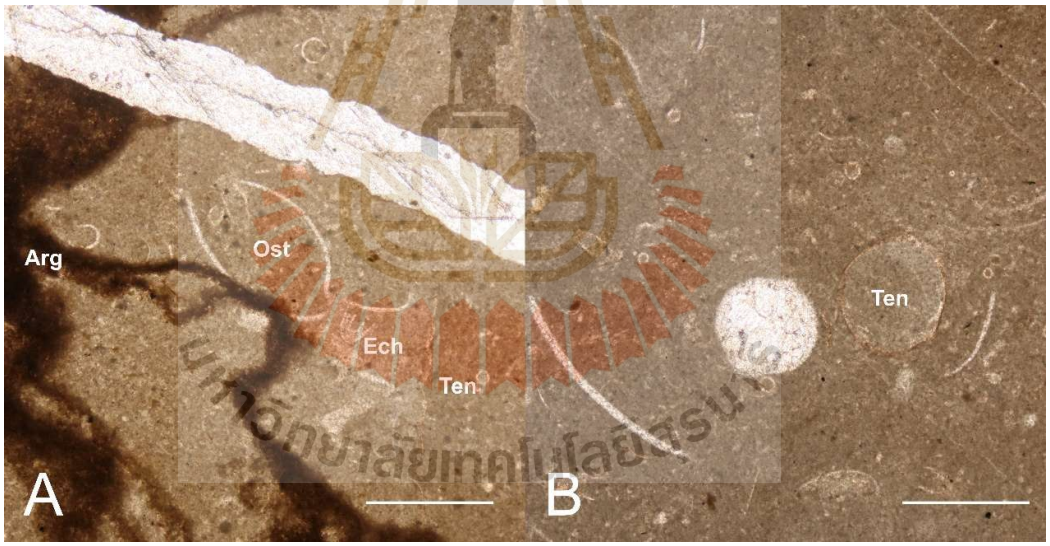

Figure 6.6 Photomicrographs of sample U2U under ppl, scale bar = 1 mm. A. bioclastic wackestone with longitudinal cross-sectioned tentaculitoid (Ten), echinoderm (Ech), cross-sectioned ostracod shell (Ost), argillaceous seams (Arg) and microfilaments. B. bioclastic wackestone with transverse cross-sectioned tentaculitoid (Ten) and microfilaments.

In conclusion, the middle subunit is interpreted as having been deposited in a subtidal below the fair-weather wave base, low energy conditions to deep marine environment, representing a shift to a deeper depositional setting relative to the lower subunit.

6.1.3 The upper subunit

The upper subunit consists of limestone interbedded with black shale. Thin section analysis was limited to the limestone, as samples from the black shale beds could not be successfully obtained. The limestone contains unsorted, fine-grained bioclasts with size variations between samples. Most bioclasts are less than 1 mm in size; however, sample U3U shows a higher proportion of bioclasts exceeding 1 mm, all embedded within a lime mud matrix. These bioclasts contribute more than 10% of the total volume, with sample U3L contributing approximately 30–50%, sample U3M 50–60%, and sample U3U more than 50%. Based on this composition, the subunit is classified as fine-grained bioclastic sparse wackestone for sample U3L, and bioclastic packed wackestone for samples U3M and U3U. While Figure 6.11 depicts packed

Figure 6.7 Photomicrographs of sample U3L under ppl, scale bar = 1 mm. A. bioclastic wackestone with longitudinal cross-sectioned tentaculitoid (Ten) and abundant cross-sectioned tentaculitoid (circular or ellipse shape). B. bioclastic wackestone with longitudinal cross-sectioned *styliolina* (Sty), pyrite (Pyr) and cross-sectioned of other tentaculitoid (circular or ellipse shape).

tentaculitoids resembling a grain-supported texture which only occurs in a thin layer, the overall composition of sample U3U supports classification as packed wackestone when the sample is considered in its entirety. The bioclasts in the upper subunit are predominantly composed of tentaculitoids, with occasional trilobite fragments (Figure 6.9B). Argillaceous seams are still observed in sample U3M (Figure 6.9), while pyrite is present in all samples (Figures 6.7–6.9, 6.10A).

According to Flügel (2010), fine-grained bioclastic wackestone dominated by pelagic organisms such as tentaculitoids corresponds to SMF 3-TENT. This microfacies is typically associated with basin (FZ 1-B) and open deep shelf (FZ 3) settings within Wilson's facies zone.

In the lower part of the upper subunit, the occurrence of minor benthic organisms (e.g. trilobites), along with bioturbation and brachiopods reported by Itsarapong et al. (2023), suggests an open deep shelf setting where benthic life persists

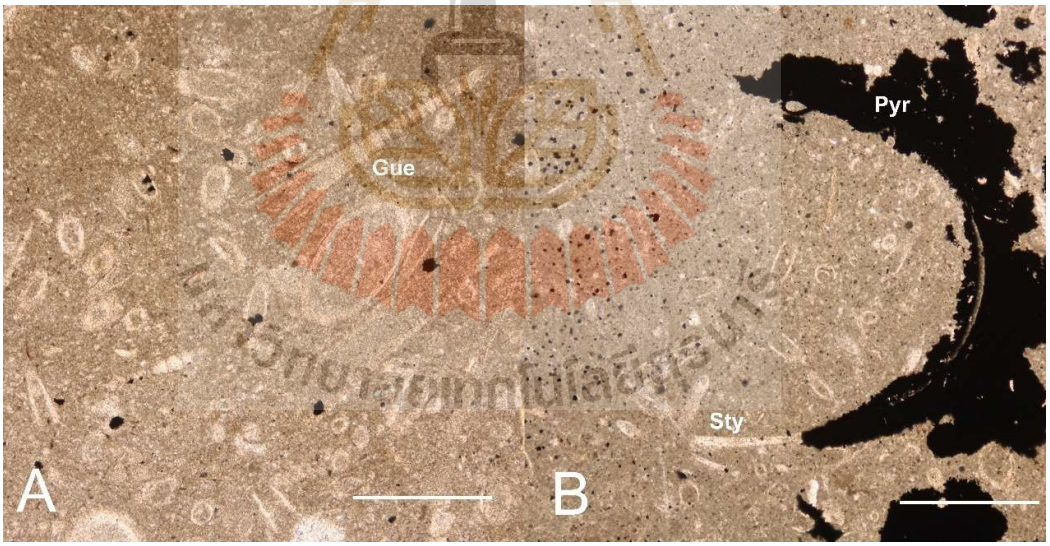

Figure 6.8 Photomicrographs of sample U3L under ppl, scale bar = 1 mm. A. bioclastic wackestone with longitudinal cross-sectioned *Guerichina* (Gue) and abundant cross-sectioned tentaculitoid (circular or ellipse shape). B. bioclastic wackestone with longitudinal cross-sectioned *styliolina* (Sty), pyrite (Pyr) and cross-sectioned of other tentaculitoid (circular or ellipse shape).

(Flügel, 2010). The presence of bioturbation and benthic fauna, despite the dominance of pelagic organisms, rules out anoxic conditions that would typically eliminate benthic communities (Allison et al., 1995). Moreover, pyrite within this subunit, observed replacing or surrounding fossils (Figures 6.8B, 6.10A), likely reflects bacterial sulfate reduction of organic matter rather than persistent euxinic conditions. As noted by Berner (1984), under euxinic conditions (absence of oxygen, elevated hydrogen sulfide) pyrite can form throughout bottom waters regardless of organic matter position.

In the upper part of the upper subunit, bioclasts remain dominated by tentaculitoids (dacryoconarids), consistent with SMF 3-TEN. The matrix is composed of a dark, organic-rich substrate, accounting for approximately 50% of the matrix volume. Some layers display thin, tentaculitoid-rich beds (Figure 6.11) that are devoid of benthic fauna. This shift reflects a transition to a deeper marine environment, where declining oxygen levels likely suppressed benthic activity and bioturbation.

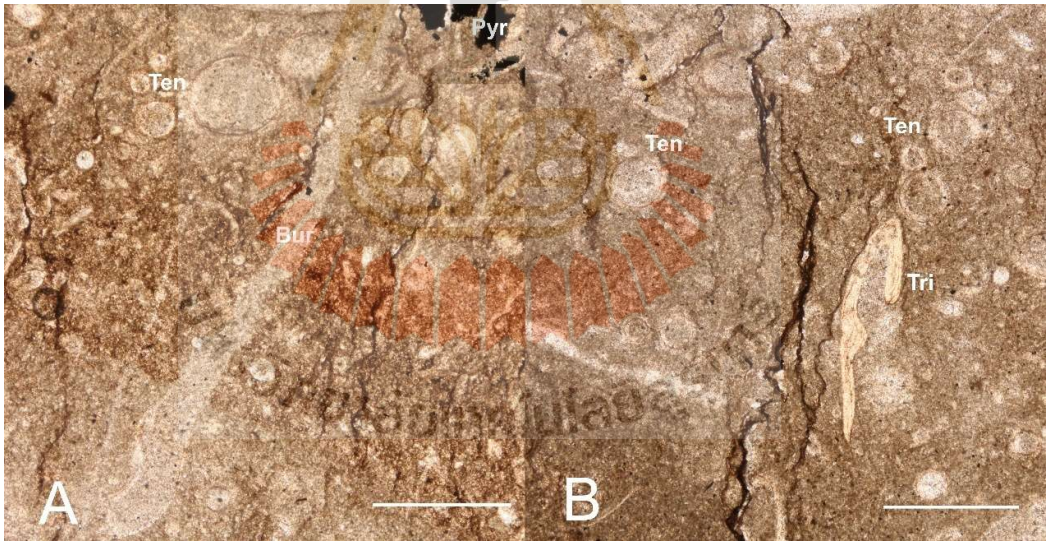

Figure 6.9 Photomicrographs of sample U3M under ppl, scale bar = 1 mm. A. bioclastic wackestone with abundant cross-sectioned tentaculitoid (Ten), pyrite (Pyr), argillaceous seams and burrow (Bur). B. bioclastic wackestone with abundant cross-sectioned tentaculitoids (Ten), trilobite fragment (Tri) and argillaceous seams.

In conclusion, the upper subunit is interpreted as a deep marine environment. The lower and middle part retain enough oxygen to sustain benthic communities, but the upper part reflects a significant shift to low-oxygen conditions, effectively reduces or eliminates benthic organisms, particularly within the tentaculitoid-rich beds.

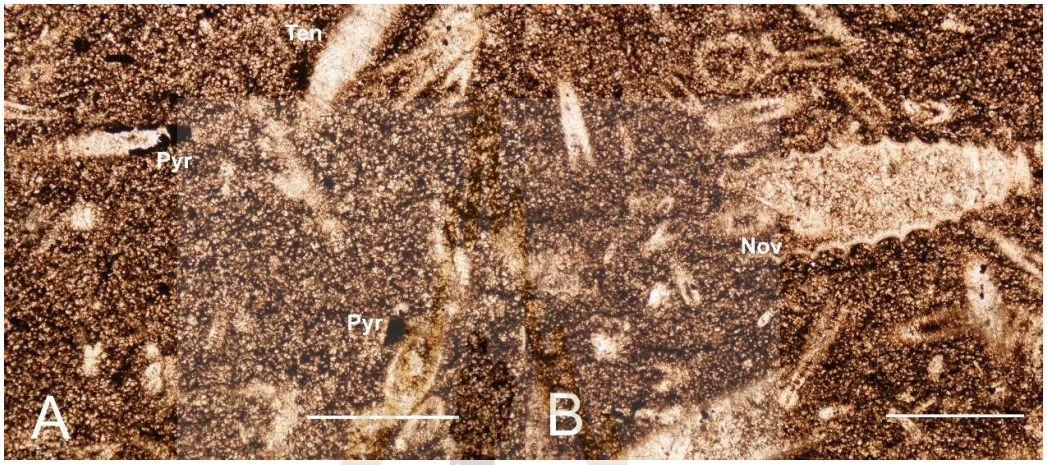

Figure 6.10 Photomicrographs of sample U3U under ppl, scale bar = 1 mm. A. abundant longitudinal cross-sectioned tentaculitoids and *Nowakia* (Nov). B. abundant longitudinal cross-sectioned tentaculitoids and the cross-sectioned *Nowakia* (Nov) and *Styliolina* (Sty).

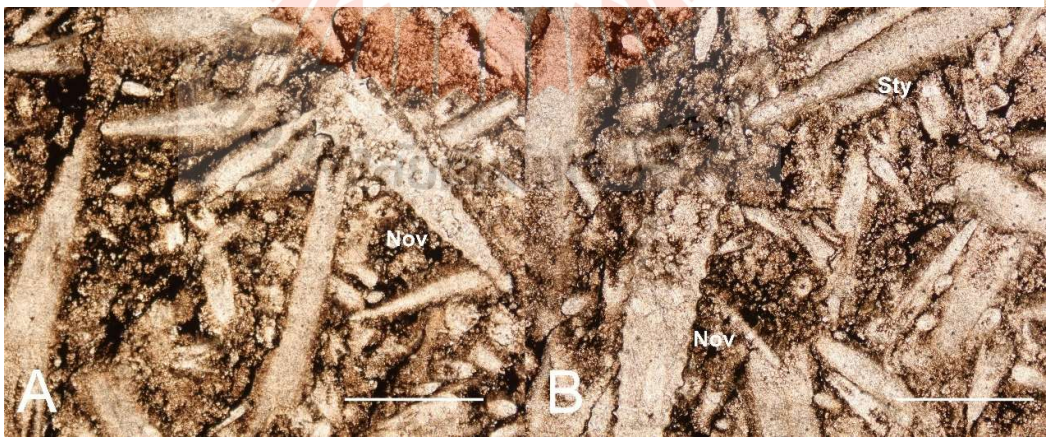

Figure 6.11 Photomicrographs of sample U3U under ppl, scale bar = 1 mm. A. bioclastic wackestone with abundant cross-sectioned tentaculitoids (Ten) and pyrite (Pyr). B. bioclastic wackestone with abundant cross-sectioned tentaculitoids and cross-sectioned *Nowakia* (Nov).

CHAPTER VII

DISCUSSION AND CONCLUSION

This chapter provides a discussion and conclusion on the paleoenvironments of the Ban Thung Samed section, based on analyses of ostracod assemblages and thin sections. It highlights the stratigraphic shift from subtidal to deep marine settings, focusing on changes in faunal composition and environmental conditions, and concludes with recommendations for future research directions.

7.1 Discussion

7.1.1 Paleoenvironment of Ban Thung Samed section

The ostracods recovered from the study section were found only in samples 19KT01-07 ranges from the lower to middle subunits. These ostracods belong to 6 suborders, Podocopina, Metacopina, Palaeocopina, Paraparchiticopina, Platycopina, and Eridostraca.

The most diverse group is the superfamily Bairdiocypridoidea from Podocopina, representing 50% of the total species, with 17 species identified. This superfamily includes 4 families: Pachydomellidae (genera *Ampuloides* and *Microcheilinella*), Bairdiocyprididae (genera *Bairdiocypris* and *Baschkirina*?), Rectellidae (genus *Rectella*), and Krausellidae (genus *Pseudorayella*).

The superfamily Bairdioidea is the second most prevalent group, also within Podocopina, contributing 17.6% of the species diversity. This group is represented by 4 species from 2 families: Acratiidae (genus *Acratia*) and Bairdiidae (genera *Bairdia* and *Fabalicypris*), along with Bairdioidea indet.

The superfamily Healdioidea, part of the suborder Metacopina, is represented by the family Healdiidae, with 4 species across 3 genera (*Cytherellina*, *Healdia*, and *Kummerowia*?), accounting for 11.7% of the total species.

The superfamily Aparchitoidea, belonging to the suborder Palaeocopina, is represented by the family Aparchitidae, which includes 3 species from the genera *Aparchites* and *Brevidorsa*, making up 8.7% of the species.

The superfamily Paraparchitoidea, from the suborder Paraparchiticopina, is represented by 2 species from the family Paraparchitidae (genera *Samarella* and *Coelonella*), accounting for 5.8% of the total species.

Only one species from the superfamily Kloedenelloidea (family Knoxitidae), tentatively identified as *Knoxiella* sp., was found in the suborder Platycopina, contributing 2.9% of the total species. Additionally, a single taxon from the suborder Eridostraca, identified as Eridoconchidae indet., also accounts for 2.9% of the species (Figure 7.1).

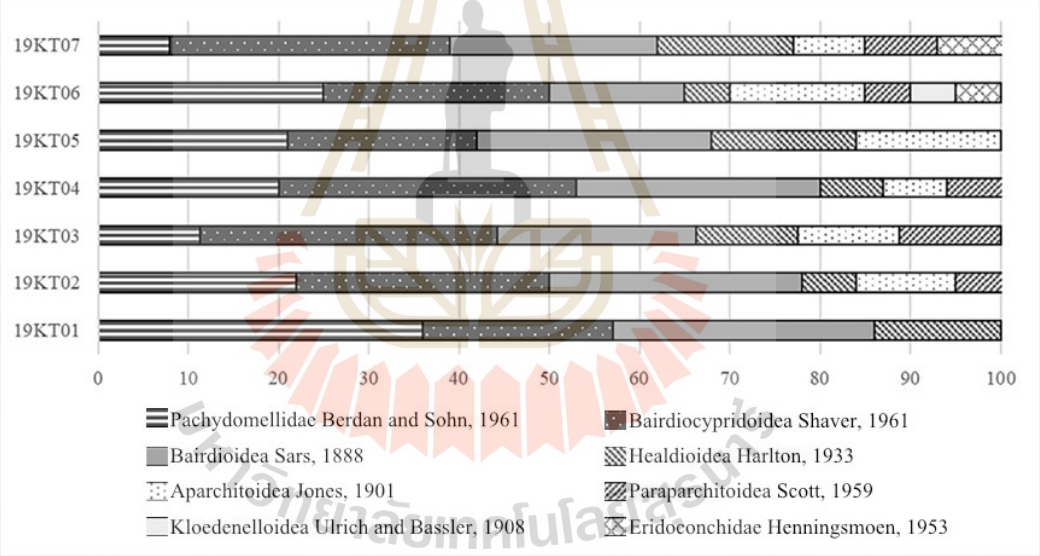

Figure 7.1 Percentage distribution of ostracod species by superfamily and family in the Ban Thung Samed section.

Understanding the taphonomy of fossilized ostracod assemblages is essential for reconstructing paleoenvironments. Ostracod deposition in sediment can be influenced by various factors, with currents being particularly significant. Currents can sort and transport ostracod shells, resulting in assemblages with distinct

characteristics, such as containing only adults, only juveniles, or a high ratio of disarticulated valves to carapaces. Such assemblages are less reliable for paleoenvironmental interpretation, as they do not represent the environment where the ostracods originally lived and died (Boomer et al., 2003). In contrast, the ostracod assemblage in the study section consists entirely of carapaces, with no disarticulated valves, and includes both adults and juveniles (see Promduang and Chitnarin, 2025). This composition suggests deposition in a low-energy current environment, making the assemblage well-suited for paleoenvironmental reconstruction.

The ostracod fauna in the study section is predominantly composed of Bairdiocypridoidea, with Bairdioidea as a secondary group, while Healdioidea, Aparchitoidea, Paraparchitoidea, Kloedenelloidea, and Eridoconchidae are present in minor or rare occurrences. This ostracod assemblage corresponds with the Eifelian Mega-Assemblage (Assemblage III), indicating a shallow marine environment below the fair-weather wave base. The relative proportions of families show minimal variation across sampling levels, suggesting a stable depositional environment. While a small increase in kloedenellids and eridoconchids is observed in samples 19KT06 and 19KT07 (Figure. 7.1), this is not significant enough to indicate a transition to the shallower conditions of Assemblage II. The lack of Leperditicopid ostracods eliminates the possibility of Assemblage 0 shallow environment, while lack of Myodocopid ostracods excludes the pelagic conditions associated with the Entomozoacean Mega-Assemblage. The ratio between Podocopida and Metacopida fluctuates without a clear trend, making it unreliable for interpreting water-depth variations. In the upper section, ostracods disappear, likely due to a change of facies from a carbonate-dominated to a clastic-dominated environment. This shift is less suitable for benthic ostracods, either because the new conditions are unfavorable for their survival or because poor fossil preservation in clastic sediments makes fossil recovery difficult.

The paleoenvironmental interpretation derived from the ostracod assemblage, which covers only the lower and middle subunits, aligns with results from thin section analysis. Both suggest deposition below the fair-weather wave base,

transitioning into deeper water environments in the upper subunit where pelagic organisms dominate. In the upper subunit, where ostracods are absent, the presence of benthic fauna such as trilobites and gastropods, along with bioturbation evidence (burrows) observed in thin section analysis and noted by Itsarapong et al. (2023), indicates that the deep marine environment maintained sufficient oxygen levels to support benthic communities. The evidence suggests this environment was neither anoxic nor dysaerobic until the transition into a tentaculitoid-rich bed with a reduction in benthic fauna in the uppermost part of the section.

This interpretation is further supported by studies from Fortey (1989) and Crônier and Fortey (2006), who identified Early Devonian trilobites such as *Plagiolaria poothaii* Kobayashi and Hamada, 1968 in black shale from Member 1 of the original Pa Samed Formation. These trilobites, with reduced eyes, represent an atheloptic assemblage adapted to deep-water benthic conditions. Boucot et al. (1999) examined Early Devonian brachiopods from original Pa Samed Formation and interpreted the paleoenvironments as deep marine deposits at depths of 150 to 200 meters, influenced by moderate current activity. Their conclusion was based on evidence of disarticulated brachiopod valves and trilobites. However, the interpretation of moderate currents appears to contradict the findings of this study, which suggest deposition under low-energy current conditions. Agematsu et al. (2006a) studied tentaculitoids from the black shale of the original Pa Samed Formation, including evidence from thin sections. The thin section revealed tentaculitoids scattered randomly on the bedding plane, with no signs of sorting or parallel alignment, suggesting deposition under low-energy current conditions. In contrast, the disarticulated brachiopod valves and trilobites reported by Boucot et al. may have resulted from benthic organism activity or could reflect differences in depositional environments between the studied beds, as Boucot et al. did not specify the sampling horizon. Further research is required to resolve these discrepancies.

7.2 Conclusion

The study section named “Ban Thung Samed” belongs to revised Kuan Tung Formation of Itsarapong et al. (2023), ranges approximately 50 meters, and well-bedded rocks are continuously exposed. The average bedding orientation is 080°/40 (strike/dip). This section consists of lower, middle, and upper subunits. The lower subunit primarily consists of medium to thick layers of reddish-grey limestone interspersed with thin argillaceous layers. The middle subunit is characterized by medium bedded reddish-grey limestone interbedded with black shale. The upper subunit is composed of sequences of black shales and thin to medium-bedded dark grey limestones, with an increasing proportion of black shales towards the top. The limestone in the study section comprises of fine-grained bioclastic sparse wackestone in the lower and middle subunits includes the lower of upper subunit and for the middle and upper of upper subunit, limestone is classified as bioclastic packed wackestone. Bioclasts in the lower subunit are generally small, measuring less than 1 mm in size, and include tentaculitoids, gastropods, trilobites, and microfilaments. In the middle subunit, bioclasts are more abundant and similar in size to those in the lower subunit, with only a few specimens exceeding 1 mm, the assemblage includes tentaculitoids, gastropods, ostracods, echinoderms, and microfilaments. In contrast, the upper subunit is dominated by tentaculitoids, most of which are larger than 1 mm.

The age of Ban Thung Samed section ranges from Late Silurian to Early Devonian (from late Ludlow to late Pragian or earliest Emsian). Based on the occurrence of Late Silurian – Early Devonian conodont group (*Ozarkodina*, *Belodella*, *Pseudooneotodus*, *Wurmiella*, and *Zieglerodina* and an index fossil *Ozarkodina crispa* in the lower subunit make it late Ludlow. The age of the upper subunit can only correlate with previous works based on the tentaculitoids-graptolites bearing black shale which indicate Early Devonian (late Pragian or earliest Emsian).

A total of 586 complete ostracod carapaces, including both adults and juveniles, were identified, representing 34 species from 17 genera, belonging to 6 superfamilies including Bairdiocypridoidea, Bairdioidea, Healdioidea, Aparchitoidea,

Paraparchitoidea, and Kloedenelloidea. Additionally, 103 conodont specimens were identified, encompassing 7 species from 5 genera: *Ozarkodina*, *Belodella*, *Pseudooneotodus*, *Wurmiella*, and *Zieglerodina*. The tentaculitoid fossils were classified as *Nowakia* sp., *Guerichina* sp., and *Striatostyliolina* sp.

The Ban Thung Samed section records a transition from subtidal conditions below the fair-weather wave base to deeper marine settings dominated by pelagic organisms. The lower and middle subunits supported diverse benthic communities in well-oxygenated environments, while the upper subunit reflects deeper, low-oxygen conditions that reduced benthic fauna.

7.3 Recommendations for future studies

1) As previously mentioned, the current conodont sampling is insufficient to precisely determine the Silurian-Devonian boundary, and the upper part of the section is vaguely defined. A more comprehensive biostratigraphic analysis is required to better define these boundaries and enhance our understanding of the stratigraphic transitions.

2) The abundance of conodont elements presents an opportunity for isotopic analysis, which could provide new insights into the paleoenvironment of this section.

REFERENCES

Abushik, A. F., Ivanova, V. A., Kotchetkova, N. M., Martinova, G. P., Neckaja, A. I., & Rozhdestvenskaja, A. A. (1960). New Palaeozoic ostracodes of the Russian and Siberian platforms, the Urals and Pechora Range. In: *New Species of Ancient Plants and Invertebrates of the USSR*, *Moscow*, *2*: 280–366, 492-517 [in Russian].

Adamczak, F. (1976). Middle Devonian Podocopida (ostracoda) from Poland; Their morphology, systematics, and occurrence. *Senckenbergiana Lethaea*, *57*: 265-467.

Agematsu, S., Sashida, K., Salyapongse, S., & Sardsud, A. (2006a). Lower Devonian tentaculite bed in the Satun area, Southern Peninsular Thailand. *Journal of Asian Earth Sciences*, *26(6)*: 605-611.

Agematsu, S., Sashida, K., Salyapongse, S., & Sardsud, A. (2006b). Ordovician-Silurian boundary graptolites of the Satun area, Southern Peninsular Thailand. *Paleontological Research*, *10*: 207-214.

Agematsu, S., Sashida, K., Salyapongse, S., & Sardsud, A. (2007). Ordovician conodonts from the Satun area, Southern Peninsular Thailand. *Journal of Paleontology*, *81(1)*: 19-37.

Agematsu, S., Sashida, K., Sarsud, S. and Machida, N., 2017. Ordovician- Silurian-Devonian: Significance of fossil assemblages at Tarutao, Khao Noi, and Kuan Tung, Satun Aspiring Geopark. In S. Techawan and A. Surinkum (eds). *DMR-CCOP-TNCU Technical Seminar on "Biostratigraphy and Karst Morphology of Satun Aspiring Geopark"*, Department of Mineral Resource, Thailand: 23-27.

Al Omari, M. M. H., Rashid, I. S., Qinna, N. A., Jaber, A. M., & Badwan, A. A. (2016). Chapter two - calcium carbonate. In: H. G. Brittain (Ed.), *Profiles of drug substances, excipients and related methodology*. Academic Press, pp. 31-132.

Allison, P. A., Wignall, P. B., & Brett, C. E. (1995). Palaeo-Oxygenation: Effects and Recognition. *Geological Society, London, Special Publications, 83(1)*: 97-112.

Anderson, M. A. (2003). A study of conodont genera *Belodella* and *Neopanderodus* with emphasis on faunas from Eastern Australia. *CFS Courier Forschungsinstitut Senckenberg*: 463-491.

Bancroft, A. M., & Cramer, B. D. (2020). Silurian conodont biostratigraphy of the East-Central Appalachian Basin (Eastern USA): Re-examination of the C.T. Helfrich collection. *Bulletin of Geosciences*, *95(1)*: 1-22.

Bandel, K., & Becker, G. (1975). Ostracoden aux Paläozoischen pelagischen kalken der Karnischen Alpen (Silurium bis Unterkarbon). *Senckenbergiana lethaea*, *56*: 1-83.

Barrande, J. (1852). Système silurien du centre de la Bohême: *1re partie: Recherches paléontologiques. Prague: Chez l'auteur et éditeur*.

Bateson, W. (1886). The ancestry of the chordata. *Quarterly Journal of Microscopical Science. 26*: 535–571

Becker, G. (1964). Palaeocopida (Ostracoda) aus dem Mitteldevon der Sötenicher Mulde (N-Eifel). *Senckenbergiana lethaea, 45*: 43–113.

Becker, R. T., Marshall, J. E. A., Da Silva, A. C., Agterberg, F. P., Gradstein, F. M., & Ogg, J. G. (2020). Chapter 22 - the Devonian Period. In: F. M. Gradstein, J. G. Ogg, M. D. Schmitz, & G. M. Ogg (Eds.), *Geologic time scale 2020*. Elsevier, pp. 733-810.

Bennett, C., Siveter, D., Davies, S., Williams, M., Wilkinson, I., Browne, M., & Miller, C. (2012). Ostracods from freshwater and brackish environments of the Carboniferous of the Midland Valley of Scotland: The early colonization of terrestrial water bodies. *Geological Magazine*, 149: 366-396.

Benson, R. H., Berdan, J. M., van den Bold, W. A., Hanai, T., Hessland, I., Howe, H. V., Kesling, R. V., Levinson, S. A., Reyment, R. A., Moore, R. C., Scott, H. W., Shaver, R. H., Sohn, I. G., Stover, L. E., Swain, F. M., & Sylvester-Bradley, P. C. (1961). Systematic description. In: R. C. Moore and C. W. Pitrat (Eds.), *Treatise on invertebrate paleontology, part Q arthropoda 3 crustacea ostracoda*. Geological Society of America, Boulder and University of Kansas Press, Lawrence, pp. 99-421.

Berdan, J. M., & Sohn, I. G. (1961). Family Pachydomellidae Berdan & Sohn, N. Fam. In: R. C. Moore (Ed.), *Treatise on invertebrate paleontology, part Q, arthropoda 3*

crustacea ostracoda. Geological Society of America and University of Kansas Press., Lawrence, pp. 373.

Berner, R. A. (1984): Sedimentary pyrite formation: an update. Geochim. *Cosmochim. Acta, 48*: 605-615

Bergström, S. M. (1981). Family Balognathidae - Family Ulrichodinidae. In: R. A. Robison (Ed.), *Treatise on invertebrate paleontology, part w, supplement 2 conodonta*. Geological Society of America and the University of Kansas, Lawrence.

Bischoff, G., & Sannemann, D. (1958). Unterdevonische conodonten aus dem Frankenwald. *Notizblatt des hessisches Landesamt für Bodenforschung zu Wiesbaden, 86*: 87-110.

Blumenstengel, H. (1970). Zur paläontologie und biostratigraphie des paläozoikums und mesozoikums europas. *Freiberger Forschungshefte*, C256: 7-63.

Boomer, I., Horne, D. J., & Slipper, I. J. (2003). The use of ostracods in palaeoenvironmental studies, or what can you do with an ostracod shell?. *The Paleontological Society Papers, 9*: 153-180.

Boomer, I., Whatley, R., Bassi, D., Fugagnoli, A., & Loriga, C. (2001). An Early Jurassic Oligohaline ostracod assemblage within the marine carbonate platform sequence of the Venetian Prealps, Northeast Italy. *Palaeogeography, Palaeoclimatology, Palaeoecology, 166(3)*: 331-344.

Bouček, B. (1964). The tentaculites of Bohemia: Their morphology, taxonomy, ecology, phylogeny and biostratigraphy. *Publishing House of the Czechoslovak Academy of Sciences, Prague*: 215.

Bouček, B., & Prantl, F. (1960). Nekolik nomenklatorických poznámek k nadrádu tentaculitoidea (Ljašenko). *Časopis Národního Musea – Oddíl Prírodovedný*: 198-199.

Bouček, B., & Prantl, F. (1961). Über einige neue tentaculiten-gattungen aus dem böhmische Devon. *Vest. Ustr. ust. geol., 36*: 385-388.

Boucot, A. J., Cocks, L. R. M., & Racheboeuf, P. R. (1999). Early Devonian brachiopods from Satun Province, Southern Thailand. *Journal of Paleontology, 73(5)*: 850 – 859.

Brandão, S. N., Hoppema, M., Kamenev, G. M., Karanovic, I., Riehl, T., Tanaka, H., Vital, H., Yoo, H., & Brandt, A. (2019). Review of ostracoda (Crustacea) living below the carbonate compensation depth and the deepest record of a calcified ostracod. *Progress in Oceanography, 178*: 102144.

Branson, E. B., & Mehl, M. G. (1933). Conodont studies. *University of Missouri Studies, 8*: 1-343.

Briggs, D. E. G. (1992). Conodonts: A major extinct group added to the vertebrates. *Science, 256(5061)*: 1285-1286.

Bunopas, S. (1981). *Paleogeographic history of Western Thailand and adjacent parts of Southeast Asia – a plate tectonic interpretation*. PhD thesis, Victoria University of Wellington, New Zealand. (Reprinted in 1982 as Geological Survey Division, Department of Mineral Resources, Geological Survey Paper, No.5, special issue).

Burrett, C., Fang, X., Li, W., Thassanapak, H, & Udchachon, M. (2024). The first scyphocrinitid loboliths from Thailand. *Proceedings of the Geologists' Association, 135(1)*: 131-136.

Burrett, C., Udchachon, M., & Thassanapak, H. (2021). The Truong Son, Loei-Phetchabun, and Kontum Terranes in Indochina: Provenance, rifting, and collisions. *Frontiers in Earth Science*, 9.

Casier, J-G., (1988). Présence de Cypridinacea (ostracodes) dans la partie Supérieure du Frasnien du Bassin de Dinant. *Bulletin de l'Institut Royal des Sciences Naturelles de Belqique, Sciences de la Terre, 58*: 89-94.

Casier, J-G. (2004). The mode of life of Devonian Entomozoacean ostracods and the Myodocopid mega-assemblage proxy for hypoxic events. *Bulletin de l'Institut Royal des Sciences Naturelles de Belqique, Sciences de la Terre, 74-suppl*.: 73-80.

Casier, J-G. (2007). Guide de l'excursion: Les ostracodes du Dévonien moyen et Superieur du Synclinorium de Dinant. In: J. G. Casier (Ed.), *Résumé des communications et guide de l'excursion de la 22ième Réunion des ostracodologistes de langue française, Bruxelles*: Institut royal des Sciences naturelles de Belgique, pp. 25-79.

Casier, J-G. (2017). Ecology of Devonian ostracods: Application to the Frasnian/Famennian boundary bioevent in the type region (Dinant Synclinorium, Belgium). *Palaeobiodiversity and Palaeoenvironments, 97(3)*: 553-564.

Casier, J-G., & Lethiers, F. (1997). *Micronewsomites* et *Decoranewsomites*, deux nouveaux genres d'ostracodes Dévoniens. *Revue de micropaléontologie, 40(2)*: 125-130.

Casier, J-G., & Préat, A., (1996). Ostracods and sedimentology from the Eifelian-Givetian transition in the marble quarry of Pic De Vissou (Montagne Noire, France). *Bulletin des Centres de Recherches Elf Exploration Production, 20*: 367-387.

Casier, J-G., Kasimi, R., & Preat, A. (1995). Les ostracodes au passage Eifelien/Givetien a Glageon (Avesnois, France). *Geobios, 28(4)*: 487-499.

Casier, J-G., Lethiers, F., & Baudin, F. (1999). Ostracods, organic matter and anoxic events associated with the Frasnian/Famennian boundary in the Schmidt quarry (Germany). *Geobios*, 32(6): 869-881.

Casier, J-G., Lebon, A., Mamet, B., & Préat, A. (2005). Ostracods and lithofacies close to the Devonian-Carboniferous boundary in the Chanxhe and Rivage sections, northeastern part of the Dinant Basin, Belgium. *Bulletin de l'Institut Royal des Sciences Naturelles de Belqique, Sciences de la Terre*. 75. 95-126.

Casier, J.-G., Devleeschouwer, X., Petitclerc, E., & Préat, A. (2011). Ostracods, rock facies and magnetic susceptibility of the Hanonet Formation/Trois-Fontaines Formation boundary interval (Early Givetian) at the Mont D'Haurs (Givet, France). *Bulletin de l'Institut royal des Sciences naturelles de Belgique, 81*: 63–96.

Chaodumrong, P., Assavapatchara, S., & Jongautchariyakul, S. (2004). *Final report on comparative research on Permian strata and fauna between West Yunnan and West Thailand*: Research project funded by national research council of Thailand. 1-235.

Chaodumrong, P., Xiangdong, W., & Shuzhong, S. (2007). Permian lithostratigraphy of the Shan-Thai Terrane in Thailand: Reservoir of the Kaeng Krachan and Ratburi Groups, in Tantiwanit, W., Ed. In Chief. *Proceedings of the International*

Conference on Geology of Thailand: Towards sustainable development and sufficiency economy, Bangkok, November 21-22, 2007, Department of Mineral Resources.

Chapman, F. (1904). New or little-known Victorian fossils in the National Museum. Part III: Some Palaeozoic Pteropoda. *Proceedings of the Royal Society of Victoria*, *16*, 336–342.

Chitnarin, A., & Ketwetsuriya, C. (2021). Middle Permian ostracod fauna from the Khao Khad Formation (Indochina Terrane), Central Thailand. *Annales de Paléontologie, 107*: 102521.

Chitnarin, A., Crasquin, S., Forel, M-B., & Tepnarong, P. (2017). Ostracods (Crustacea) of the Early-Middle Permian (Cisarulian-Guadalupian) from Central Thailand (Indochina Block): Part II, Orders Podocopida, Platycopida and Myodocopida. *Geodiversitas, 39(4)*: 651-690.

Chitnarin, A., Crasquin, S., Charoentitirat, T., Tepnarong, P., & Thanee, N. (2012). Ostracods (Crustacea) of the Early - Middle Permian from Central Thailand (Indochina Block). Part I.: Order Palaeocopida. *Geodiversitas, 34*: 801-835.

Chitnarin, A., Crasquin, S., Chonglakmani, C., Broutin, J., Grote, P. J., & Thanee, N. (2008). Middle Permian ostracods from Tak Fa limestone, Phetchabun Province, Central Thailand. *Geobios, 41*: 341-353.

Cocks, L. R. M., & Fortey, R. A. (1997). A new Hirnantia fauna from Thailand and the biogeography of the Latest Ordovician of South-East Asia. *Geobios, 20*: 117-126.

Cooper, B. J. (1974). New forms of *Belodella* (Conodonta) from the Silurian of Australia. *Journal of Paleontology, 48(6)*: 1120-1125.

Cooper, C. L. (1946). Pennsylvanian ostracodes of Illinois. *Illinois State Geological Survey Bulletin, 70*: 1-177.

Cornell, S. R., Brett, C. E., & Sumrall, C. D. (2003). Paleoecology and taphonomy of an Edrioasteroid-dominated hardground association from tentaculitid limestones in the Early Devonian of New York: A paleozoic Rocky Peritidal Community. *PALAIOS, 18(3)*: 212-224.

Corradini, C. (2007). The conodont genus *Pseudooneotodus* Drygant from the Silurian and Lower Devonian of Sardinia and the Carnic Alps (Italy). *Bollettino della Società Paleontologica Italiana, 46*: 139–148.

Corradini, C., & Corriga, M. G. (2010). Silurian and Lowermost Devonian conodonts from the Passo Volaia Area (Carnic Alps, Italy). *Bollettino della Societa Paleontologica Italiana, 49*: 237-253.

Corradini, C., Corriga, M. G., Männik, P., & Schönlaub, H. P. (2015). Revised conodont stratigraphy of the Cellon Section (Silurian, Carnic Alps). *Lethaia, 48(1)*: 56-71.

Corradini, C., Corriga, M. G., Pondrelli, M., & Suttner, T. J. (2020). Conodonts across the Silurian/Devonian boundary in the Carnic Alps (Austria and Italy). *Palaeogeography, Palaeoclimatology, Palaeoecology, 549*: 109097.

Corriga, M. G., & Corradini, C. (2019). The conodont apparatus of *Zieglerodina Eladioi* (Valenzuela-Ríos, 1994). *Bollettino della Societa Paleontologica Italiana, 58*: 181-185.

Corriga, M. G., Corradini, C., & Walliser, O. (2014). Upper Silurian and Lower Devonian conodonts from Tafilalt, Southeastern Morocco. *Bulletin of Geosciences, 89*: 183-200.

Coryell, H. N., & Billings, G. D. (1932). Pennsylvanian ostracoda of the Wayland Shale of Texas. *American Midland Naturalist, 13(4)*: 170-189.

Crasquin-Soleau, S., Vaslet, D., & Le Nindre, Y-M. (2005). Ostracods as markers of the Permian/Triassic boundary in the Khuff Formation of Saudi Arabia. *Palaeontology, 48(4)*: 853-868.

Crasquin, S. (1985). Nouvelles especes d'ostracodes Dinantiens (France, Belgique, Canada). *Revue de Paleobiologie*, *4*: 79-109.

Crasquin, S., & Horne, D. J. (2018). The palaeopsychrosphere in the Devonian. *Lethaia, 51(4)*: 547-563.

Crônier, C., & Fortey, R. A. (2006). Morphology and ontogeny of an Early Devonian Phacopid trilobite with reduced sight from Southern Thailand. *Journal of Paleontology, 80(3)*: 529-536.

Delo, D. M. (1930). Some Upper Carboniferous ostracods from the shale basin of Western Texas. *Journal of Paleontology, 4*: 152-178.

Department of Mineral Resources. (2013). Zoning for geological and mineral resource managements, Satun Province, Peninsular Thailand. Department of Mineral Resources, Bangkok, Thailand: 123.

Department of Mineral Resources. (2014). Lithostratigraphy, faunal assemblages, biodiversity, paleocology and environment of deposition of the Cambrian-Permian rocks in Satun Province, Peninsular Thailand. Bureau of Geological Survey, Department of Mineral Resources, Bangkok, Thailand: 221.

Department of Mineral Resources. (2018). Summary of the geology and palaeontology of the proposed Satun Geopark Peninsular Thailand, Burrett, C. F., Chaodumrong, P. Mineral Resources Research and Development Center, Bangkok, pp. 100.

Dill, H. G., Luppold, F. W., Techmer, A., Chaodumrong, P., & Phoonphun, S. (2004). Lithology, micropaleontology and chemical composition of calcareous rocks of Paleozoic through Cenozoic Age (Surat Thani Province, Central Peninsular Thailand): Implications concerning the environment of deposition and the economic potential of limestones. *Journal of Asian Earth Sciences, 23(1)*: 63-89.

Donoghue, P. C. J., Forey, P. L., & Aldridge, R. J. (2000). Conodont affinity and chordate phylogeny. *Biological Reviews, 75(2)*: 191-251.

Drygant, D. M., (1974). Simple Silurian and Lower Devonian conodonts from the Volyn–Podolia. *Paleontologičeskij Sbornik, 10(2)*: 64-70.

Dunham, R. J. (1962). Classification of Carbonate Rocks According to Depositional Texture. In: Ham, W. E. (Ed.), *Classification of Carbonate Rocks*, Aapg, Tulsa,. 108-121.

Dzik, J. (1976). Remarks on the evolution of Ordovician conodonts. *Acta Palaeontologica Polonica, 21*: 395-455.

Egorov, V. G. (1950). Ostracoda of the Frasnian stage of the Russian Platform, I, Kloedenellidae. *Ministry of Oil Industry, Moscow Office All-Soviet Sci. Research Geol. Prospecting Inst.*: 1-175 [In Russian].

Egorov, V. G. (1953). Ostracods of the Frasnian stage of the Russian Platform. Volume 2: Bairdiidae, Hollinidae, Kirkbyidae. *Moscow — Ibid.*, 1–135 [In Russian].

Ethington, R. L. (1959). Conodonts of the Ordovician Galena Formation. *Journal of Paleontology, 25*: 257-292.

Farrell, J. (2004). Siluro-Devonian conodonts from the Camelford limestone, Wellington, New South Wales, Australia. *Palaeontology, 47*: 937-982.

Farsan, N. M. (1994). Tentaculiten: ontogenese, systematik, phylogenese, biostratonomie und morphologie. *Abhandlungen der Senckenbergische Naturforschende Gesellschaft, 547*: 1-128.

Ferretti, A., Corriga, M. G., Slavík, L., & Corradini, C. (2022). Running across the Silurian/Devonian boundary along Northern Gondwana: A conodont perspective. *Geosciences, 12(43)*: 1-25.

Fisher, D. W. (1962). Small conoidal shells of uncertain affinities, P. W98-W143. In: R. C. Moore (Ed.), *Treatise on invertebrate paleontology, pt. w, miscellane*. Geological Society of America and University of Kansas Press, Lawrence.

Flügel, E. (2010). Microfacies of carbonate rocks: Analysis, interpretation and application. *Springer-Verlage, Berlin*, 976 pp.

Fortey, R. A. (1989). An Early Devonian trilobite fauna from Thailand. *Alcheringa: An Australasian Journal of Palaeontology, 13(4)*: 257-267.

Geis, H. L. (1932). Some ostracodes from the Salem limestone, Mississippian, of Indiana. *Journal of Paleontology, 6*: 149-188.

Geis, H. L. (1933). Microcheilinella, a new name for the ostracode genus *Microcheilus*. *Journal of Paleontology, 7*: 112.

Gramm, M. N., & Ivanova, V. A. (1975). The ostracod *Paraparchites minax* Ivanov, Sp. Nov. from the Permian of the U.S.S.R., and its muscle-scar field. *Palaeontology, 18(3)*: 551–561.

Green, O. R. (2001). Extraction techniques for phosphatic fossils. In: O. R. Green (Ed.), *A manual of practical laboratory and field techniques in palaeobiology*. Springer Netherlands, Dordrecht, pp. 318-330.

Gründel, J. (1962). Zur taxonomie der ostracoden der Gattendorfi a-Stufe Thüringens. *Freiberger Forschungshefte, 151*: 51-105.

Gügel, B., De Baets, K., Jerjen, I., Schuetz, P., & Klug, C. (2017). A new subdisarticulated Machaeridian from the Middle Devonian of China: Insights into taphonomy and

taxonomy using X-Ray microtomography and 3d-analysis. *Acta Palaeontologica Polonica, 62*: 237-247.

Guillam, E., Forel, M-B., Song, J. J., & Crasquin, S. (2022). Late Devonian– Early Carboniferous ostracods (Crustacea) from South China: taxonomy, diversity and implications. *European Journal of Taxonomy, 804*: 1-62.

Gürich, G. (1896). Das Palaeozoicum im Polnischen Mittelgebirge. *Zapisky I. Mineralog. Obcestva, 32(2)*: 1-539.

Hagen, D., & Kemper, E. (1976). Geology of the Thong Pha Phum area (Kanchanaburi Province, Western Thailand). *Geologisches Jahrbuch, B21*: 53-91.

Hahn, L. and Siebenhüner, M. (1982). Explanatory notes (Paleontology) on the geological maps of Northern and Western Thailand 1: 250,000: Sheets Nan, Chiang Rai, Phayao, Chiang Dao, Chiang Mai, Li, Thong Pha Phum. *Bundesanst. für Geowiss. u. Rohstoffe*, 79.

Hall, J. (1843). Natural history of New York, *Geology of New York, Part IV* . Albany.

Harlton, B. H. (1933). Micropaleontology of the Pennsylvanian Johns Valley shale of the Ouachita Mountains, Oklahoma, and its relationship to the Mississippian Caney shale. *Journal of Paleontology, 7*: 3-29.

Hass, W. H. (1959). Conodonts from the Chappel limestone of Texas. *U. S. Geological Survey Professional Paper, 294-J*: 365-400.

Hassan, M. H. A., Erdtmann, B. D., Wang, X., & Peng, L. C. (2013). Early Devonian graptolites and tentaculitids in Northwest Peninsular Malaysia and a revision of the Devonian-Carboniferous stratigraphy of the region. *Alcheringa: An Australasian Journal of Palaeontology, 37(1)*: 49-63.

Henningsmoen, G. (1953). Classification of Paleozoic straight-hinged ostracods. *Norsk Geologisk Tidsskrift, 31*: 185-288.

Hladil, J., Cejchan, P., & Berousek, P. (1991). Orientation of the conical tests of tentaculites: Internal waves in aqueous environment. *Casopis pro mineralogii a geologii, 36*: 115-130.

Hladil, J., Simcik, M., Ruzicka, M. C., Kulaviak, L., & Lisy, P. (2014). Hydrodynamic experiments on Dacryoconarid shell telescoping. *Lethaia, 47(3)*: 376-396.

Hou, H., Wan, Z., & Xian, S. (1988). Devonian stratigraphy, paleontology and sedimentary facies of Longmenshan, Sichuan, Beijing. *Geol. Publ. House*: 487 [in Chinese with English summary].

Horne, D. J. (2003). Key events in the ecological radiation of the ostracoda. *The Paleontological Society Papers, 9*: 181-202.

Horne, D. J. (2005). Microfossils | Ostracoda. In: R. C. Selley, L. R. M. Cocks and I. R. Plimer (Eds.), *Encyclopedia of Geology*. Elsevier, Oxford, pp. 453-463.

Hušková, A., & Slavík, L. (2020). In search of Silurian/Devonian boundary conodont markers in carbonate environments of the Prague Synform (Czech Republic). *Palaeogeography, Palaeoclimatology, Palaeoecology, 549*: 109126.

Iglikowska, A. (2014). Stranded: The conquest of fresh water by marine ostracods. *Paleontological Research, 18*: 125-133.

Itsarapong, K., Mitmark, S., Keamsontie, V., & Mitsrisai, P. (2023). Stratigraphy of Kuan Tung Formation, Satun UNESCO Global Geopark, Satun. In *GEOTHAI 2023 "Building upon Thai geological knowledge towards sustainable development.", 5-7 september 2023.* Department of Mineral Resources, Bankok, Thailand.

Jain, S. (2020). *Fundamentals of invertebrate palaeontology: Microfossils*. Springer India, New Delhi, pp. 323.

Jarzynka, A., & Filipiak, P. (2009). Organic remains of tentaculitids: New evidence from Upper Devonian of Poland. *Acta Palaeontologica Polonica, 54*: 111-116.

Javanaphet, J. C. (1969). Geology Map of Thailand, Scale 1:1,000,000. Department of Mineral Resources, Bangkok, Thailand.

Jasin, B. (2015). *Posidonomya* (Bivalvia) from Northwest Peninsular Malaysia and its significance. *Sains Malaysiana, 44(2)*: 217-223.

Jeppsson, L., Fredholm, D., & Mattiasson, B. (1985). Acetic acid and phosphatic fossils: A warning. *Journal of Paleontology, 59(4)*: 952-956.

Jones, P. J. (2010). Latest Devonian (Strunian) ostracoda from the Buttons Formation, Bonaparte Basin, Northwest Australia: Their biostratigraphy, palaeoecology and biostratigraphic Links. *Memoir Association of Australasian Association of Palaeontologists, 39*: 261-323.

Jones, P. J., & Holl, H. B. (1869). Notes on the Palaeozoic bivalved Entomostraca, No. IX. Some Silurian species. *Annals and Magazine of Natural History, London (ser. 4) 3*: 221-227.

Jones, T. R. (1855). Notes on Palæozoic bivalved Entomostraca. No. I. Some species of Beyrichia from the Upper Silurian limestones of Scandinavia. *Annals and Magazine of Natural History, 16(92)*: 81-92.

Jones, T. R. (1889). Notes on the Paleozoic bivalved Entomostraca, No. 27. On some North American (Canadian) species. *Annals and Magazine of Natural History, 3(6)*: 377-387.

Kegel, W. (1932). Zur kenntnis Palãozoischen ostrakoden, 2. Bairdiidae aus dem Mitteldevon des Rheinischen Schiefergebirges. *Jahrbuch der Preussischen Geologischen Landesanstalt zu Berlin, 52*: 245-250.

Kershaw, S., Chitnarin, A., Noipow, N., Forel, M-B., Junrattanamanee, T., & Charoenmit, J. (2019). Microbialites and associated facies of the Late Ordovician system in Thailand: Paleoenvironments and paleogeographic implications. *Facies, 65(3)*: 35.

Khodalevich, A. N., & Chernik, V. V. (1973). Konodonty iz zhiv etskikh otlozhenii vostochnogo sklona Iuzhnogo Ural. *Trudi Sverdlovskogo ordena trudovogo krasnogo znameni gornogo instituta, 93*: 27-41.

Klapper, G., & Vodrazkova, S. (2013). Ontogenetic and intraspecific variation in the Late Emsian - Eifelian (Devonian) conodonts *Polygnathus serotinus* and *P. bultyncki* in the Prague Basin (Czech Republic) and Nevada (Western U.S.). *Acta geologica Polonica, 63*: 153-174.

Kobayashi, T. (1957). Upper Cambrian fossils from Peninsular Thailand. *Journal of Faculty of Science, University of Tokyo, 10*: 367-382.

Kobayashi, T., & Hamada, T. (1968). A Devonian Phacopid recently discovered by Mr. Charan Poothai in Peninsular Thailand. *Geology and Palaeontology of Southeast Asia, 4*: 22-28.

Lardeux, H. (1969). Les tentaculites d'europe occidentale et d'afrique du Nord. Cahiers de paleontologie. *Editions du Centre National de la Recherche Scientifique. Paris*: 1-238.

Larsson, K. (1979). Silurian tentaculitids from Gotland and Scania. *Fossils and Strata, 11*: 1-180.

Latreille, P. A. (1802). Histoire naturelle, générale et particulière des Crustacés et des insectes. *Histoires des Cypris et des Cytherées, 8(4)*: 232-254.

Legrand, P. (1986). The Lower Silurian graptolites of Oued in Djerane: A study of populations at the Ordovician-Silurian boundary. *Geological Society, London, Special Publications, 20(1)*: 145-153.

Lethiers, F., & Crasquin-Soleau, S. (1988). Comment extraire les microfossiles a tests calcitiques des roches calcaires dures. *Revue de Micropaléontologie, 311*: 56-61.

Li, Y. W. (1989). The Discovery of Ordovician ostracods from Erlang Mountain, Sichuan. *Bulletin of the Chengdu Institute of Geology and Mineral Resources, Chinese Academy of Geological Sciences, 10*: 131–149 [in Chinese with English Abstract].

Li, Y. X. (1995). Famennian tentaculites from Luofu, Guangxi: Survivors Bed 67 of F/F extinction event. *Journal of Guilin Institute of Technology, 15(2)*: 157–170 [In Chinese with English abstract].

Ljashenko, G. P. (1957). Coniconchia, a new class of extinct mollusca. *Akademia Nauk, SSSR Leningrad, Doklady, 117(6)*: 1049-1052.

Lyaschenko, G. P. (1959). Konikonchii Devona tsentral'nykh i vostochnykh oblastey Russkoy Platformy. *Leningrad, VNIGNI,* : 1–220.

Long, J. A., & Burrett, C. F. (1989). Early Devonian conodonts from the Kuan Tung Formation, Thailand: Systematics and biogeographic considerations. *Records of the Australian Museum, 41(2)*: 121–133.

Maillet, S., Dojen, C., & Milhau, B. (2013). Stratigraphical distribution of Givetian ostracods in the type-area of the Fromelennes Formation (Fromelennes, Ardennes, France) and their relationship to global events. *Bulletin of Geosciences, 88*: 865-892.

Maillet, S., Milhau, B., Vreulx, M., & Sanchez de Posada, L. (2016). Givetian ostracods of the Candás Formation (Asturias, North-Western Spain): Taxonomy, stratigraphy, palaeoecology, relationship to global events and palaeogeographical implications. *Zootaxa, 4068*: 1-78.

Maneerat, W. (2021). *Stratigraphy and Paleoenvironment of Thong Pha Phum Group in Kanchanaburi Province*. Chulalongkorn University Theses and Dissertations (Chula ETD), 89 pp.

Marshall, J. E. A., & Telnova, O. P. (2012). Tentaculitids in palynological preparations: New evidence from the Famennian (Late Devonian) of Southern Timan. *Paleontological Journal, 46(3)*: 228-230.

Mathieson, D., Mawson, R., Simpson, A., & Talent, J. (2016). Late Silurian (Ludlow) and Early Devonian (Pragian) conodonts from the Cobar Supergroup, Western New South Wales, Australia. *Bulletin of Geosciences, 91*: 583-652.

McCoy, F. (1851). On some new Cambro–Silurian fossils. *Annals and Magazine of Natural History. 8*: 387-443

McCoy, F., & Griffith, R. J. S. (1844). A synopsis of the characters of the carboniferous limestone fossils of Ireland. Printed at the University Press by M.H. Gill, Dublin, 207 pp.

McGairy, A., Komatsu, T., Williams, M., Harvey, T., Miller, C., Phong, N. D., Legrand, J., Yamada, T., Siveter, D., Bush, H., & Stocker, C. (2021). Ostracods had colonized estuaries by the Late Silurian. *Biology Letters, 17*: 7.

Meesook, A. (2014). Lithostratigraphy, faunal assemblages, biodiversity, paleoecology and environment of deposition of the Cambrian-Permian rocks in Satun Province, Peninsular Thailand. Bureau of Geological Survey Technical Report 39/2557, Department of Mineral Resources, Bangkok 10400, Thailand (unpublished). 1-235.

Meidla, T., Tinn, O., Salas, M., Williams, M., Siveter, D., Vandenbroucke, T., & Sabbe, K. (2013). Chapter 21 biogeographical patterns of Ordovician ostracods. *Geological Society, London, Memoirs,*: 337-354.

Metcalfe, I. (2017). Tectonic evolution of Sundaland. *Bulletin of the Geological Society of Malaysia, 63*: 27-60.

Moore, R. C. (1961). Ostracoda. In R. C. Moore (Ed.): *Treatise on invertebrate paleontology, part q, arthropoda 3: Crustacea*. Geological Society of America and University of Kensas Press, Lawrence, Kansas.

Morris, R. W., & Hill, B. H. (1952). New ostracoda from the Middle Silurian Newsom shale of Tennessee. *Bulletins of American Paleontology, Ithaca, New York., 34(142)*: 5-22.

Müller, G. W. (1894). Die ostrakoden des Golfes von Neapel und der angrenzenden Meeresabschnitte. *Herausgegeben von der zoologischen Station zu Neapel, 21*: 1-404.

Murphy, M. A. and Matti, J. C. (1983). Lower Devonian conodonts (Hespericus-Kindlei Zones), Central Nevada. *University of California Publications in Geological Sciences, 123*: 82.

Murphy, M. A., Valenzuela-Ríos, J. I., & Carls, P. F. (2004). On classification of Pridoli (Late Silurian)-Lochkovian (Early Devonian) Spathognathodontidae (conodonts). *University of California, Riverside, Campus Museum Contribution*.

Nazik, A., Königshof, P., Ariuntogos, M., Waters, J. A., & Carmichael, S. K. (2020). Late Devonian ostracods (Crustacea) from the Hushoot Shiveetiin Gol section (Baruunhuurai Terrane, Mongolia) and their palaeoenvironmental implication and palaeobiogeographic relationship. *Palaeobiodiversity and Palaeoenvironments, 101(3)*: 689-706.

Neckaja, A. I. (1952). New ostracode species from the Ordovician strata of the Northwestern part of the Russian Platform. *Trudy Vsesoyuznogo Neftyanogo Nauchno-issledovatelskojo Geologorazvedochnogo Instituta, 5*: 217–232 [in Russian].

Neckaja, A. I. (1958). New species and genera of ostracodes of the Ordovician and Silurian of the Russian Platform. *Trudy Vsesoûznogo neftânogo naučno–issledovatel'skogo geologorazvedočnogo instituta (VNIGRI), 60*: 349-373 [in Russian].

Neckaja, A. I. (1966). Ostracods from the Ordovician and Silurian of the USSR. *Tr. Vsesoyuz. Nauchno–Issled. Geol.–Razved. Inst., 251*: 1-103.

Neckaja, A. I. (1973). Ostrakody Ordovika I Silura SSSR. *Vsesoyuznyi Neftyanoi Nauchno-Issledovatel'skii Geologo-Razvedochnyi Institut, Trudy, 324*: 1-88.

Olempska, E. (1979). Middle to upper Devonian ostracoda from the Southern Holy Cross Mountains, Poland. *Palaeontologia Polonica, 41*: 49-162

Olempska, E., Nazik, A., Çapkınoğlu, Ş., & Saydam Demiray, D. G. (2015). Lower Devonian ostracods from the Istanbul area, Western Pontides (Nw Turkey): Gondwanan and peri-Gondwanan affinities. *Geological Magazine, 152*: 298-315.

Ottonello, D., & Romano, A. (2011). Ostracoda and Amphibia in temporary ponds: Who is the prey? unexpected trophic relation in a mediterranean freshwater habitat. *Aquatic Ecology, 45(1)*: 55-62.

Pander, C. H. (1856). Monographie der fossilen fische des Silurischen systems der Russisch-Baltischen gouvernements. *St Petersburg: Buchdruckerei der Kaiserlichen Akademie der Wissenschaften*: 1-91.

Perrier, V., & Siveter, D. J. (2013). Chapter 22 testing Silurian palaeogeography using 'European' ostracod faunas. *Geological Society, London, Memoirs, 38(1)*: 355-364.

Philip, G. M. (1965). Devonian conodonts from the Tyers area, Gippsland, Victoria. *Proceedings of the Royal Society of Victoria, 79*: 95-117.

Pitakpaivan, K., Ingavat, R., & Pariwatvorn, P. (1969). Fossils of Thailand (Vols. 1-3). Geological Survey Division, Department of Mineral Resources.

Polenova, E. N. (1952). Ostracoda of the upper part of the Jivetjki Formation of the Russian Platform (Middle Devonian from Bores in the Central Volga Area). *All-Union Petrol.Sci.-Res.Geol.Expl.Inst., Leningrad (VNIGRI) Trans.N.S.*: 1-15.

Polenova, E. N. (1955). Ostrakody Devona Volgo-Uralskoj Oblasti. Tr. VNIGRI n. ser. 87. In Bykova, E. V. and Polenova, E. N. (Eds): *Foraminifery, radiolyarii i ostrakody devona Volgo-Uralskoj oblasti*. Lenningrad: 191-319.

Polenova, E. N. (1968). Ostrakody nizhnego Devona Salaira. Tom'chumyshskii Gorizont. *Moscow: Nauka*.

Posner, V. M. (1951). Ostracoda of the Lower Carboniferous of the Western Arm of the Submoscow Basin. *All-Union Petrol.Sci.-Res.Geol.Expl.Inst., Leningrad (VNIGRI)* Trans.

Promduang, A., & Chitnarin, A. (2025). Late Silurian – Early Devonian marine ostracods from Kuan Tung Formation, Satun Province, Southern Thailand. *Revue de Micropaléontologie, 86*: 100817.

Purnell, M. A., Philip, C. J. D., & Aldridge, R. J. (2000). Orientation and anatomical notation in conodonts. *Journal of Paleontology, 74(1)*: 113-122.

Racheboeuf, P., Casier, J-G., Plusquellec, Y., Toro, M., Mendoza, D., Carvalho, M., Hérissé, A., Paris, F., Fernández-Martínez, E., Tourneur, F., Broutin, J., Crasquin, S., & Janvier, P. (2012). New data on the Silurian-Devonian palaeontology and biostratigraphy of Bolivia. *Bulletin of Geosciences, 87(2)*: 269–314.

Rasmussen, J., & Stouge, S. (2018). Baltoscandian conodont biofacies fluctuations and their link to Middle Ordovician (Darriwilian) global cooling. *Palaeontology, 61*: 391-416.

Reed, F. R. C. (1915). Supplementary memoir on new Ordovician and Silurian fossils from the Northern Shan States. *Palaeontologica Indica (new series), 6*: 1-123.

Rigo, M., & Joachimski, M. M. (2010). Palaeoecology of Late Triassic conodonts: Constraints from oxygen isotopes in biogenic apatite. *Acta Palaeontologica Polonica, 55*: 471-478.

Rodriguez-Lazaro, J., & Ruiz-Muñoz, F. (2012). Chapter 1 - a general introduction to ostracods: Morphology, distribution, fossil record and applications. In: D. J. Horne, J. A. Holmes, J. Rodriguez-Lazaro and F. A. Viehberg (Eds.), *Developments in Quaternary Sciences*. Elsevier, pp. 1-14.

Roemer, F.A., 1843, Die Versteinerungen des Harzgebirges. *Hannover, Hahn'sche Hofbuchhandlung*, pp. 26–32.

Roundy, P. V. (1926). Mississippian Formations of San Saba County, Texas. U.S. *Geological Survey Professional Paper, 146*: 5-8.

Rozhdestvenskaja, A. A. (1959). Ostracodes of the Devonian Terrigenous Beds of Western Bashkiria and Their Stratigraphic Significance. In: E. V. Chibrikova and A. A. Rozhdestvenskaja (Eds.), *Contributions to the Paleontology and Stratigraphy of the Devonian and Older Deposits of Bashkiria*. Academy of Sciences S.S.S.R., Moscow, pp. 117-247 [in Russian].

Rozhdestvenskaja, A. A. (1972). Ostracodes from the Upper Devonian of Bashkiria. *Acad. Nauk. SSSR., Bashkirian fil., Instit. Geol*.: 1-194 (in Russian).

Saesaengseerung, D., & Saiid, N. B. M. (2016). Carboniferous Radiolarian Fauna from Radiolarian-Bearing Rocks Along the Malaysia-Thailand Border and Their

Depositional Environments. In: *Geoscience for the Society, 52nd Annual CCOP Session, 1st November.* Bangkok.: 17.

Salas, M. J., Vannier, J., & Williams, M. (2007). Early Ordovician Ostracods from Argentina: Their Bearing on the Origin of Binodicope and Palaeocope Clades. *Journal of Paleontology, 81(6)*: 1384-1395.

Sansom, I., Smith, M., Armstrong, H., & Smith, M. (1992). Presence of the Earliest Vertebrate Hard Tissue in Conodonts. *Science, 256(5061)*: 1308–1311.

Sars, G. O. (1866). Oversigt af norges marine ostracoder. *Forhandlinger i Videnskabs-Selskabet i Christiania, 1865(1)*: 1-130.

Sars, G. O. (1888). Nye bidrag til kundskaben om Middelhavets invertebratfauna. 4. ostracoda mediterranea. *Archiv for Mathematik og Naturvidenskab, 12*: 173-324.

Schallreuter, R., Kruta, M., & Marek, L. (1996). Ordovician (Dobrotivá Formation) ostracodes and trilobites from Ejpovice (Bohemia) and their relations to faunas of Northern and Western Europe. *Paläontologische Zeitschrift, 70*: 439-460.

Schindler, E. (2012). Tentaculitoids – an enigmatic group of Palaeozoic fossils. In: J. A. Talent (Ed.), *Earth and life: Global biodiversity, extinction intervals and biogeographic perturbations through time*. Springer Netherlands, Dordrecht, pp. 479-490.

Scott, H. W. (1959). Type species of *Paraparchites* Ulrich & Bassler. *Journal of Paleontology, 33*: 670-674.

Shaver, R. H. (1961). Family Bairdiocyprididae Shaver, N. Fam. In: R. C. Moore (Ed), *Treatise on invertebrate paleontology: part q. arthropoda 3. ostracoda*. Geological Society of America and University of Kansas Press, New York and Lawrence, Kansas., pp. 364-365.

Siveter, D. J. (2008). Ostracods in the Palaeozoic?. *Senckenbergiana lethaea, 88(1)*: 1-9.

Siveter, D. J., Vannier, J. M. C., & Palmer, D. (1991). Silurian Myodocopes: Pioneer pelagic ostracods and the chronology of an ecological shift. *Journal of Micropalaeontology, 10(2)*: 151-173.

Song, J. J., Crasquin, S., & Gong, Y. (2016). Ostracods of the Late Devonian Frasnian/Famennian transition from Western Junggar, Xinjiang, Northwest China. *Alcheringa: An Australasian Journal of Palaeontology, 41(2)*: 250-276.

Song, J., Crasquin, S., & Gong, Y. (2018). Ostracods (Crustacea) as shelf to basin indicators: Evidence from Late Devonian Yangdi and Nandong sections in Guangxi, South China. *Journal of Micropalaeontology, 37*: 257–281.

Song, J. J., Crasquin, S., & Gong, Y. (2019). Late Devonian benthic ostracods from Western Junggar, Northwest China: Implications for palaeoenvironmental reconstruction. *Geological Journal, 54(1)*: 91-100.

Song, J. J., Guo, W., Huang, J-Y., Zhang, Y-C., Chen, Z-Y., Sun, Y-C., Ma, J., & Qie, W-K. (2022). Silurian ostracods from the Nyalam Region, Southern Tibet, China and their implications on palaeoenvironment and palaeobiogeography. *Journal of Palaeogeography, 11(1)*: 85-96.

Suphakdee, P. (2017). The Paleozoic lithostratigraphy and faunal assemblage of the Pa Samet Area, La Ngu District, Satun Province, Bureau of Geological Survey, Department of Mineral Resources, Bangkok, Thailand.

Stauffer, C. R. (1940). Conodonts from the Devonian and associated clays of Minnesota. *Journal of Paleontology, 14*: 417-435.

Stewart, G. A. (1930). Additional species from the silica shale of Lucas County, Ohio. *Ohio Journal of Science, 30(1)*: 52-58.

Stewart, G. A. (1936). Ostracodes of the silica shale, Middle Devonian, of Ohio. *Journal of Paleontology, 10*: 739-763.

Sweet, W. C. (1988). The Conodonta: Morphology, taxonomy, paleoecology, and evolutionary history of a long-extinct animal phylum. *Oxford Monographs on Geology & Geophysics, 10*: 1-212.

Sweet, W. C., & Donoghue, P. C. J. (2001). Conodonts: Past, present, future. *Journal of Paleontology, 75(6)*: 1174-1184.

Takahashi, Y., Agematsu, S., Rahman, M. N. A., & Sashida, K. (2017). Lowermost Devonian conodonts from the Setul Group, Northwestern Peninsular Malaysia. *Journal of Geological Society of Japan, 123*: 989-997.

Tansuwan, W., Chaodumrong, P., & Teansiri, P. (1979). Geological map of Changwat Satun, Scale 1 : 250,000. Department of Mineral Resources, Bangkok, Thailand.

Thassanapak, H., Udchachon, M., Chareonmit, J., & Burrett, C. (2019). Early Permian radiolarians from Southern Thailand, the deglaciation of Gondwana and the age of the Basal Ratburi Group. *Palaeoworld, 29(3)*: 552-567.

Tiyapairat, S. (2004). Geological Map of Ban Pak Bara (4922 Iv), 1:50,000 Scale.: Department of Mineral Resources, Bangkok, Thailand.

Udchachon, M., Thassanapak, H., Burrett, C., & Feng, Q. (2022). The boundary between the Inthanon Zone (Palaeotropics) and the Gondwana-derived Sibumasu Terrane, Northwest Thailand-evidence from Permo-Triassic limestones and cherts. *Palaeobiodiversity and Palaeoenvironments, 102(2)*: 383-418.

Ulrich, E. O., & Bassler, R. S. (1908). New American Paleozoic ostracoda. Preliminary revision of the Beyrichiidae, with descriptions of new genera. *Proceedings of the United States National Museum, 35*: 277-340.

Ulrich, E. O., & Bassler, R. S. (1923). Paleozoic ostracoda: Their morphology, classification and occurence. *Maryland Geological Survey*: 271-391.

Vandekerkhove, J., Namiotko, T., Hallmann, E., & Martens, K. (2012). Predation by macroinvertebrates on *Heterocypris incongruens* (Ostracoda) in temporary ponds: Impacts and responses. *Fundamental and Applied Limnology, 181(1)*: 39-47.

Valenzuela-Ríos, J. I. (1994). Conodontos del Lochkoviense y Praguiense (Devónico Inferior) del Pirineo Central Español. *Memorias del Museo Paleontologico de la Universidad de Zaragoza, 5*: 1-142.

Viira, V., & Aldridge, R. J. (1998). Upper Wenlock to Lower Prídolí (Silurian) conodont biostratigraphy of Saaremaa, Estonia, and a correlation with Britain. *Journal of Micropalaeontology, 17(1)*: 33-50.

Vinn, O. (2010). Adaptive strategies in the evolution of encrusting tentaculitoid tubeworms. *Palaeogeography, Palaeoclimatology, Palaeoecology, 292*: 211-221.

Vinn, O., Hove, H. A. T., Mutvei, H., & Kirsimäe, K. (2008). Ultrastructure and mineral composition of Serpulid tubes (Polychaeta, Annelida). *Zoological Journal of the Linnean Society London, 154*: 633-650.

Walliser, O. H. (1964). Conodonten des Silurs. *Abhandlungen der Hessischen Landesamtes Bodenforschung, 41*: 1-106.

Wang, S. Q. (1983). Ostracods from the Devonian Sipai Formation of Guangxi. *Memoirs of Nanjing Institute of Geology and Palaeontology, 18*: 111–154 [In Chinese with English abstract].

Wang, S. Q. (2015). Ordovician and Silurian ostracoda of China. *University of Science and Technology of China Press, Hefei*: 1-272 [in Chinese with English abstract].

Wang, X-F., Zeng, Q-L., Zhou, T-M., Ni, S-Z., Xu, G-H., Sun, Q-Y., Li, Z-L., Xiang, L-W., & Lai, C-G. (1983). Latest Ordovician and earliest Silurian faunas from the Eastern Yangste Gorges, China, with comments on the Ordovician-Silurian boundary. *Bulletin of the Yichang Institute of Geology and Mineral Resources, 6*: 95-127.

Weddige, K. (1977). Die conodonten der Eifel-Stufe im typusgebiet und in Benachbarten Faziesgebieten. *Senckenbergiana lethaea, 58*: 271–419.

Wei, F. (2019). Conch size evolution of Silurian–Devonian tentaculitoids. *Lethaia, 52(4)*: 454-463.

Wei, F., Gong, Y., & Yang, H. (2012). Biogeography, ecology and extinction of Silurian and Devonian tentaculitoids. *Palaeogeography, Palaeoclimatology, Palaeoecology, 358-360*: 40-50.

Wei, M., Li, Y. W., Jiang, Z. W., & C., X. L. (1983). Subclass ostracoda. In: Chengdu Institute of Geology and Mineral Resources (ed.) *Palaeontological atlas of Southwest China, Guizhou. Volume of microfossils*: 23–254. Geological Publishing House, Beijing. [In Chinese.].

Williams, M., & Siveter, D. (1996). Lithofacies-influenced ostracod associations in the Middle Ordovician Bromide Formation, Oklahoma, USA. *Journal of Micropalaeontology, 15*: 69-81.

Williams, M., Komatsu, T., Nguyen, P. D., Siveter, D. J., McGairy, A., Bush, H., Goodall, R. H., Harvey, T., H. P. , Stocker, C., Legrand, J., Yamada, T., & Miller, C. G. (2023).

Ostracods from the Upper Silurian Si Ka Formation, Northern Vietnam, and their paleobiogeographical significance. *Paleontological Research, 27(3)*: 261-276.

Williams, M., Siveter, D. J., Salas, M. J., Vannier, J., Popov, L. E., & Ghobadi Pour, M. (2008). The earliest ostracods: The geological evidence. *Senckenbergiana lethaea, 88(1)*: 11-21.

Wood, G. D., Miller, M. A., & Bergstrom, S. M. (2004). Late Devonian (Frasnian) tentaculite organic remains in palynological preparations, Radom-Lublin Region, Poland. *Association of Australasian Palaeontologists, 29 (Memoir)*: 253-258.

Wongwanich, T. (1990). *Lithostratigraphy, sedimentology and diagenesis of the Ordovician carbonates, Southern Thailand*: University of Tasmania, Unpublished Ph.D. Thesis. 1-215.

Wongwanich, T. (2001). Lower Palaeozoic. In: Bunopas, S., Piyasin, S., Nutasari, N. (Eds.), Geology of Thailand. Department of Mineral Resources, Bangkok, Thailand. ISBN: 9747733633, : 53–110 [in Thai].

Wongwanich, T., & Boucot, A. J. (2011). Devonian. In: M. F. Ridd, A. J. Barber and M. J. Crow (Eds.), *The Geology of Thailand*. Geological Society of London, pp. 53-70.

Wongwanich, T., Burrett, C. F., Chaodumrong, P., & Tansathein, W. (1990). Lower to Mid Palaeozoic stratigraphy of Mainland Satun Province, Southern Thailand. *Journal of Southeast Asian Earth Sciences, 4(1)*: 1-9.

Wongwanich, T., Boucot, A. J., Brunton, C., House, M., & Racheboeuf, P. (2004). Namurian fossils (Brachiopods, Goniatites) from Satun Province, Southern Thailand. *Journal of Paleontology, 78*: 1072-1085.

Wongwanich, T., Tansathien, W., Leevongcharoen, S., Paengkaew, W., Thiamwong, P., Chaeroenmit, J., & Saengsrichan, W. (2002). The Lower Paleozoic rocks of Thailand. *The symposium on geology of Thailand*. 26-31 August 2002, Bangkok, Thailand: 16 – 21.

Yasuhara, M., Cronin, T. M., & Martínez Arbizu, P. (2008). Abyssal ostracods from the South and Equatorial Atlantic Ocean: Biological and paleoceanographic implications. *Deep Sea Research Part I: Oceanographic Research Papers, 55(4)*: 490-497.

Ziegler, W. (1956). Unterdevonische Conodonten, insbesondere aus dem Schnauer und dem ZorgensisKalk. *Notizblatt des Hessischen Landesamtes fUr Bodenforschung 84*: 93-106.

Ziegler, W. (1960). Conodonten aus dem Rheinischen Unterdevon (Gedinnium) des Remscheider Sattels (Rheinisches Schiefergebirge). *Paläontologische Zeitschrift, 34(2)*: 169-201.

BIOGRAPHY

Anucha Promduang was born on March 27, 1996, in Nakhon Ratchasima Province, Thailand. He earned his Bachelor's Degree in Geological Engineering from Suranaree University of Technology in 2019. Following this, he pursued a Master's Degree in the Civil, Transportation, and Geo-Resources Engineering Program at the Institute of Engineering, Suranaree University of Technology. Between 2019 and 2022, during his postgraduate studies, he served as a laboratory teaching assistant at the School of Geotechnology and worked as a research assistant with the Georesources Research Unit at the same institution.